# Synthesis of Biomass Based Microcrystalline Cellulose for Food Packaging Application

*Thesis submitted in partial fulfillment of the requirements*

*for the degree of*

**DOCTOR OF PHILOSOPHY**

**by**

*Banhisikha Debnath*

*Roll No.: 196152101*


**Centre for the Environment**

**Indian Institute of Technology Guwahati**

**Guwahati 781039, India**

**January 2025**

# Synthesis of Biomass Based Microcrystalline Cellulose for Food Packaging Application




*Banhisikha Debnath*

# DEDICATION

*To my beloved parents and husband for their prayers, love, encouragement, and unconditional support*

**Centre for the Environment**

**Indian Institute of Technology Guwahati**

**Guwahati 781039, India**

# STATEMENT

I hereby declare that the content embodied in the thesis entitled "**Synthesis of Biomass Based Microcrystalline Cellulose for Food Packaging Application**" is the result of investigations carried out by me at the Centre for the Environment, Indian Institute of Technology Guwahati, India, under the guidance of Prof. Mihir Kumar Purkait. In keeping with the general practice of reporting scientific observations, due acknowledgements have been made wherever the work described is based on the findings of other investigators.

Banhisikha Debnath

**Centre for the Environment**

**Indian Institute of Technology Guwahati**

**Guwahati 781039, India**

# CERTIFICATE

It is certified that the work reported in the thesis entitled "**Synthesis of Biomass Based Microcrystalline Cellulose for Food Packaging Application**", by **Banhisikha Debnath**, has been carried out under my supervision. The work documented in this thesis has not been submitted to any other University or Institute for the award of any degree or diploma.

This thesis in my opinion, has reached the standard fulfilling the requirements for the award of the degree of Doctor of Philosophy in accordance with the regulations of the institute.

**Dr. Mihir Kumar Purkait**

Professor

Department of Chemical Engineering

Indian Institute of Technology Guwahati

Guwahati 781039, India

# Acknowledgements

*This thesis becomes a reality with the kind support and help of many individuals. It is a genuine pleasure to express my sincere gratitude to all who helped me in the completion of this thesis.*

*First and foremost, I would like to thank* ***God*** *for giving me strength and encouragement throughout all the challenging moments of completing this thesis.*

*I wish to express my deepest gratitude and appreciation for my supervisor* ***Prof. Mihir Kumar Purkait*** *for providing me invaluable guidance throughout the various stages of my research journey. I am indebted to him for his positive inputs and constant encouragement throughout the journey. I am grateful to him for his great support in every way which helped me to finish this work. His guidance and encouragement helped me in all the time of experiments and writing of this thesis. I could not have imagined having a better supervisor and advisor. It has been a rich and rewarding experience, and the memories will always be cherished.*

*I would like to extend my sincere gratitude to my doctoral committee members* ***Prof. Chandan Das*** *(Department of Chemical Engineering),* ***Prof. S. K. Majumder*** *(Department of Chemical Engineering), and* ***Prof. Lal Mohan Kundu*** *(Department of Chemistry) for their valuable suggestions and constructive criticism during the project evaluations, which helped me to make necessary improvements in various stages of my research work.*

*I am extremely grateful to my* ***thesis examiners*** *for their insightful advice that helped me improve the quality of the thesis.*

*I would like to acknowledge Department of Chemical Engineering and the centres for providing me various facilities required for my analysis and characterization during the research work specifically,* ***Research lab, Computer lab, and Analytical Lab Facility*** *(Centre for the Environment) and* ***Central Instrument Facility*** *(CIF), Indian Institute of Technology Guwahati.*

*I am also grateful to all the* ***faculty*** *and* ***staff*** *members of the Centre for the Environment for helping and providing me the necessary facilities and resources.*

**Acknowledgements**

*I would like to thank my lab* ***seniors*** *(Dr. Thangsei Nengneilhing Baite, Dr. Deepti Nair, Dr. Ankush D Sontake, Dr. Piyal Mondal, Dr. Niladri Samanta, Dr. Pranjal Pratim Das, Mr. Anweshan Ghosh, and Dr. Simons Dhara) and* ***colleagues*** *(Prangan, Mukesh, Satish, Lokesh) for always being there when I needed them.*

*I am immensely grateful to my* ***friends*** *(Debolina, Sumona, Mousumi and Gariyoshi,) who are a constant source of support through all my ups and downs. I can never thank them enough for all the ways they have supported me and stood by me in each and every step of the journey. I am very thankful to my relatives and all my well-wishers who are directly or indirectly involved in my research journey.*

*My final words go to my family whom I am abundantly blessed with for all their unconditional love, sacrifices and encouragement. I am greatly indebted to my* ***father*** *(****Mr. Ranjit Debnath****),* ***mother (Mrs. Kabita Debnath)*** *and* ***husband (Mr. Arindam Das)*** *whose unwavering support made it possible for me to come so far. I would also like to express my gratitude to my* ***father-in-law (Er. Amar Kumar Das)*** *and* ***mother-in-law (Mrs. Swapna Das)*** *for their constant support during my PhD journey.*

*Banhisikha Debnath*

# Abstract

The primary objective of this thesis is the extraction of crystalline cellulose derivative i.e., microcrystalline cellulose (MCC) from lignocellulosic waste biomass elephant grass and tea factory waste and exploration of its potential application in the food packaging sector. MCC was extracted from elephant grass (*Pennisetum purpureum*) through successive bleaching method. The elephant grass derived microcrystalline cellulose (E-MCC) was used as a reinforcing agent in bioplastic corn starch film to improve its packaging properties. MCC was also synthesized from tea factory waste by a novel superfast technique using microwave heating. The synthesized tea waste microcrystalline cellulose (TWMCC) was employed as reinforcing filler in polyvinyl alcohol (PVA) film and studied for its potential application in food packaging. The abstract of this work is shown below.

Nowadays, the development of biodegradable packaging materials from natural renewable sources has attained great attraction in the research field to mitigate environmental problems and the depletion of resources. In this regard, starch-based films are effective for food packaging due to their low cost and eco-friendliness. In the present study, microcrystalline cellulose (MCC) was synthesized from elephant grass biomass and characterized using X-ray diffraction (XRD), Fourier transform infrared spectroscopy (FTIR), Field emission scanning electron microscopy (FESEM), and Thermogravimetric analysis (TGA). The prepared E-MCC was then employed as reinforcement in corn starch films to improve their properties, and the fabricated films were characterized using FTIR, FESEM, TGA, water contact angle, moisture content, and tensile strength testing. The addition of 1% E-MCC significantly enhanced the thermal stability of the films by increasing the peak degradation temperature from 312.3 (neat starch film) to 321 °*C*. The water contact angle value of the pure starch film

was 19.52°, which increased to 98.83° with the incorporation of 5% E-MCC. The mechanical strength of the film increased from 6.03 MPa (neat film) to 22.33 MPa (5% E-MCC). The findings in the study reveal that MCC synthesized from elephant grass is a promising reinforcing agent that can considerably enhance the various properties of corn starch films for food packaging applications.

The potential of the wastes generated in the industries during tea production processes for the extraction of MCC was also explored in this study. MCC was isolated from industrial black tea waste using microwave heating instead of conventional heating and avoiding the traditional acid hydrolysis method. Microwave increased the reaction speed significantly and resulted in very quick delignification and bleaching of black tea waste to isolate MCC in white powdered form. FTIR, XRD, FESEM, and TGA analysis were then carried out to investigate the chemical functionality, crystallinity, morphology, and thermal properties, respectively, of the synthesized tea waste MCC. The characterization results demonstrated that cellulose with a short rough fibrous structure having an average particle size of around 23 µm was extracted. The results of FTIR and XRD demonstrated unequivocally that all amorphous non-cellulosic compounds had been eliminated. The microwave-extracted black tea waste MCC showed 89.77% crystallinity and good thermal properties, indicating that it could be a promising filler material for preparing polymer composites. Therefore, microwave-assisted delignification and bleaching can be used as a suitable, energy-efficient, time-saving and low-cost method for extracting MCC from the black tea waste produced in tea factories which can serve as a renewable, abundant, and cheap source of valuable crystalline cellulose derivatives.

The tea waste derived microcrystalline cellulose was then incorporated in PVA polymer matrix to improve its properties for food packaging applications. The properties of the prepared composite films were investigated using FTIR, FESEM, TGA, water contact angle meter, moisture content and solubility determination, water vapour permeability testing, UTM and UV-vis spectroscopy analysis. Strong hydrogen bonding between the hydroxyl groups of PVA and TWMCC forms a dense network structure, which prevents water molecules from entering the polymer matrix. As a result, both water resistance and water vapour barrier properties of the TWMCC reinforced PVA films improved significantly. TWMCC content of 5 wt% increased the water contact angle of PVA film to 81.54°, while pure PVA film had a much lower contact angle of 29.31°. Incorporation of 3 wt% TWMCC increased the tensile strength of the PVA composite film by about 2 folds (from 9.11±1.15 to 18.5±1.93 MPa). TWMCC also improved the thermal stability and UV-blocking capability of the composite films. When used for fruit packaging, the PVA composite film containing 5 wt% TWMCC showed excellent performance in extending fruit shelf life by preserving grapes up to 18days, while unpacked grapes lost marketability within one week. Findings from the current study show that lignocellulosic biomass are renewable, cheap and eco–friendly sources of valuable crystalline derivatives of cellulose that have promising potential to be used as filler materials in bio-based packaging materials for food preservation, which can substitute the traditional petroleum-based food packaging and minimize the global plastic pollution issue.

# Research Publications

**Journal publications related to thesis work**

**Published**

1. **Debnath, B.**, Duarah, P., Haldar, D., and Purkait, M. K. Improving the properties of corn starch films for application as packaging material via reinforcement with microcrystalline cellulose synthesized from elephant grass. *Food packaging and shelf life*, 34 (2022) 100937. https://doi.org/10.1016/j.fpsl.2022.100937
2. **Debnath, B.**, Duarah, P., and Purkait, M. K. Microwave-assisted quick synthesis of microcrystalline cellulose from black tea waste (*Camellia sinensis)* and characterization. *International Journal of Biological Macromolecules*, 244 (2023) 125354. https://doi.org/10.1016/j.ijbiomac.2023.125354
3. **Debnath, B.**, Duarah, P., and Purkait, M. K. Sustainable utilization of tea factory waste-derived microcrystalline cellulose as filler material for food packaging films. *ACS Sustainable Resource Management*, 12 (2024) 2518-2529. https://doi.org/10.1021/acssusresmgt.4c00165
4. **Debnath, B.**, Haldar, D., and Purkait, M. K. A critical review on the techniques used for the synthesis and applications of crystalline cellulose derived from agricultural wastes and forest residues. *Carbohydrate polymers*, 273 (2021) 118537. https://doi.org/10.1016/j.carbpol.2021.118537
5. **Debnath, B.**, Haldar, D., and Purkait, M. K. Potential and sustainable utilization of tea waste: A review on present status and future trends. *Journal of environmental chemical engineering*, 9 (2021) 106179. https://doi.org/10.1016/j.jece.2021.106179

## Research Publications

### Chapters related to thesis work

1. **Debnath, B.,** and Purkait, M.K. (2023). Sustainable Utilization of Tea Waste. In: Ramawat, K., Mérillon, JM., Arora, J. (eds) Agricultural Waste: Environmental Impact, Useful Metabolites and Energy Production. Sustainable Development and Biodiversity, vol 31, 245-275. Springer. https://doi.org/10.1007/978-981-19-8774-8_11

### Books related to thesis work

1. Purkait, M.K., Haldar, D., and **Debnath, B**. Technological advancements in product valorization of tea waste. Publisher: **Elsevier,** (2023). **ISBN: 978-0-443-19239-5**

### Other publications apart from thesis work

1. **Debnath, B.**, Haldar, D., and Purkait, M. K. Environmental remediation by tea waste and its derivative products: A review on present status and technological advancements. *Chemosphere*, 300 (2022) 134480. https://doi.org/10.1016/j.chemosphere.2022.134480
2. Duarah, P., **Debnath, B**., and Purkait, M. K. Synthesis of antibacterial fluorescent carbon dots and green coal-like hydrochar from tea Industry byproducts via hydrothermal carbonization. *Industrial Crops and Products*, 221 (2024) 119364. https://doi.org/10.1016/j.indcrop.2024.119364
3. Duarah, P., Joardar, S., **Debnath, B**., and Purkait, M. K. Optimized extraction of polyphenols from tea factory waste and cost-effective drying methods for sustainable utilization. *Bioresource Technology Reports*, 26 (2024) 101833. . https://doi.org/10.1016/j.biteb.2024.101833

# CONTENTS

**CONTENTS**

# LIST OF FIGURES

## LIST OF FIGURES

# LIST OF TABLES

## LIST OF TABLES

# Nomenclature

## Notations

| | |
|---|---|
| $2\theta$ | Diffraction angle |
| $I_{002}$ | Maximum intensity of crystalline phase |
| $I_{am}$ | Intensity of the amorphous phase |
| $\mu$ | Micron |
| $M_1$ | Initial weight before drying |
| $M_2$ | Final weight after drying |

## Abbreviations

| | |
|---|---|
| ANOVA | Analysis of variance |
| C | Carbon |
| CAGR | Compound annual growth rate |
| CCD | Central composite design |
| cm | Centimetre |
| C-MCC | Commercial microcrystalline cellulose |
| CrI | Crystallinity index |
| DC | Degree of crystallinity |
| DI | Deionized |
| DP | Degree of polymerization |
| DTG | Differential thermogravimetry |
| EG | Elephant grass |
| E-MCC | Elephant grass derived microcrystalline cellulose |
| FESEM | Field emission scanning electron microscope |
| FTIR | Fourier transform infrared spectroscopy |
| g | Grams |

| | |
|---|---|
| h | Hour |
| $H_2O_2$ | Hydrogen peroxide |
| $H_2SO_4$ | Sulphuric acid |
| HCl | Hydrochloric acid |
| $HNO_3$ | Nitric acid |
| kHz | Kilo Hertz |
| kN | Kilonewton |
| KOH | Potassium hydroxide |
| L | Litre |
| m | Metre |
| M | Molar |
| M.W. | Molecular weight |
| mg | Milligram |
| min | Minute |
| mL | Millilitre |
| mm | Millimetre |
| NaOH | Sodium hydroxide |
| NaClO | Sodium hypochlorite |
| $NaClO_2$ | Sodium chlorite |
| $Na_2SO_3$ | Sodium sulphite |
| nm | Nanometres |
| MC | Moisture content |
| MCC | Microcrystalline cellulose |
| MPa | Megapascal |
| P | Pascal |

| | |
|---|---|
| PVA | Polyvinyl alcohol |
| $R^2$ | Root mean square |
| RH | Relative humidity |
| RI | Refractive index |
| RPM | Rotations per minute |
| RSM | Response surface methodology |
| s | Seconds |
| SR | Swelling ratio |
| TGA | Thermogravimetric analyzer |
| TW | Tea waste |
| TWMCC | Tea waste derived microcrystalline cellulose |
| UV – Vis | UV – Visible |
| UV | Ultra-violet |
| v | Volume |
| w | Weight |
| wt% | Weight percentage |
| WS | Water solubility |
| WVP | Water vapour permeability |
| WVTR | Water vapour transmission rate |
| XRD | X-ray diffraction |

# Chapter 1

# Introduction, Literature Review, Objectives and Organization of the Thesis

*This chapter discusses a brief summary of the fundamentals of crystalline derivatives of cellulose. The state-of-the art literature on extraction of microcrystalline cellulose from lignocellulosic biomass using conventional as well as advanced methods is summarized. The potential utilization of the biomass derived crystalline cellulosic derivatives as reinforcing agents in polymer composites are explored here. Furthermore, the potential application of crystalline cellulose in the food packaging sector is elaborated. Finally, the objectives of the present work and the outline of the thesis work is highlighted.*

## 1.1. Background

The rapid growth of human population along with industrial development is increasing the worldwide demand of energy which is presently maintained by the traditional fossil sources. Excessive use of energy and the consequent depletion of natural resources are the major issues in the recent era and hence, the environment friendly sustainable development is of more interest in the research field. One significant way to mitigate the environmental concern is to utilize the naturally available renewable materials and eco-friendly biomass-based products. The valorization of biomass is an encouraging strategy to achieve such objectives (C. Wang et al., 2021). Biomass is generally characterized as the biodegradable organic fraction of various waste materials such as agricultural wastes, forest residues, and industrial wastes. Agricultural waste usually includes plant-based waste materials such as leaves, shoots, cereal straw, grass, vine pruning, roots,

and fruit peels. Forest residues include trunks of old tree, sawdust, bark, pruning and roots (Moustakas et al., 2020). Generally, agricultural wastes are generated at a rapid rate with an average annual increase rate of 5-10% which attributes towards negative environmental impacts because of the random disposal or burning of such wastes lead to pollution of the aquatic environment, soil, and air. So, proper utilization of waste biomass residues through conversion and valorization is of high demand to control its harmful effects on the environment (B. Wang et al., 2016).

## 1.2. Lignocellulosic biomass

Lignocellulosic biomass represents an abundant and underutilized resource with potential applications across various scientific and industrial domains. Global annual production of lignocellulosic biomass is estimated to be over 181.5 billion tonnes, underscoring the vast potential for its utilization, but only around 8.2 billion tonnes of lignocellulose biomass is utilized by different application areas (Mujtaba et al., 2023). Lignocellulosic biomass, derived primarily from agricultural crops and forest residues, is a significant natural carbon reservoir composed of plant-derived materials. The main constituents of lignocellulosic biomass are carbohydrate polymers (cellulose, hemicellulose, pectin) and non-carbohydrate polymers (lignin, proteins). Cellulose consists of glucose units forming linear microfibrils with regions of high crystallinity and amorphous structures, interconnected by hydrogen bonds into cellulose fibers. Hemicellulose is a highly branched low molecular weight biopolymer comprising of 5-C pentose monomers (xylose, arabinose), 6-C hexose monomers (galactose, mannose, glucose) and sugar acids (glucuronic, galacturonic, cinnamic and methyl galacturonic acid). Hemicellulose is of amorphous structure with less degree of polymerization,

which makes it more susceptible towards disintegration into its monomeric units. Lignin is the 2nd most amply available biopolymer on the earth after cellulose, consisting of aromatic rings of phenylpropane units linked together by different chemical bonds such as β-O-4 ether linkages, some carbon–oxygen and carbon–carbon bonds (Debnath et al., 2021a). The increasing focus on sustainable development and environmental stewardship has prompted significant interest in the valorization of lignocellulosic waste, a prominent byproduct of agricultural and industrial activities. Lignocellulosic waste includes agricultural wastes, woody forest residues, pulp and paper industry wastes, municipal solid wastes, energy crops residues and so on. These waste materials contain cellulose (35–50%), hemicellulose (20–35%), and lignin (10–25%) as their major components. Such lignocellulosic wastes exhibit numerous environmental benefits due to their natural abundance, renewability, low cost, and minimum energy requirement for conversion.

## 1.3. Crystalline cellulose derivatives

Cellulose is the most abundant natural biopolymer available on this planet which is generally utilized as a renewable, biodegradable, and environment-friendly resource of value-added products. It is a semi-crystalline polysaccharide having high molecular weight and composed of D-glucose monomers connected by β-(1,4)-glycosidic bonds. The structural configuration of cellulose is composed of crystalline and amorphous regions. The presence of O–H group in cellulose facilitates its modification into various derivative products (Haldar & Purkait, 2021; Halder et al., 2019; Salama, 2020). Microcrystalline (MCC) is one of the most common and widely used crystalline

derivatives of cellulose. It is a white, odorless, crystalline, fine powder having diameter of 50 μm and length in the range of 100-1000 μm. Partial hydrolysis of the amorphous regions present in cellulose results in the formation of MCC. So, both crystalline and amorphous regions may be present in MCC. In the last few decades, MCC has gained immense attention in the research field for its specific properties such as biodegradability, bio-compatibility, non-toxicity, large surface area and high mechanical strength which make them promising candidates for applications in various fields (Haldar & Purkait, 2020b; Mishra et al., 2019). Various lignocellulosic biomass wastes such as left-over portions of food crops (straws of rice, wheat, maize, sunflower, corn stover), perennial plants and forest residues like woody biomass are frequently used as the abundant sources of crystalline cellulosic derivatives. Utilization of these resources is considered as a sustainable approach as they do not compete with food production (Debnath et al., 2021a).

Various industries around the world have started the bulk scale production of MCC over the past decade. At present, most of the industries are using forest residues such as wood chips or wood pulp for the manufacturing of crystalline cellulose, whereas some of them utilize agricultural residues also (Haldar & Purkait, 2020b). The global demand of MCC is increasing rapidly which may be attributed to its potential application in food and beverages preservation, biomedical and pharmaceutical fields, cosmetics, and personal care products manufacturing. The worldwide MCC market based on woody and non-wood (agricultural) biomass is expected to grow from 938 million USD in the year 2019 to 1315 million USD by 2024 (CAGR being 7%). The major companies fulfilling the growing demand of MCC are DowDuPont and Avantor Performance

Materials Inc. in the US, Asahi Kasei Chemicals Corporation in Japan, DFE Pharma GmbH & Co.KG and JRS Pharma GmbH & Co.KG in Germany, Huzhou City Linghu Xinwang Chemical Co., Ltd. in China, Roquette in France, Rayonier Advanced Materials in Finland, Gujarat Microwax Limited and Sigachi Industrial Pvt. Ltd. in India. Another report shows that the rise in the global MCC market was 5.5% in the year 2020 and it will reach to 1.6 billion USD by 2027 at a projected CAGR of 8% over the forecasted period of 2020-2027. Biomass availability and cost are considered as the crucial factors for the bulk scale industrial production of biomass-based MCC. Therefore, with respect to economical and commercial aspects, agricultural wastes and forest residues with ample availability, rich cellulose content and less lignin fraction should be selected for the synthesis of crystalline cellulose derivatives (Debnath et al., 2021a).

## 1.4. Application of microcrystalline cellulose in polymer composites

Over the past decades, the crystalline cellulose derivatives attracted great attention as reinforcing agents or filler in the matrices of polymer composites. They possess huge potential to replace the traditional petroleum-derived reinforcing materials in the production of polymer composites for applications in different fields like packaging materials, building materials, automotive and household products (Trache et al., 2016). Green composites were prepared through sonication followed by solution casting of polyvinyl alcohol (PVA) reinforced with MCC extracted from sago seed shells. The synthesized PVA-MCC films showed improved thermal stability, good transparency

and their tensile strength also increased slightly after incorporating 1 wt% of MCC into the polymer matrix (Naduparambath et al., 2018). MCC isolated from pepper (*Piper nigrum L.*) bio-waste was successfully utilized for the formation of sustainable bio-composites. MCC was synthesized via hydrothermal assisted alkaline treatment and acid hydrolysis method (using HCl) and about 86% yield of MCC was obtained. The doping of the prepared MCC into the polymer matrices of seaweed and chitosan enhanced the tensile strength of the composite films significantly, indicating the applicability of the MCC as reinforcing material in bio-composites replacing the conventional plastic filler (Holilah et al., 2021). Many literatures also reported the usefulness of surface modified MCC for polymer composite production. Bessa et al. isolated MCC from giant reed (*Arundo donax L.*) through acid hydrolysis and functionalized them with amine groups. The modified MCC was then used as reinforcing agent in bisphenol A-based benzoxazine composites and their kinetic curing behaviour was tested. The modified MCC reinforced composites exhibited a single curing stage as compared to the intricate polymerization of the neat composites and the average activation energy of the curing process also reduced from 89 kJ/mol to 80 kJ/mol (Bessa et al., 2021).

## 1.5 Elephant grass biomass

Elephant grass (*Pennisetum purpureum*) is a renewable and sustainable resource that generally grows in tropical regions. This grass is popular for its easy cultivation, high yield, and nutrient availability. It is lignocellulosic biomass with high cellulose and hemicellulose contents, typically in the range of 31–41 wt% and 15–47 wt%,

respectively (Kongkeitkajorn et al., 2020; Phitsuwan et al., 2016). Elephant grass grows abundantly in the North-Eastern states of India, particularly in Assam, because of the heavy rainfall in this region. But it grows so rapidly and extensively that it is usually considered a waste material, and people cut or burn this grass to control its growth which in turn causes negative environmental impacts (Haldar & Purkait, 2020c). Hence, employing elephant grass for the synthesis of valuable MCC can be a sustainable way of managing this waste biomass. Moreover, the production of elephant grass is water efficient as compared to other conventional lignocellulosic biomass like rice, sugarcane. The requirement of water for the production of 1 kg of rice and sugarcane is 3000-5000 and 1500-3000 L, respectively, whereas only 800-1000 L of water is required for the producing 1kg of elephant grass. Therefore, elephant grass biomass can preferably be used in place of rice husk or sugarcane bagasse for large-scale production of MCC, even in countries with water shortages (Debnath, Duarah, et al., 2022).

## 1.6. Tea industry waste: a potential source of microcrystalline cellulose

Tea is a non-alcoholic beverage that ranks second in popularity worldwide, right after water. According to estimates, tea is consumed every day throughout the globe in amounts between 18 and 20 billion cups. Around 6.3 million tonnes of tea were consumed globally in 2020, and by 2025, that number is projected to increase to up to 7.4 million tonnes. Because of its immense popularity and growing demand, tea production around the world has experienced remarkable growth over the past few

decades (Debnath et al., 2021b; Debnath, Haldar, et al., 2022). The International Tea Committee (ITC) reports that worldwide tea output will grow from its 2017 level of around 5.72 million tonnes to a maximum of 6.46 million tonnes in 2021 ("Tea Board of India, Global Tea website," 2022). China is the world's largest tea producer, and is often regarded as tea's origin. India, second only to China, is a major tea producer and also a leading tea consumer of the world. As per the reports of the International Tea Organization, India, having nearly 579,000 acres of land dedicated to tea cultivation, contributes around 27.4% of the global annual tea production (Duarah et al., 2023).

As reported by the Tea Board of India, more than 1.34 million tonnes of tea was produced in India in the financial year 2021-2022, mainly driven by the states of Assam and West Bengal. The North-Eastern state of Assam is the largest tea-growing state in India, contributing over 50% of the country’s tea production (Basumatary et al., 2018; Kumar et al., 2021). Enormous amounts of waste are produced during the various tea processing procedures employed in the tea industry in the form of wasted tea stems, leaves, and buds. Such wastes, if not disposed of properly, may lead to severe environmental pollution problems. In India, the estimated production of tea waste in the 2020-2021 financial year was near about 25 million kilograms (Debnath et al., 2023). The tea factories are facing many challenges in handling these huge quantities of waste since there is no proper tea waste management system available in the country. As a result, a significant amount of waste produced by tea manufacturers ends up in landfills or is composted, burned, or incinerated, which contributes to a variety of environmental problems such as soil, water, and air pollution (Chowdhury et al., 2016; Debnath et al.,

2021b). Therefore, valorization and utilization of tea factory wastes for their sustainable management are of high importance in the research field nowadays.

## 1.7. Bio-based sustainable food packaging materials

The packaging materials commonly used for food preservation are raising the environmental concern as they are mostly of non-biodegradable nature and only a small percentage of plastics are recycled. The traditional plastic materials are difficult to break down, and hence they generate huge quantities of waste that accumulate on the terrestrial and marine environment, resulting in severe environmental issues. Moreover, the excessive usage of plastic for packaging is causing depletion of the natural resources (crude oil, natural gas, and coal) (Debnath, Duarah, et al., 2022). Therefore, research efforts are constantly being directed toward the utilization of various biopolymers for the development of green, sustainable, and eco-friendly food packaging to mitigate the environmental problems associated with plastic packaging. Starch films are biodegradable, environment-friendly, and safe to be used as packaging materials (Malherbi et al., 2019; Yuan & Chen, 2021). Starch can be extracted from various plants, among which corn starch (CS) is the most predominant one. The high amylose content of corn starch facilitates the formation of strong, stiff films that are suitable for food packaging (Othman et al., 2021). However, starch films generally possess poor thermal, mechanical, and moisture barrier properties. The introduction of reinforcing agents into the polymer matrix of starch can substantially improve the properties of starch films for packaging purposes (Merci et al., 2019). Cellulosic materials are found to be effective as reinforcement in corn starch films (Collazo-Bigliardi et al., 2019a;

Shih & Zhao, 2021). Crystalline cellulose derivatives are successfully incorporated into starch films to improve their thermal resistance, mechanical strength, and gas and water barrier properties. The O–H groups present in cellulose favour the reinforcement by interacting with the polymer matrix (Collazo-Bigliardi et al., 2019b).

Polyvinyl alcohol (PVA) is another eco-friendly and biocompatible polymer with various advantages such as excellent film-forming capability, chemical resistance, high oxygen barrier capacity, outstanding biodegradability, and non-toxicity (Baite et al., 2022; Souza et al., 2024). However, PVA is highly hydrophilic in nature due to the presence of abundant hydroxyl groups. The inherent low mechanical strength, poor thermal, UV-blocking, and water barrier properties restrict the applications of PVA in food packaging (Aloui et al., 2016). Therefore, PVA is generally blended with fillers or other biopolymers to improve its properties for packaging applications.

One of the main requirements for a good food packaging material is that it should be resistant to water and have good barrier properties against oxygen and moisture to keep the food products safe. Therefore, it is essential to investigate environmentally friendly methods for improving the hydrophobic properties of biopolymers-based packaging materials.

## 1.8. State of the art literature review

With a brief overview of the contemporary research, this section outlines the outcome of various literatures so as to identify few promising areas of research that needs to be addressed in this thesis. The state-of-the-art literature has been presented for synthesis and utilization of microcrystalline cellulose from lignocellulosic biomass.

### 1.8.1. Synthesis of microcrystalline cellulose from lignocellulosic biomass

MCC shows excellent potential for industrial applications such as food, cosmetics, pharmaceutical, and reinforcement in polymer composites. Biomass-based extraction of cellulose derivatives is observed to be environmentally friendly and suitable for industrial applications (Trache et al., 2016). MCC can be synthesized from different lignocellulosic biomass such as rose stems (Ventura-Cruz et al., 2020), sweet sorghum (Ren et al., 2019), sugarcane bagasse (Thiangtham et al., 2020), tea waste (Zhao et al., 2018) and so on. Ventura-Cruz et al. successfully utilized rose stem wastes for the synthesis of MCC possessing high crystallinity and good thermal properties (Ventura-Cruz et al., 2020). MCC isolated from roselle fibers exhibited higher crystallinity (78%) than that of commercial-microcrystalline cellulose (C-MCC, crystallinity 74%) and improved thermal stability as compared to the roselle pulp (Kian et al., 2017). Shao et al. used corncob for the production of MCC with higher economic feasibility as compared to C-MCC (Shao et al., 2020). The various methods adopted for the synthesis of MCC from lignocellulosic biomass are described in **Table 1.1.**

**Table 1.1** Preparation of MCC from lignocellulosic biomass

| **Biomass and structural composition** | **Techniques used** | **Characterization techniques used** | **References** |
|---|---|---|---|
| Waste cotton fabrics (WCFs)<br><br>[Cellulose 95–99 wt%] | **Chemical method:**<br>Phosphotungstic acid (0.69-6.25 mmol/L), 130–170 °C, 4–8 h. | FTIR, XRD, TGA, SEM, particle size and contact angle | (Hou et al., 2019) |

| | | | |
|---|---|---|---|
| Sweet sorghum<br><br>[Cellulose 33.8 wt%, Hemicellulose 19.7 wt%, Lignin 23.4 wt%] | **Alkaline treatment:** 0.03 g/mL NaOH, 50 °C, 70 min.<br><br>**Bleaching:** 0.03 g/mL $Na_2SO_3$ and 0.06 g/mL NaClO, 80 °C, 120 min.<br><br>**Acid hydrolysis:** HCl. | SEM, XRD, FTIR, TGA | (Ren et al., 2019) |
| Rice husk | **Alkali treatment:** 4 M NaOH, 80 °C, 24 h.<br><br>**Bleaching:** NaClO (12.5% pure), 40 °C, 1 h.<br><br>**Acid hydrolysis:** 4 M $H_2SO_4$ (98% pure), 60 °C, 1 h. | HR-SEM, FTIR, TGA and laser particle size analyser | (Sim, Bae, Choi, Choi, et al., 2016) |
| Cotton wool | **Bleaching:** 30% (v/v) $H_2O_2$, room temperature, 1 h.<br><br>**Acid hydrolysis:** $H_2SO_4$, 50 °C, 4 h. | SEM, FTIR, XRD, TGA, XPS, VSM | (Rashid et al., 2017) |
| Date seeds | **Dewaxing:** Chloroform and ethanol (2:1).<br>**Delignification:** 17.5% (w/v) NaOH, 90 °C, 3 h.<br>**Bleaching:** NaClO, 80 °C, 45 min.<br>**Acid hydrolysis:** 2.5 N HCl, (105 ± 2) °C, 45 min. | FTIR, Raman, XRD, SEM, TGA | (Abu-Thabit et al., 2020) |

| | | | |
|---|---|---|---|
| Waste cotton fibres<br>[Cellulose ~95-99% (w/w)] | 0.0-1.0 mol/L HCl, 110–170 °C. | SEM, TGA, XRD, FTIR, contact angle testing | (Shi et al., 2018) |
| Soybean hulls | **Reactive extrusion:** NaOH and $H_2SO_4$ subsequently, 110 °C. | FTIR, SEM, TGA, XRD, $^{13}C$ CP MAS NMR, water sorption isotherm | (Merci et al., 2015) |
| Oil palm empty fruit bunch | **Bleaching:** 15% (v/v) acidified NaClO, 80 °C, 2 h.<br><br>**Alkaline treatment**: 17.5% (w/v) NaOH, room temperature, 2 h.<br><br>**Acid hydrolysis:** $H_2SO_4$ [45%, 55% and 65%(v/v)], 45 °C, 45 min. | XRD, FTIR, TEM | (Pujiasih et al., 2018) |
| Pomelo peel | **Alkaline treatment and bleaching:** 4 wt% NaOH and 0.9% (v/v) $H_2O_2$, 80 °C, 4 h. 80% acetic acid and 68% $HNO_3$, 100 °C, 15 min.<br><br>**Acid hydrolysis:** 6 wt% HCl, 90 °C, 100 min. | FTIR, XRD, SEM, TGA, | (Liu et al., 2018) |
| Corn husk fibres<br><br>[Cellulose 50–55 wt%, Hemicellulose 39.4 wt%, Lignin 7.5 wt%] | **Pre-treatment:** 10 wt% NaOH, 120 °C, 60 min. 0.1% (w/v) acetic acid and anaerobic consortium (30 days old).<br><br>**Bleaching:** 0.3% (w/v) $H_2O_2$, 0.1% (w/v) NaOH and 0.15% (w/v) sodium silicate, 80 °C, 60 min.<br><br>**Acid hydrolysis:** 2.5 N HCl. | SEM, FTIR, XRD, Differential Scanning Calorimetry | (Kambli et al., 2017) |
| Sugarcane bagasse<br><br>[Cellulose 45–50 wt%] | **Alkaline treatment:** 10% (w/v) NaOH, 80 °C, 4 h.<br><br>**Bleaching:** 10% (v/v) $H_2O_2$ and 0.5 M NaOH, 60 °C, 2 h.<br><br>**Hydrolysis:** 4 M HCl, 80 °C, 1 h. | FTIR, XRD, FE-SEM | (Thiangtham et al., 2020) |

| | | | |
|---|---|---|---|
| Sago seed shells<br><br>[α-Cellulose 36.5 ± 1 wt%, Hemicellulose 22.5 ± 1 wt%] | **Dewaxing:** Ethanol and toluene (2:1), 5 h.<br><br>**Bleaching:** 0.7% (w/v) $NaClO_2$, 80 °C, 5 h, pH 5 and 17.5% (w/v) NaOH, 1 h.<br><br>**Acid hydrolysis:** 2.5 N HCl, boiling temperature, 15 min. | FTIR, TGA, XRD, SEM, TEM, AFM | (Naduparambath & Purushothaman, 2016) |
| Rice straw | **Alkali treatment:** 4% (w/v) KOH, microwave irradiation, 60 °C, 30 min, and 2.5% (v/v) $H_2O_2$, 45 °C, 10 min.<br><br>**Acid treatment:** Acetic acid, microwave irradiation, 60°C, 30 min.<br><br>**Preparation of MCC:** 12% (v/v) HCL, 50 °C, 30 min, microwave irradiation. 4% (w/v) NaOH, microwave irradiation, 60 °C, 10 min. | FTIR, XRD, SEM | (Fan et al., 2017) |
| Wheat Straw | **Dewaxing:** Methanol and hexane, 6 h.<br><br>**Delignification:** 2 wt% NaOH, 2 h.<br><br>**Bleaching:** 0.7 wt% $NaClO_2$, 1 h.<br><br>**Acid hydrolysis:** i) 64% (v/v) $H_2SO_4$ at 40 °C.<br><br>ii) 2.5 N HCL, 1 h and 64% (v/v) $H_2SO_4$. | SEM, particle size, true density by a gas displacement pycnometer. | (Krivokapić et al., 2020) |
| Corncob<br><br>[Cellulose 44.1 wt%] | **Chemical treatment:** 1 mol/L HCl, 90 °C, 1 h and acetic acid, $NaClO_2$, 75 °C, 1 h. | SEM, laser particle size analyser, XRD, FTIR, $N_2$-sorption | (Shao et al., 2020) |

From **Table 1.1**, it was observed that MCC is mostly prepared using the conventional acid-base methods. Various advanced techniques like reactive extrusion, microwave irradiation, hydrothermal method, ultrasound assisted method and steam explosion are also being employed nowadays. Most of the methods involve an efficient pretreatment of the biomass for the removal of the outermost lignin barrier for the exposure of cellulose and hemicellulose towards further treatments and the reaction conditions of different methods are varied depending on the biomass type (Haldar & Purkait, 2020a). To modify the properties of the natural fibres present in waste biomass, both physical and chemical treatments are frequently used. Chemical treatment improves the strength and surface geometry of the fibres (Arsyad et al., 2015), whereas physical treatment mainly leads to reduction of size and increase in surface area of the biomass manifesting decrease in the degree of polymerization. Physical pretreatment is anticipated by non-thermal plasma, ultrasound, microwave, and mechanical comminution such as milling, chipping, and grinding (Haldar & Purkait, 2020a; Halder et al., 2019).

The various steps involved with the conventional preparation of MCC are illustrated in **Fig. 1.1**. From the figure, it is seen that initially the raw biomass is subjected to preliminary treatment such as washing/boiling with distilled water, drying, grinding, and screening to remove the surface contaminants or soluble impurities for the formation of powdered biomass with uniform particle size. In the next step, the biomass is treated with alkali which effectively removes lignin, hydrolyses hemicellulose, and subsequently reduces the polymerization of cellulose. Delignification is followed by bleaching for further purification of the biomass. The final step i.e. acid hydrolysis is performed to depolymerize the waste biomass to produce MCC. The most commonly

used chemical reagents for alkaline delignification are NaOH (Abu-Thabit et al., 2020; Zhao et al., 2018) and KOH (Fan et al., 2017). Bleaching is usually carried out employing $NaClO_2$, NaClO, $H_2O_2$ and acetic acid. For acid hydrolysis, $H_2SO_4$ (Rashid et al., 2017; Zhao et al., 2018) and HCl (Abdul Khalil et al., 2018; Baruah et al., 2020) are mostly employed.

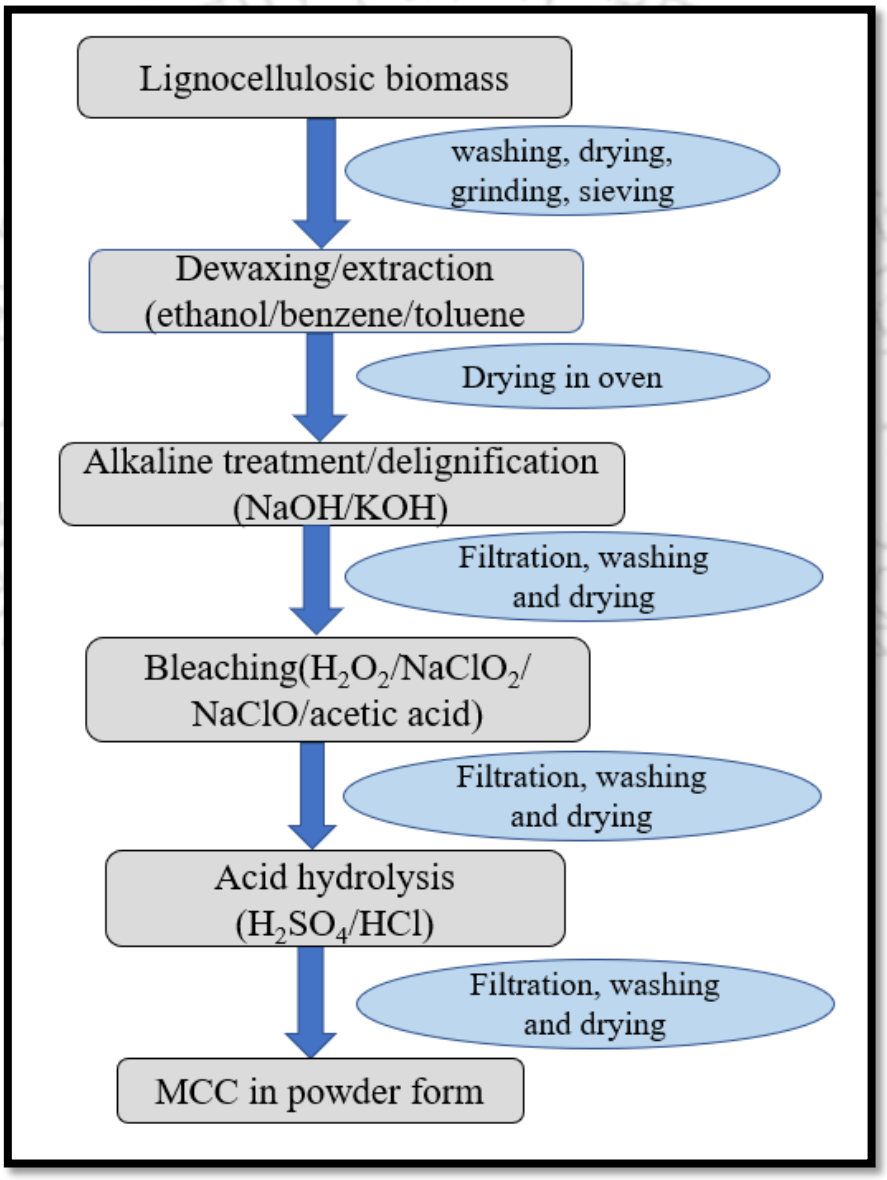


**Figure 1.1** Flowchart of conventional MCC synthesis from lignocellulosic biomass

The mechanism involved in acid hydrolysis process is illustrated in **Fig. 1.2**. During acid hydrolysis of the bleached biomass, $H^+$ ions from acid moves towards the amorphous regions present in cellulose, easily attacks them to break the 1,4-β-glycoside linkages and forms multiple hydronium ions ($H_3O^+$). As the glycosidic bonds disintegrate, the amorphous structure of cellulose starts to decay, while the crystalline areas of cellulose remain intact as they exhibit higher resistance towards acid attack, thus leading to the formation of microcrystalline cellulose (MCC) (Trache et al., 2016; Xie et al., 2018).

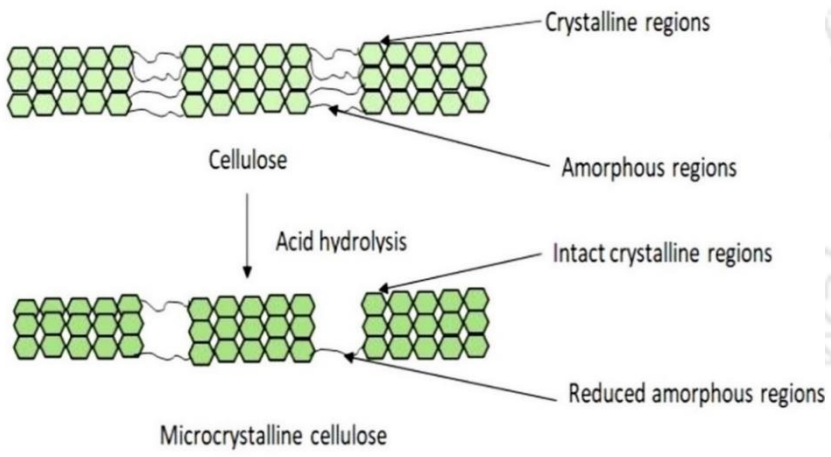


**Figure 1.2.** Mechanism involved in acid hydrolysis of cellulose.

Recently many studies are reported on the modification of the conventional methods. In this view, Ventura-Cruz et al. (Ventura-Cruz et al., 2020) demonstrated the synthesis of MCC from rose stems through successive delignification by using alkaline hydrogen peroxide ($H_2O_2$) and obtained MCC with enhanced thermal stability and higher degree of crystallinity (DC). This method is advantageous over the conventional techniques as

it doesn't involve acid hydrolysis, high temperature or high pressure. The increase in DC of the synthesized MCC indicates that, alkaline peroxide efficiently removed the non-cellulosic fraction, particularly lignin from the biomass. Alkaline hydrogen peroxide treatment without using concentrated acids can produce MCC with properties comparable to those synthesized by acid hydrolysis (Kuznetsov et al., 2018; Ventura-Cruz et al., 2020).

### 1.8.2. Potential applications of microcrystalline cellulose in packaging materials

Microcrystalline cellulose reinforced polymer composites are found very useful for packaging applications. Polypropylene composite embedded with MCC can be used effectively as packaging material for microwave application. MCC was isolated from cotton and incorporated into polypropylene matrix by using a brabender internal mixer while employing maleic anhydride as coupling agent. The addition of 20 wt% MCC into the polymer matrix remarkably improved the thermal and mechanical properties of the composites and provided the features of microwavable packaging (Ummartyotin & Pechyen, 2016). Wang et al. produced multilayer polyethylene terephthalate (PET) bottles with edible films for packaging of rosebud beverages. The edible films with superior mechanical proprieties were prepared by blending chitosan, MCC, whey protein isolate and PET together. The produced PET bottles showed significantly enhanced barrier performance by preventing the loss of polyphenols, improved the soluble solids content, color indices, pH and browning degree of the beverages and extended the beverage shelf life by 38 days when stored at 4 °C (Z.-C. Wang et al.,

2021). Chen et al. prepared MCC filled thermoplastic starch composites for packaging material. MCC was introduced into the starch matrix through extrusion and hot pressing-technique and the composite films with 6 wt% MCC possessed better tensile strength and water vapor permeation with lower water contact angle than that of the neat films (Chen et al., 2020).

### 1.8.3. Cellulose reinforcement in starch-based packaging films

Several cellulosic materials have been utilized for enhancing the packaging performance of corn starch films. Reinforcement with cellulose fibers extracted from rice and coffee husk in corn starch films significantly improved the various properties of corn starch films desirable for packaging applications such as tensile strength and barrier properties (Collazo-Bigliardi et al., 2019a). Incorporation of cellulose nanofiber significantly enhanced the thermal and water resistance properties of starch films for application as muffin liner (Shih & Zhao, 2021). Yuan and Chen demonstrated the formation of corn starch films with excellent thermal and mechanical properties reinforced with nanocellulose for antibacterial packaging (Yuan & Chen, 2021).

MCC has been found to be effective in improving the properties of cassava starch films for food packaging. Incorporation of MCC increased the tensile strength, opacity and Young's modulus of the starch films, while moisture content, water solubility, elongation at break and water vapour permeability of the films decreased with the addition of MCC (Yao Désiré et al., 2021). Chen et al. incorporated MCC as fillers into the starch matrix of thermoplastic starch and observed increase in the tensile strength with 6 wt% MCC addition, while the water vapour permeation decreased. Water contact

angle also decreased with the increased MCC loading (Chen et al., 2020). Another study demonstrated the synthesis of MCC from soyabean hulls and its application as reinforcement in cassava starch films. The addition of 2.5 wt% MCC led to films with lower solubility, water vapor permeability, hygroscopicity and improved flexibility than pure starch film (Merci et al., 2019).

**Possible scope for further research on the synthesis of microcrystalline cellulose from waste biomass and its application in the packaging field**

It is envisaged from the state of art literatures that most of the methods used for synthesizing MCC from biomass sources involves hydrolysis using concentrated acid. Such conventional preparation of MCC involving acid hydrolysis is not desirable for bulk scale production because acid causes corrosive effects on various plant equipment, making it unfeasible with respect to industrial aspects. The drawbacks of using concentrated mineral acids in MCC production can be eliminated by replacing the acid hydrolysis with alkaline hydrolysis and subsequent treatment with hydrogen peroxide. However, use of alkaline peroxide to extract MCC from biomass sources is rarely reported in the literature. Further, there is no reported work on the synthesis of microcrystalline cellulose from elephant grass biomass. Also, the application of elephant grass-derived MCC for reinforcement in corn starch films is not reported to date. Hence, there is a scope to explore the potential of elephant grass for the synthesis of microcrystalline cellulose and application of the synthesized MCC as reinforcing agents in corn starch films for sustainable and eco-friendly food packaging.

### 1.8.4. Microwave-assisted extraction of microcrystalline cellulose from waste biomass

The extraction of cellulose is a solid-liquid extraction process, and microwave-assisted extraction is considered the best extraction technique for extracting lignin-cellulose components. The conventional cellulose extraction methods have the limitations of poor yield, the requirement of bulk amounts of solvent, and time consumption. The different steps used in the conventional methods of MCC synthesis require high temperatures (75-80 °C) for a long duration of about 2-4 hours (Pujiasih et al., 2018; Sim, Bae, Choi, Islam, et al., 2016; Zhao et al., 2018). Microwave heating is an emerging and advanced technique for matter transfer from plant matrix in a reduced extraction time. Microwave irradiation heating can increase the speed of a chemical reaction even at lower temperatures. The microwave-assisted technique facilitates cell rupturing and the release of components from biomass into the extracting solvent. Mass transfer from the ruptured cells expedites solvent penetration, resulting in the complete extraction of the lingo-cellulosic contents (Rizwan et al., 2021). Therefore, microwave-assisted extraction techniques have gained quite popularity in recent times for the extraction of lingo-cellulosic components from biomass (Azlan et al., 2022; Mao et al., 2023; Singh et al., 2017).

Tea waste (TW) is lignocellulosic, comprising cellulose, hemicellulose, and lignin. Waste tea was reported to contain 16–18% cellulose, 68.2% hemicellulose, and 18.8% lignin. The high cellulose content of tea waste makes it suitable for synthesising crystalline cellulose derivatives (Debnath et al., 2021b). Tea leaves waste obtained from

tea factories was employed as raw material for the synthesis of cellulose nanocrystals, which were then successfully utilized as reinforcement in polymer composites (Abdul Rahman et al., 2017; Handoko & Yusuf, 2021). MCC isolated from oolong tea processing waste was reported to maintain cellulosic structure and good thermal stability. Such tea waste-derived MCC may be used as a stabilizer to fabricate food-grade Pickering emulsion (Zhao et al., 2018; Zheng et al., 2022). Black tea waste reportedly contains high cellulose content of around 28.3%, and it was found to be a promising source for the extraction of cellulose nanocrystals (Xu et al., 2023).

**Possible scope for further research on synthesis of microcrystalline cellulose from tea industry waste using microwave-assisted method**

From the available literature, it is observed that tea waste produced in the industries during tea manufacturing is a readily available, abundant, cellulose-rich, and cheap biomass. However, the utilization of industrial black tea waste for extracting MCC is scant. Furthermore, conventional acid hydrolysis using concentrated sulfuric acid was used in the available literature on the synthesis of MCC from oolong tea waste (Zhao et al., 2018). No work is reported on the use of microwave-assisted alkaline peroxide bleaching technique for the synthesis of MCC from black tea waste. Thus, there is a scope to explore the potential of industrial black tea waste for synthesizing MCC and to investigate the effectiveness of microwave heating during the various treatment steps used for biomass-based MCC synthesis.

### 1.8.5. Polyvinyl alcohol composite films for food packaging

Polyvinyl alcohol is a biocompatible polymer which is extensively utilized in food industry as well as biomedical, domestic, and construction sectors. Considering its nontoxic and safe profile, PVA has earned the generally recognized as safe (GRAS) status, making it suitable for producing food packaging films. However, PVA is deficient in desirable characteristics for materials used in food packaging, such as moisture barrier, mechanical strength, antimicrobial, antioxidant, and UV barrier properties (Nguyen and Lee, 2022). Many inorganic fillers have been used to prepare PVA composites with improved properties. However, poor interfacial compatibility between inorganic fillers and PVA negatively affects some properties such as mechanical behaviour of the composites. Moreover, incorporation of expensive inorganic fillers diminishes the biodegradability of PVA composite films. To fabricate environment-friendly biodegradable food packaging materials, green resources like biomass derived fillers are highly desirable to substitute the inorganic fillers (Baite et al., 2022).

As discussed earlier, cellulose fibres have received widespread interest as fillers in composite films because of their abundant natural availability, environment-friendliness, biodegradability, biocompatibility, renewability, and remarkable mechanical strength. Various cellulosic materials including cellulose microfibers (Puttaswamy et al., 2017a), cellulose nanofibers (Ueda et al., 2022), cellulose nanocrystals (Aloui et al., 2016) were successfully incorporated as reinforcement into the polymer matrix of PVA films to enhance the performance of PVA films in terms of

thermal, mechanical, and barrier properties, thus producing green composites for food packaging. Improvement of structural properties and mechanical strength of PVA was attained from cellulose microfibers reinforcement (Puttaswamy et al., 2017b). Cellulose extracted from corn husk fibres increased the tensile strength of PVA film by about 29% in comparison to neat PVA due to the formation of strong hydrogen bonding between PVA and cellulose fibres (Ratna et al., 2023). Cellulose nanofibers synthesized from wheat straw improved the surface hydrophobicity, thermal stability and tensile strength of PVA composite films considerably (Yang et al., 2020). Ulaganathan et al. prepared PVA and cellulose nanocrystal blended film. The bio-nanocomposite films maintained high transparency level (transmittance of ~90% in the visible region in UV–vis), suggesting their effectiveness for food packaging (Ulaganathan et al., 2022). Tummala et al. developed a highly transparent macroporous hydrogel with more than 90% water content by combining PVA and nanocellulose. Due to the addition of nanocellulose, the composite hydrogel had a refractive index close to water and showed excellent UV blocking property (Tummala et al., 2016). Rice straw derived cellulose microfibrils and cellulose nanofibrils were incorporated as reinforcement into PVA matrix. The rice straw cellulose nanofibrils/PVA composite films exhibited more uniform fibre dispersion, better mechanical properties, and transparency. However, the rice straw cellulose microfibrils/PVA composite films showed stronger water resistance i.e., hydrophobicity than the nanofibril/PVA composite films. Both the cellulose microfibril and nanofibril reinforced PVA films showed improved thermal stability (Z. Wang et al., 2018).

Feng et al. reported the reinforcement of rice straw derived cellulose microfibers in PVA films. The composite film showed significantly higher mechanical strength (37.54 ± 0.77 MPa) as compared to pure PVA (25.88 ± 2.97 MPa) film. In addition to that, the prepared composite films had a transmittance of over 80% in the visible light range, and exhibited excellent UV blocking property. However, strengthening of PVA films using cellulose microfibers with larger size was found to be difficult (Feng et al., 2022).

**Possible scope for further research on the application of black tea waste derived microcrystalline cellulose as reinforcement in food packaging films**

It was observed from the available literatures that, despite having excellent film forming ability, the application of PVA films in food packaging sector is restricted due to its low mechanical strength, poor moisture barrier and UV-blocking properties. Cellulose nanofibers and cellulose nanocrystals are widely used as reinforcement in PVA films. However, utilization of biomass derived microcrystalline cellulose as reinforcement/filler in PVA composites is scant. Therefore, studies on the reinforcement effect of MCC in PVA composites need further research. Application of black tea waste derived MCC in the packaging sector has not reported yet. Thus, there is a scope for research on how the incorporation of tea waste microcrystalline cellulose influences the physicochemical characteristics of PVA films used for food packaging.

## 1.9. Objectives of thesis work

Based on the above state of the art literature review and scope of possible work, the objectives of this thesis work are identified as below:

- Extraction of microcrystalline cellulose from elephant grass (*Pennisetum purpureum*) using alkaline hydrogen peroxide and its application as reinforcement/filler materials in corn starch films for food packaging
- Preparation and characterization of microcrystalline cellulose from tea industry waste by a novel microwave-assisted technique
- Application of tea waste derived microcrystalline cellulose as reinforcing fillers in PVA films for grapes preservation

## 1.10. Organization of the thesis

**Chapter 1** discusses the background of the problems undertaken in this work i.e. the research gap associated with the synthesis of microcrystalline cellulose from lignocellulosic waste biomass sources and their applications in the packaging sector. The objectives of the present work are also highlighted here. **Chapter 2** gives a detailed description of the experiments involved in the synthesis of microcrystalline cellulose from the waste lignocellulosic biomass of elephant grass by a non-conventional technique using alkaline hydrogen peroxide. The physicochemical characteristics of the synthesized product were investigated and compared with commercially available microcrystalline cellulose. The elephant grass derived microcrystalline cellulose was incorporated into corn starch films and its reinforcing effect on the packaging properties of the starch films were inspected. **Chapter 3** gives a complete description of the experimentation involved in the preparation of microcrystalline cellulose from industrial black tea waste under microwave heating and also under conventional heating. The synthesized products were characterized for various properties using different

techniques. Response surface methodology (RSM) analysis was carried out to optimize the experimental conditions for achieving highest crystallinity of the synthesized tea waste microcrystalline cellulose. **Chapter 4** describes the development of tea waste microcrystalline cellulose reinforced PVA composites for application as food packaging. The various physical and chemical properties of the fabricated films that are desirable for packaging application were observed using different analytical techniques. The packaging performance of the composite films were evaluated by wrapping fresh grapes samples with the films and observing the change in their visual appearance for a period of 20 days. **Chapter 5** summarizes the inferences drawn from the different works and provides some suggestions towards future research.

# Chapter 2

# Synthesis of microcrystalline cellulose from elephant grass and its application as reinforcement in corn starch films for food packaging

*This chapter gives a complete description of the experimentation involved and results thereon in the synthesis of microcrystalline cellulose from elephant grass (Pennisetum purpureum) through successive bleaching with alkaline hydrogen peroxide. The synthesized MCC was then characterized using X-ray diffraction (XRD), Fourier transforms infrared spectroscopy (FTIR), Field emission scanning electron microscopy (FESEM), and Thermogravimetric analysis (TGA). Thereafter, the elephant grass microcrystalline cellulose (E-MCC) was introduced as filler material into corn starch films which were characterized using FTIR and FESEM for physicochemical properties, and their performance was analyzed in terms of thermal stability (TGA), contact angle measurement, moisture content, water solubility and tensile strength (Universal testing machine, UTM). The background of this work is elaborated in Chapter 1, Section 1.3, 1.4, 1.5, and details of literature and the scope of work are summarized in chapter 1, Section 1.7.1, 1.7.2 1.7.3. This work has been scientifically acknowledged in the Food Packaging and Shelf Life.*

## 2.1 Experimental

### 2.1.1. Materials

Elephant grass was collected from the campus of the Indian Institute of Technology Guwahati, Assam, India. The raw biomass was dried at 60 °C for 48 h in a hot air oven, crushed into small pieces using a mixer-grinder, and screened through a mesh to obtain particles of uniform size 300-400 μm. Sodium hydroxide (SRL, India), hydrogen peroxide 30% (SRL, India), and ethanol 99.9% (Sigma Aldrich) were used for MCC synthesis. Corn starch (CS) was purchased from HiMedia, and glycerol was provided by Merck, India. All the chemicals used in this present work are of analytical grade. Deionized (DI) Milli-Q water was used throughout the experiments, including preparing the solutions and washing the samples.

### 2.1.2. Synthesis of elephant grass microcrystalline cellulose (E-MCC)

MCC was synthesized from elephant grass through successive bleaching with alkaline peroxide following the method reported by Ventura-Cruz and Tecante (Ventura-Cruz & Tecante, 2019) with some modifications. Around 10 g of dried and powdered elephant grass was dewaxed using ethanol at 80 °C for 5 h in a Soxhlet extractor with a material to solvent ratio of 1:20. Afterward, the sample was oven-dried at 50 °C until a constant weight was reached. The dewaxed sample was then subjected to alkaline treatment by mixing with 45 g/L of NaOH solution at a solid/liquid ratio of 1:12 and hydrolyzed at 80 °C for 2 h. The sample was placed in an ice bath to terminate the reaction, followed by filtration, and washing with DI water many times to achieve neutral pH. The

obtained solid was then oven-dried at 50 °C until the weight became constant. The alkaline treated sample was bleached with a mixture of 50 g/L NaOH and 160 g/L $H_2O_2$ at a solid/liquid ratio of 1:20 and hydrolyzed at 55 °C for 90 min. The treated sample was filtered and repeatedly washed using DI water until neutrality. The solid residue was oven-dried at 50 °C for 15 h to obtain a constant weight. Bleaching treatment was repeated one more time following the same procedure mentioned above to obtain the E-MCC. The pictorial representation of the synthesis process is shown in **Fig. 2.1.**

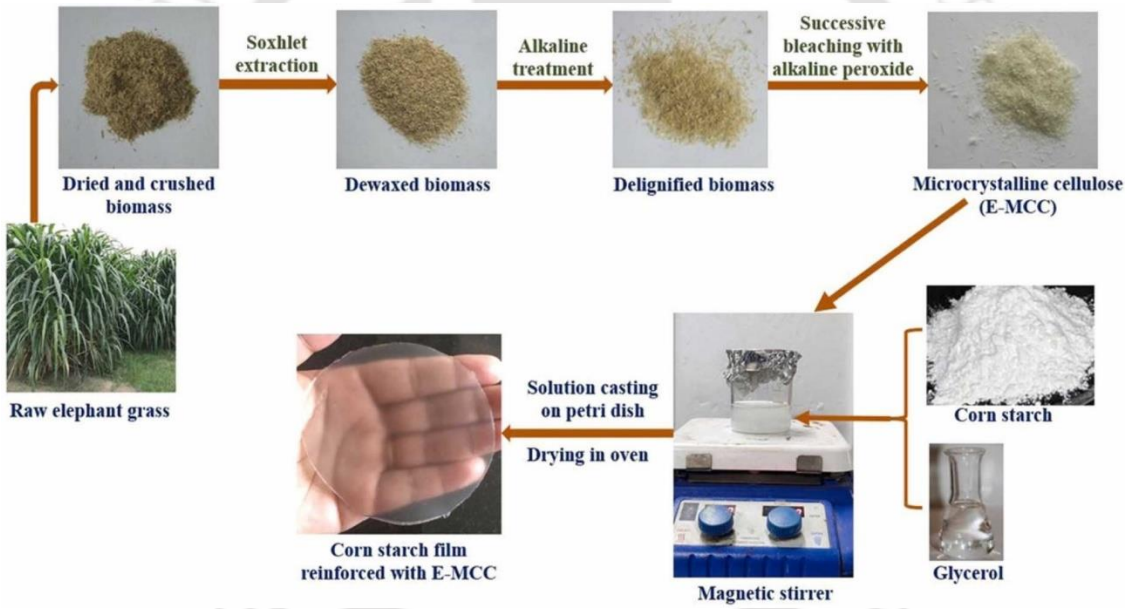


**Figure 2.1** Schematic representation of synthesis of microcrystalline cellulose from elephant grass and its incorporation into corn starch film

## 2.1.3. Preparation of MCC reinforced corn starch films

Corn starch films were prepared through solution casting according to the methods reported by others (Wang, Sui, et al., 2021; Yao Désiré et al., 2021) with some modifications in the heating temperature, stirring speed, and duration. For preparing

neat corn starch film, 4 g starch was dissolved in 100 mL DI water, heated gradually from room temperature to 90 °C, and stirred continuously at 800 rpm for 30 min using a magnetic stirrer. Thereafter, 25% glycerol (on the basis of dry starch weight) was added to the solution as a plasticizer since glycerol has good compatibility with amylose, which stimulates better mechanical properties and makes starch films flexible as well as feasible for packaging. The mixture was then stirred for another 30 min until complete gelatinization of the starch was achieved. The solution was then sonicated using an ultrasonication probe (Sonics, Model: VC 750, 20 kHz) at 30% amplitude for 10 min for the removal of air bubbles. Finally, 50 mL of the solution was poured onto a glass petri plate, followed by drying at 30 °C for 48 h. For the preparation of the MCC reinforced films, E-MCC powder of 1, 2.5, and 5 wt% (starch dry weight basis) were added to 100 mL of DI water separately and kept under constant stirring at 700 rpm for 24 h. Following that, 4 g of corn starch was added to each of the solutions, and the same procedure was used as mentioned above to prepare the neat starch film. All the films were peeled off from the petri dishes after drying and stored in a desiccator at 25 °C and 50% relative humidity (RH) for 5 days before further analysis. The corn starch films reinforced with 1, 2.5, and 5 wt% E-MCC are denoted as CS/EMCC-1, CS/EMCC-2.5, and CS/EMCC-5, respectively.

## 2.2. Characterization of the products obtained

The synthesized E-MCC and the corn starch/E-MCC composite films were characterized using various techniques as follows:

### 2.2.1. Determination of MCC yield

The yield of E-MCC was calculated based on its weight over the cellulose present in the untreated elephant grass and expressed in terms of percentage (Zhao et al., 2018).

### 2.2.2. X-ray diffraction (XRD)

The structural configuration of the prepared E-MCC was investigated by XRD pattern, using an X-ray diffractometer (Rigaku technologies, Japan; Model: Smartlab) operated at 112 mA and 45 kV. The sample was scanned through Cu Kα radiation for the diffraction angle (2θ) range of 10–90° with a step size of 0.01°. The crystallinity index (CrI) of the E-MCC was estimated by means of the following equation as reported by Zhao et al. (Zhao et al., 2018).

$$CrI = \frac{I_{002} - I_{am}}{I_{002}} \times 100 \quad (2.1)$$

Where, $I_{002}$ is the maximum intensity of the crystalline phase of MCC at 2θ = 22.5°, while $I_{am}$ is the intensity of the amorphous phase at 2θ = 18° (Tarchoun et al., 2019; Zhao et al., 2018).

### 2.2.3. Fourier-transform infrared spectroscopy (FTIR)

The functional groups present in the synthesized E-MCC were identified by analyzing the material in the 4000–400 $cm^{-1}$ region of the FTIR spectrum (Perkin Elmer, Model: Spectrum two).

### 2.2.4. Field emission scanning electron microscopy (FESEM)

The morphology of the prepared E-MCC and corn starch/E-MCC composite films were analyzed by using FESEM (Zeiss, Model: Sigma 300) operated at an accelerating voltage of 5 kV. The dried samples were placed on an aluminium stub and sputtered-coated with gold for 5 min before the analysis. Scanning was performed at 1000x magnification for E-MCC and 2000x magnification for the starch films.

### 2.2.5. Thermogravimetric analysis (TGA)

The thermal properties of the E-MCC and corn starch/E-MCC composite films were analyzed using a Thermogravimetric analyzer (Netzsch, Model: STA449F3A00) in an inert argon atmosphere (at a flow rate of 20 mL/min). The samples were heated from ambient temperature (25 °C) to 600 °C with a heating rate of 10 °C/min.

### 2.2.6. Thickness of the films

The thickness of the E-MCC reinforced corn starch films was measured by a digital micrometer (Baker, India, Model: IP65) with 1 μm accuracy. For each sample, the thickness was measured at 10 arbitrary locations, and the average value was then used to determine the mechanical properties of the bioplastic starch films (Wang, Sui, et al., 2021).

### 2.2.7. Water contact angle measurement

To investigate the wettability or hydrophobic property of the corn starch composite films, water droplet contact angle was measured using a contact angle analyzer (Holmarc, Model: HO-IAD-CAM-01B). The films were cut into 2 cm × 2 cm squares,

and 5 μL DI water was deposited on the sample surface. After 1 min, images were recorded. For each sample, three measurements were taken, and the average of the three values was reported.

### 2.2.8. Moisture content

The moisture contents of the E-MCC reinforced corn starch films were determined by the gravimetric method as described by Wang et al. (Wang, Sui, et al., 2021; Wang, Yan, et al., 2021). The films were cut into 2 cm × 2 cm square pieces, and their initial weight was noted as $M_1$. Thereafter, the samples were dried in an oven at 110 °C for 24 h, weighed again, and noted as $M_2$. Moisture content (MC) was then calculated using the following formula:

$$MC = \frac{M_1 - M_2}{M_1} \times 100\ \% \quad (2.2)$$

The results are expressed as the average values ± standard deviation of the measurements taken from three different film samples.

### 2.2.9. Water solubility

Solubility of the prepared E-MCC/corn starch composite films in water were investigated according to the method described by Wang et al. (Wang, Yan, et al., 2021). 2 cm × 2 cm square pieces of the films were precisely weighed ($M_3$) using an analytical balance and placed in conical bottles. After that, 100 mL of DI water was added to the sample and stirred in a shaker at a constant speed of 180 rpm, at 25 °C for 6 h. Finally, the solutions were filtered and dried at 110 °C for 7 h, and the samples were weighed again ($M_4$). The film solubility (WS) was calculated as follows:

$$WS = \frac{M_3 - M_4}{M_3} \times 100\ \% \quad (2.3)$$

The results are expressed as the average values ± standard deviation of the measurements taken from three different film samples.

### 2.2.10. Mechanical properties analysis

Mechanical properties of the E-MCC reinforced corn starch films, such as tensile strength, Young's modulus, and elongation at break, were determined using a Universal testing machine (5kN electromechanical UTM, ZwickRoell, Model: Z005TN Proline) at room temperature. The films were cut into rectangular strips of size 1 cm × 5 cm. The initial grip separation was 30 mm, and the samples were loaded at a crosshead speed of 10 mm/min. The measurements of each of the samples were performed in triplicates, and the reported values are the average ± standard deviation.

## 2.3. Results and discussion

### 2.3.1 Characterization of the synthesized E-MCC

#### 2.3.1.1. E-MCC yield

The compositional analysis of the raw elephant grass was performed in one of our previously reported works (Haldar & Purkait, 2020). The percentage composition of various components is given in **Table 2.1**. From the table, it was observed that the raw biomass contains 34.7 wt% of cellulose. The amount of cellulose in 10 g of elephant grass was 3.47 g. The dry weight of the MCC produced after the second bleaching step is 3.099 g. Therefore, the yield of E-MCC is calculated as follows:

$$Yield = \frac{Weight\ of\ the\ MCC\ produced}{Weight\ of\ cellulose\ in\ the\ raw\ elephant\ grass} \times 100\% \quad (2.4)$$

$$= \frac{3.099}{3.47} \times 100\%$$

$$= 89.31\%$$

**Table 2.1** Chemical composition of elephant grass based on dry weight % (w/w)

| Biomass | Cellulose | Hemicellulose | Lignin | Moisture Content | Extractives | Ash |
|---|---|---|---|---|---|---|
| Elephant grass | 34.7% | 20.2% | 19.3% | 12.4% | 6.4% | 4.9% |

**2.3.1.2. Determination of crystalline structure**

The crystalline structure of commercial MCC (C-MCC) and elephant grass MCC (E-MCC) was explored using XRD analysis. Their X-ray diffraction patterns are illustrated in **Fig. 2.2**. The synthesized E-MCC showed a similar crystalline pattern to the C-MCC. The appearance of the peaks in the diffraction pattern indicates the polycrystalline structure of the MCCs. The peaks occurring at a diffraction angle (2θ) values of 15.7°, 22.5°, and 34.6° correspond to the crystalline planes $1\bar{1}0$, 200, and 004, respectively. The XRD patterns indicated the presence of cellulose I polymorph, whereas the absence of doublet crystalline peak at 22.6° showed that no cellulose type II was present in C-MCC and E-MCC (Tarchoun et al., 2019; Ventura-Cruz et al., 2020). The crystallinity index of the C-MCC was calculated as 80%, and the synthesized E-MCC was found to have a crystallinity index of 74%. Therefore, it is evident that the MCC synthesized

from elephant grass is comparable to C-MCC, which makes it a promising candidate for commercial applications.

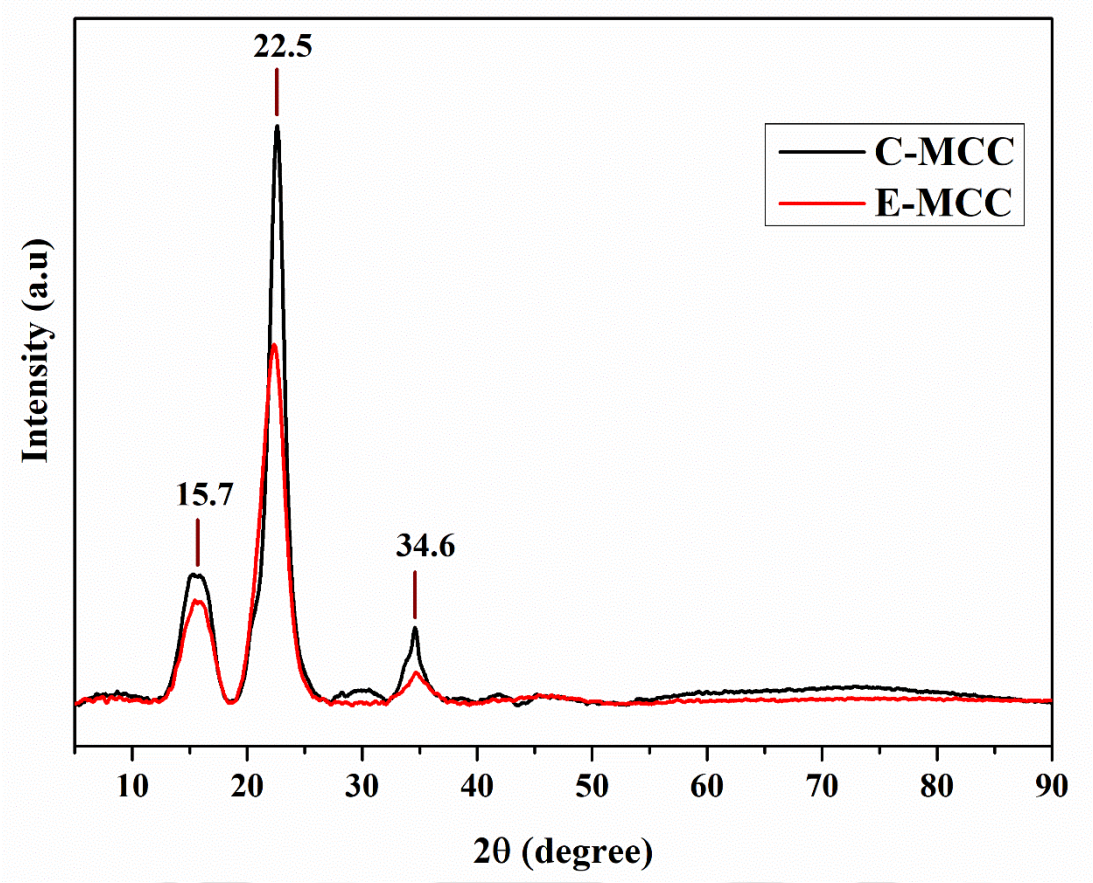


**Figure 2.2** XRD patterns of commercial microcrystalline cellulose (C-MCC) and elephant grass microcrystalline cellulose (E-MCC)

### 2.3.1.3. Analysis of chemical functionality

The FTIR spectra of C-MCC and E-MCC are presented in **Fig. 2.3**. The absorption peak at 3331cm$^{-1}$ is due to the stretching vibration of the O–H bond present in native cellulose. The absorption band around 2899 cm$^{-1}$ may be attributed to the symmetric stretching of the C–H bond of alkyl groups (Castillo et al., 2017). The absorbance peak at 1641 cm$^{-1}$ is related to the –OH bending of absorbed water and bending of the C=O

bond of the aldehyde groups (Liu et al., 2018; Rashid et al., 2017). The band at 1429 $cm^{-1}$ is contributed by symmetric bending vibration of the $–CH_2$ group, which is also termed as 'crystallinity band' (Hou et al., 2019; Rashid et al., 2017).

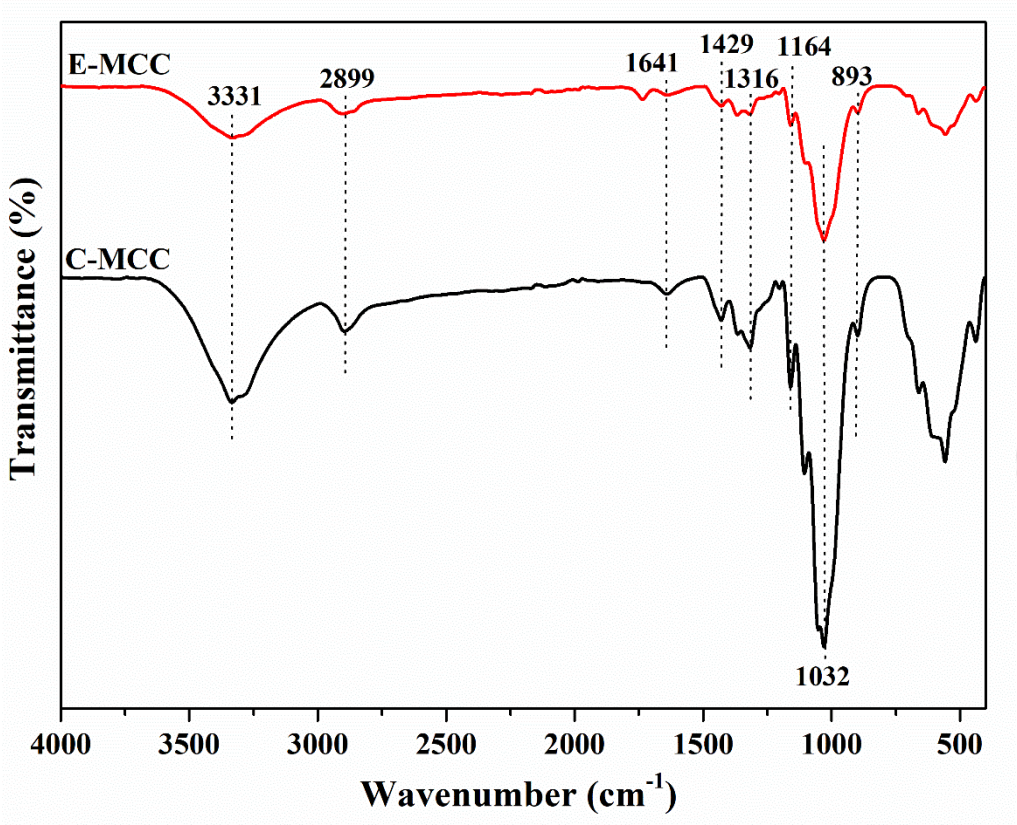


**Figure 2.3** FTIR spectra of commercial microcrystalline cellulose (C-MCC) and elephant grass microcrystalline cellulose (E-MCC)

The peak located around the 1316 $cm^{-1}$ may be ascribed to the skeletal vibration of C–O, and C–C groups, the band appearing at 1164 $cm^{-1}$ was attributed to C–O stretching vibration in the cellulose (Liu et al., 2018). The MCCs showed a strong peak at 1032 $cm^{-1,}$ which was associated with the stretching vibration of C–O–C pyranose ring skeleton and the peak at 893 $cm^{-1}$ is due to the β-1,4-glycosidic linkages in cellulose (Pujiasih et al., 2018; Rashid et al., 2017). The disappearance of characteristic

absorption peaks of lignin (1520 –1510 $cm^{-1}$) and hemicellulose (1730 –1720 $cm^{-1}$) in the FTIR spectrum of E-MCC showed that successive bleaching with alkaline $H_2O_2$ could efficiently remove the non-cellulosic constituents (lignin, hemicellulose) of elephant grass (Liu et al., 2018). The findings reveal that the synthesized E-MCC has a similar chemical structure as C-MCC.

#### 2.3.1.4. Morphology analysis

The morphology of the raw elephant grass (EG), C-MCC, and the synthesized E-MCC were studied using FESEM analysis, and the microscopic images are shown in **Fig. 2.4**. From the figure, it was seen that the raw elephant grass had a long, thick, closed, and almost non-porous fibrous structure with a smooth surface (**Fig. 2.4a**). The fibers became thinner, more exposed, and disruptive in nature with a rough surface in the E-MCC (**Fig. 2.4c**) after performing successive bleaching with alkaline peroxide because of the elimination of the lignin layer around the fibers. Similar outcomes were witnessed by Ventura-Cruz et al. (Ventura-Cruz et al., 2020). The rough surface of the E-MCC may be attributed to the cleavage of the amorphous regions of cellulose and thereby breaking the fibers into a shorter length, resulting in comparatively weaker interaction that formed cracks on the surface, making it rough (Zhao et al., 2018). **Fig. 2.4b** shows that C-MCC had rod-shaped structures having shorter lengths and smooth surfaces. The diameter of the particles of E-MCC ranged from 15-48 μm, with an average particle diameter of 29 μm. The particle size of the E-MCC is a little larger compared to the commercial one. The results reveal that the various properties of the synthesized E-MCC, like the size of particles and accumulation, were influenced by the

raw materials employed and the environmental condition present during the synthesis (Liu et al., 2018). However, the structural or morphological features of the E-MCC were found to be comparable to that of the C-MCC, indicating that this method of MCC synthesis can be useful in terms of the commercial aspect also.

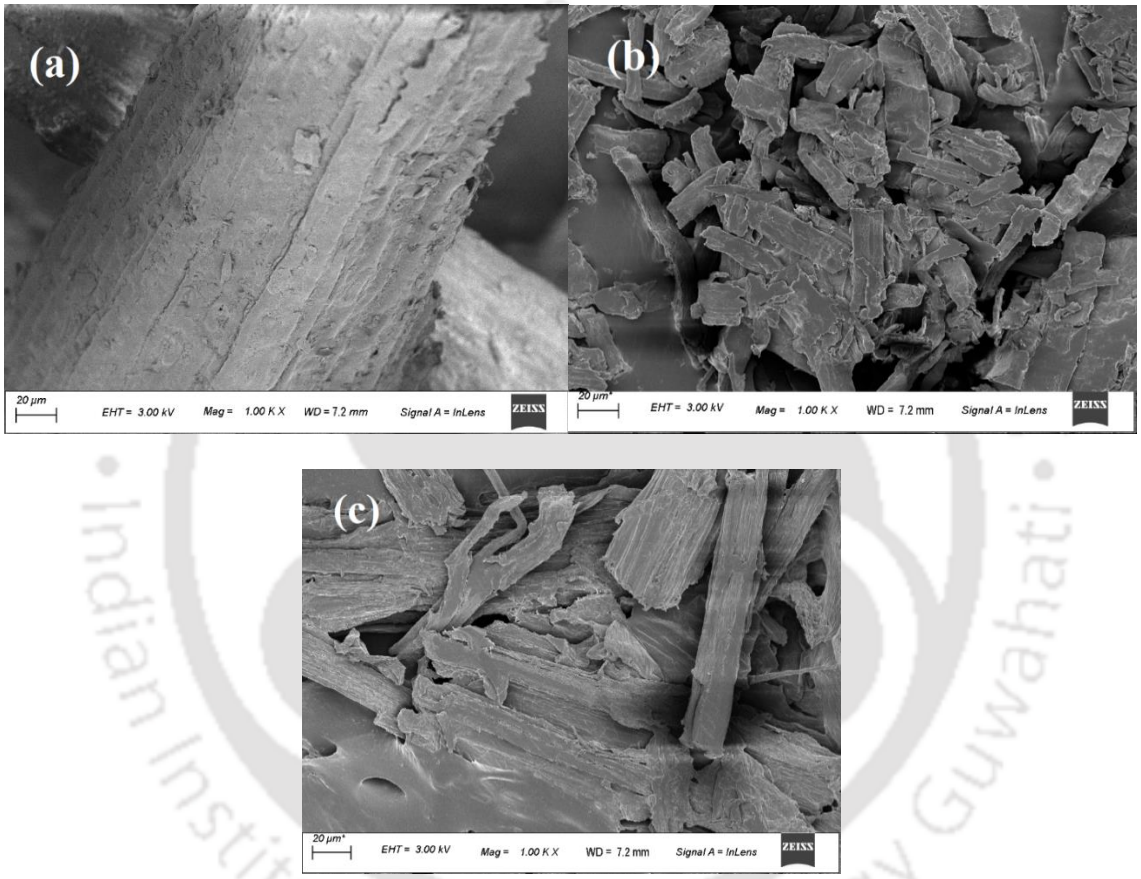


**Figure 2.4** FESEM images of **(a)** Raw elephant grass, **(b)** C-MCC, and **(c)** E-MCC

### 2.3.1.5. Analysis of thermal properties

The thermogravimetric analysis (TGA) and the derivative thermogram (DTG) curves of raw EG and the synthesized E-MCC are illustrated in **Fig. 2.5**. It was seen from **Fig. 2.5a** that the thermal decomposition of EG and E-MCC occurred in two phases. Initially, some loss of weight occurred in the temperature range of 35-100 °C, which is

attributed to the evaporation of moisture from the samples. The main thermal degradation stage was in the temperature range of 240-400 °C, which corresponds to the decomposition of cellulose and hemicellulose via depolymerization, decarboxylation, dehydration, and breaking of glycosyl units (Hou et al., 2019; Liu et al., 2018; Ventura-Cruz et al., 2020). The raw elephant grass started to decompose at around 245 °C, while the degradation of E-MCC started at around 285 °C. The results indicate that consecutive bleaching enhanced the thermal stability of the synthesized E-MCC as compared to the raw biomass, which is due to the absence of amorphous components like lignin and hemicellulose in the E-MCC. Both lignin and hemicellulose were reported to have lower degradation temperatures with respect to cellulose. Liu et al. reported that the thermal decomposition of commercial MCC starts at around 291 °C (Liu et al., 2018). Hence, it is obvious that the thermal behaviour of the synthesized E-MCC is comparable to C-MCC. The maximum weight loss for raw elephant grass was observed at 331 °C, which was lower as compared to the E-MCC, for which maximum weight loss occurred at 369 °C, indicating that the cellulose in the E-MCC is of higher purity. This result also implies that the degree of molecular ordering in E-MCC is higher, because of which more amount of heat is required to cause its thermal degradation (Kian et al., 2017). As shown in the DTG curve (**Fig. 2.5b**), the raw biomass showed a lower degradation temperature peak with the maximum value at around 330 °C, while the E-MCC exhibited a maximum temperature peak at around 370 °C. The DTG curve of the raw biomass also shows a peak at around 290 °C, which is associated with the decomposition of hemicellulose.

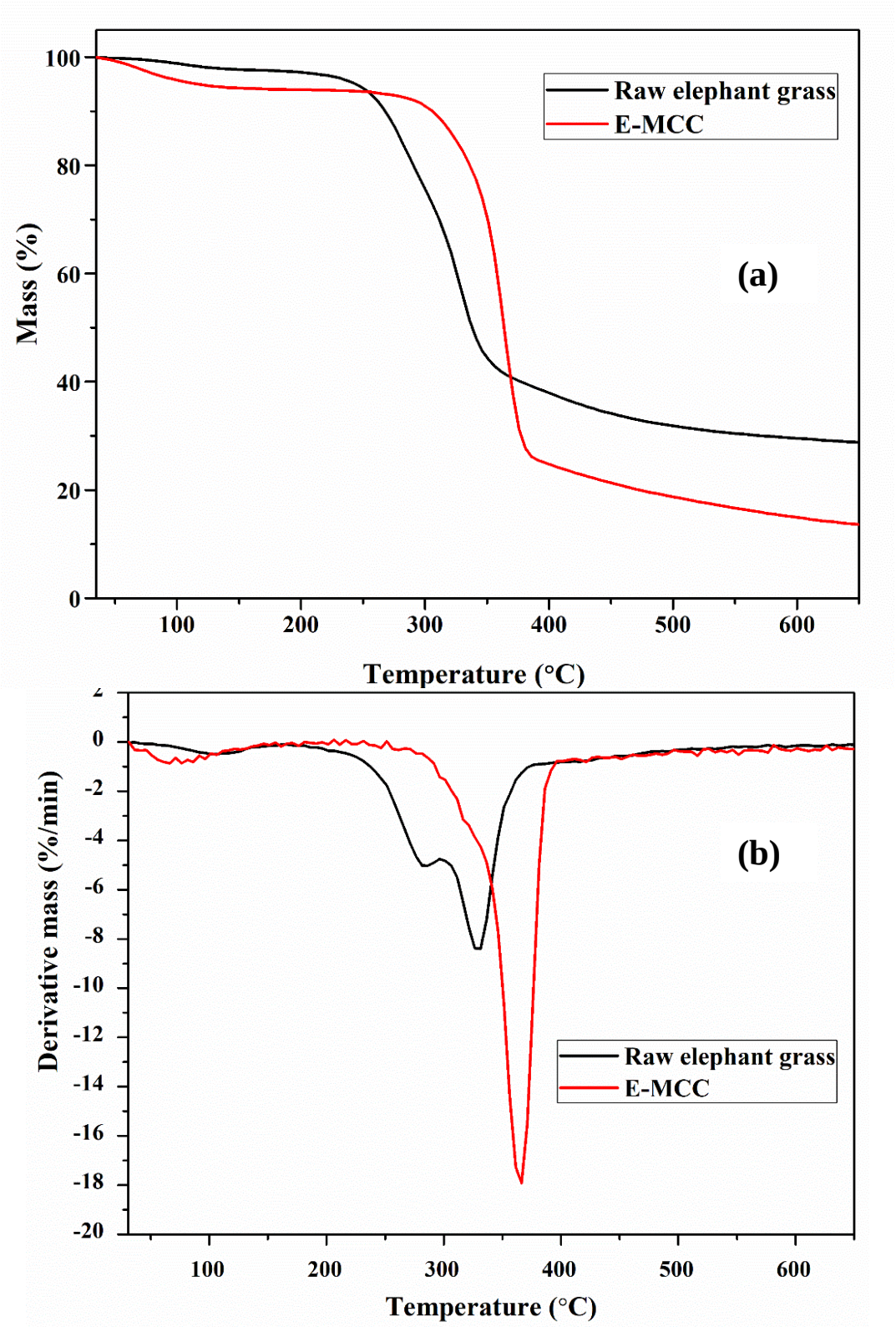


**Figure 2.5 (a)** TGA and **(b)** DTG plots of raw elephant grass and E-MCC.

However, this peak didn't appear on the curve of E-MCC, indicating the complete removal of hemicellulose (Owolabi et al., 2017). The onset degradation temperature of the E-MCC (285 °C) is higher than that of the MCC prepared from tea waste (230°C) (Zhao et al., 2018), rose stems (232 °C ) (Ventura-Cruz et al., 2020), waste cotton fabrics (240 °C) (Hou et al., 2019), pomelo peel (280 °C) (Liu et al., 2018). The DTG peak temperature of the synthesized E-MCC (370 °C) is also greater than the MCC prepared from roselle fibers (340 °C) (Kian et al., 2017), oil palm fronds (346°C) (Owolabi et al., 2017), tea waste and pomelo peel (360 °C) (Liu et al., 2018; Zhao et al., 2018). From the above observations, it can be concluded that the synthesized elephant grass MCC possesses good thermal stability, and it can be applied for the manufacturing of green bio-composites.

## 2.3.2. Characterization of the E-MCC reinforced corn starch films

### 2.3.2.1. FTIR analysis

The FTIR spectra of pure corn starch film and corn starch films filled with various concentrations of E-MCC (1, 2.5, and 5 wt%) are shown in **Fig. 2.6**. The absorption band at approximately 3288 $cm^{-1}$ is associated with the stretching vibration of the O-H bond of the intra and intermolecular bound O–H groups present in starch and glycerol (Nordin et al., 2020). The band at around 2929 $cm^{-1}$ corresponds to the stretching vibration of the C–H bond in aliphatic methyl ($–CH_3$) or methylene ($–CH_2$) groups. The strong peak at 1643 $cm^{-1}$ is ascribed to the vibrational stretching of the carbonyl group (C=O). The bands between the 1500–1300 $cm^{-1}$ range might be attributed to multiple vibration modes of –CH and –OH bending. The results are inconsistent with the work by Chen et al. (Chen et al., 2019) and Othman et al. (Othman et al., 2021).

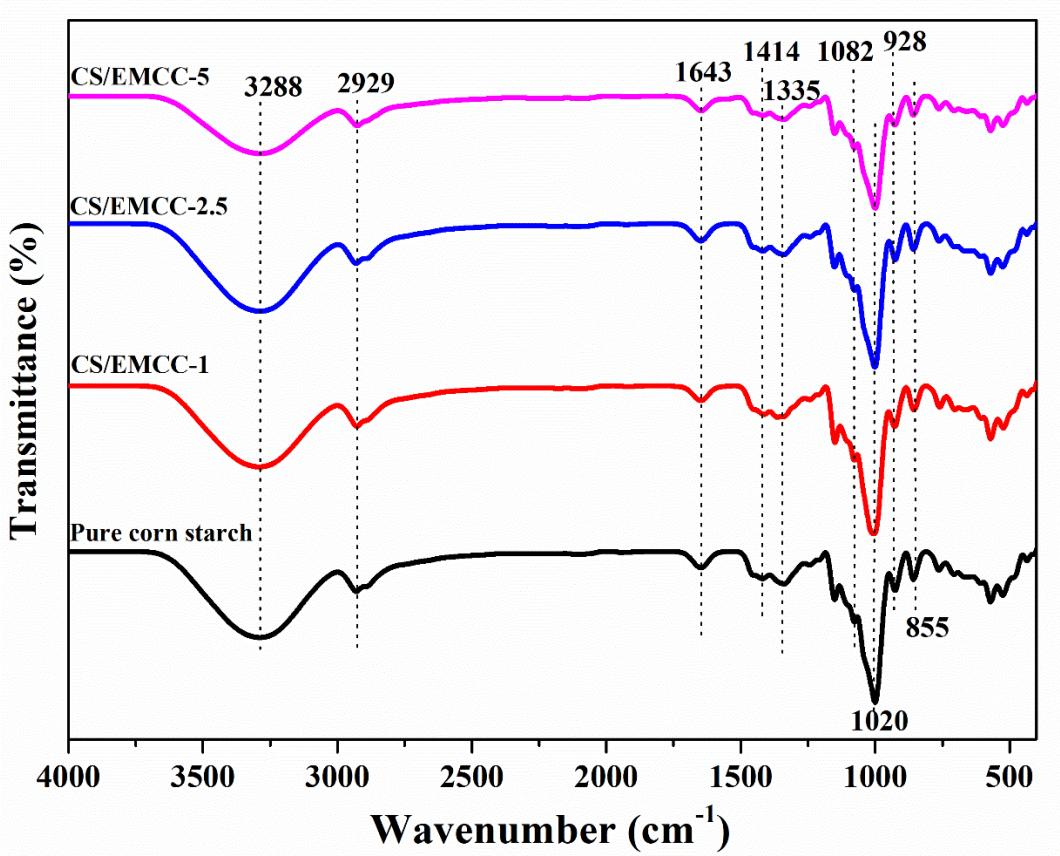


**Figure 2.6** FTIR spectra of corn starch films reinforced with different E-MCC concentrations

The peaks at 1020 and 1082 $cm^{-1}$ can be assigned to C–O stretching vibration in the functional groups C–O–C and C–O–H, respectively (Yuan & Chen, 2021). Some other works have reported that the sharp band at 1649 $cm^{-1}$ may be due to O–H bending of the absorbed water molecules in the starch films (Merci et al., 2019; Nordin et al., 2020). The peak at 928 $cm^{-1}$ represents asymmetric C–O stretching vibration from the glycosidic linkage, and the peak at 855 $cm^{-1}$ indicates symmetrical –CH and $–CH_2$ deformation in starch (Nordin et al., 2020). The FTIR spectra of the pure corn starch film and the E-MCC reinforced films are similar, indicating that all the prepared films have a similar chemical structure containing the same functional groups. This

refers to strong inter and/or intramolecular bonding between the corn starch and E-MCC, primarily via H-bonds and thereby showing promising compatibility between them (Othman et al., 2021).

#### 2.3.2.2. FESEM analysis

The surface morphology of the corn starch films reinforced with different concentrations of E-MCC are shown in **Fig. 2.7**. These images were observed using Field emission scanning electron microscopy (FESEM) to analyze the dispersion of the synthesized E-MCC in the matrices of the starch films. The pure starch film (**Fig. 2.7a**) has a homogeneous smooth surface without any pores or cracks, indicating complete disruption of the starch granules in the thermo-plasticization with water and glycerol. The E-MCC reinforced starch films also exhibited smooth surface morphology, suggesting that the E-MCC particles were well-dispersed in the starch matrix. At a lower E-MCC loading rate (1 wt% of starch dry weight), the particles seem to disperse more homogeneously in the polymer matrix (**Fig. 2.7b**). As the E-MCC loading was increased (2.5 wt% of starch dry weight), some of the fillers got agglomerated and appeared as a white domain on individual regions of the film surface (**Fig. 2.7c**). With a further increase in E-MCC loading (5 wt% of starch dry weight), larger agglomerations of E-MCC appeared on the film surface (**Fig. 2.7d**). Interactions between the O–H groups of the E-MCC and starch through hydrogen bond provided strong adhesion leading to good compatibility between them. The similarity in chemical structures of E-MCC and corn starch is the reason behind such interactions between the filler and starch matrix. This strong compatibility also contributes to the enhancement of the mechanical

properties of the films, resulting in very few cracks on the film surfaces (J. Chen et al., 2020; Merci et al., 2019).

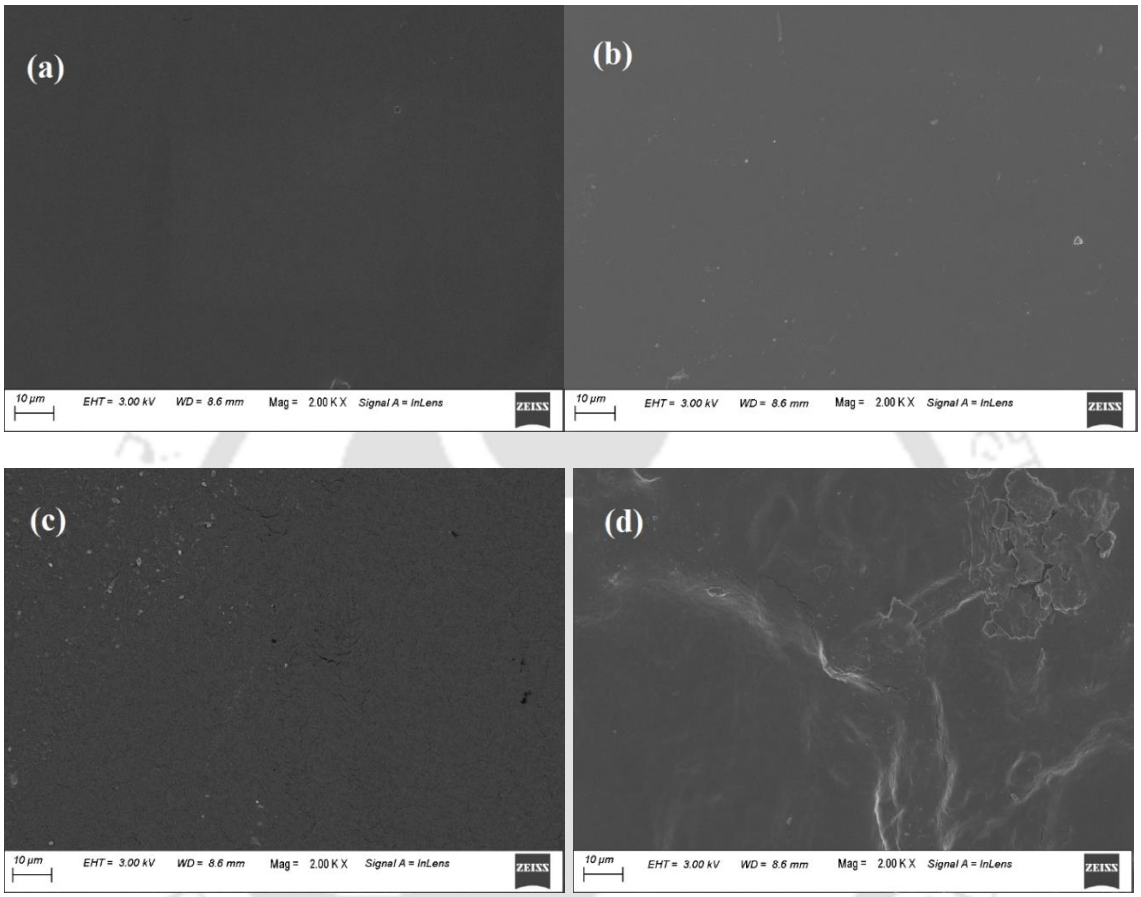


**Figure 2.7** FESEM images of (a) pure corn starch, (b) CS/EMCC-1, (c) CS/EMCC-2.5, and (d) CS/EMCC-5 film

### 2.3.2.3. TGA analysis

The TGA curves of the E-MCC reinforced corn starch films are presented in **Fig. 2.8**. All the films showed multi-stage thermal degradation curves. The first stage of weight loss ranged from room temperature to 120 °C, which is mainly attributed to the evaporation of moisture from the films. The second stage occurring in the range of 130-270 °C, is related to the loss of glycerol and water (Q. Chen et al., 2020; Othman et al.,

2021). The third stage of degradation, occurring between 280-330 °C, is mainly ascribed to the thermal decomposition of starch, overlapped with the degradation of E-MCC (J. Chen et al., 2020; Nordin et al., 2020). It was observed from the figure that with the incorporation of E-MCC into the starch matrix, the TGA curves shifted right from the pure corn starch film, indicating improved thermal stability of the E-MCC reinforced films. The reason behind this improvement is the enhanced crystallinity and rigidity of the films due to the addition of crystalline cellulose; as a result, higher temperatures were required to cause the degradation of these films (Othman et al., 2021).

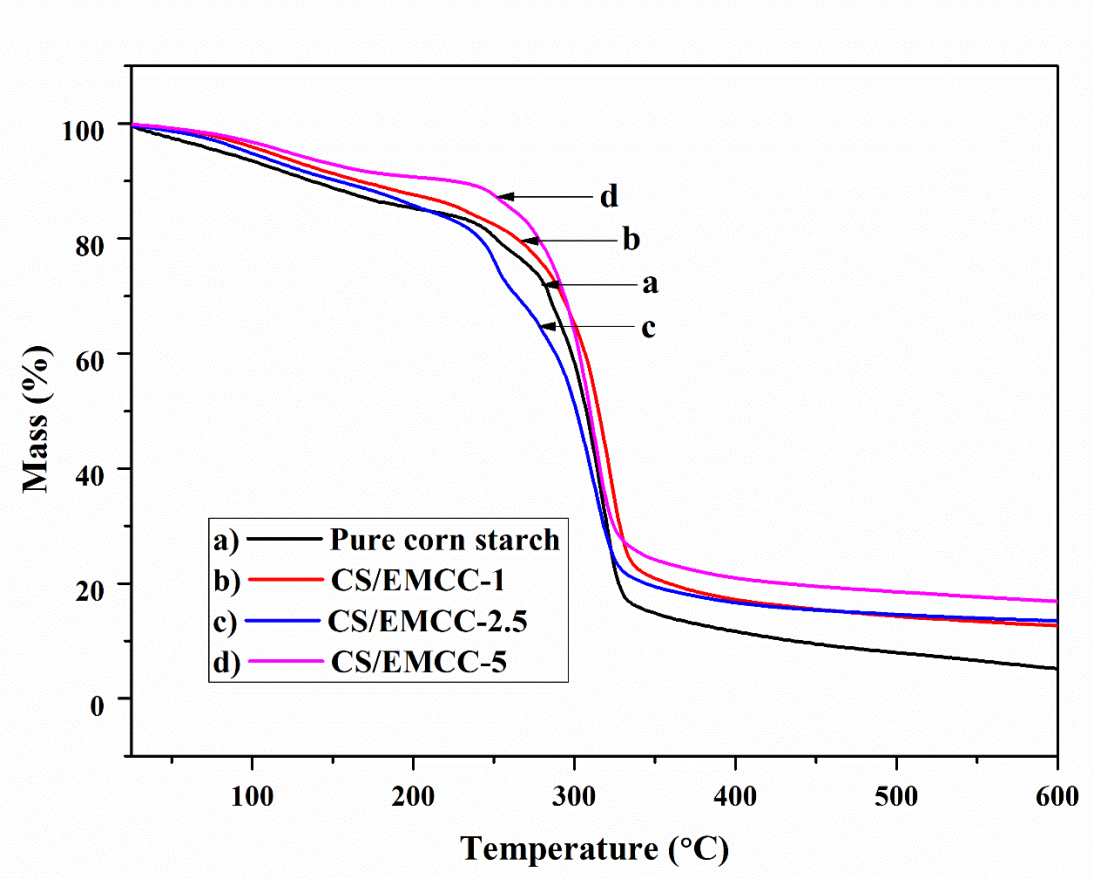


**Figure 2.8** TGA curves of corn starch films reinforced with different concentrations of E-MCC

**Table 2.2** Thermal degradation of corn starch films with different concentrations of MCC synthesized from elephant grass (E-MCC)

| Film type | Degradation temperature corresponding to percentage weight loss (°C) | | | DTG peak temperature (°C) | Residual mass (%) at 600 (°C) |
|---|---|---|---|---|---|
| | $T_{10\%}$ | $T_{25\%}$ | $T_{50\%}$ | | |
| Pure corn starch | 136.5 | 205.0 | 301.0 | 312.3 | 5.15 |
| CS/EMCC-1 | 166.5 | 231.0 | 309.5 | 321.0 | 12.68 |
| CS/EMCC-2.5 | 152.6 | 207.4 | 307.2 | 313.5 | 13.52 |
| CS/EMCC-5 | 224.5 | 261.7 | 314.7 | 312.7 | 16.89 |

**Table 2.2** represents the degradation temperature and DTG peak temperatures of the corn starch films for the four different formulations. As per **Table 2.2**, the initial weight loss (10%) and the subsequent degradation (25%, 50%) of the E-MCC reinforced films occurred at higher temperatures than the neat corn starch film. The DTG peak temperature of the CS/EMCC-1 film shifted from 312.3 °C to a higher temperature of 321.0 °C as compared to the other films implying better thermal stability. This might be associated with good interaction between starch, glycerol, and E-MCC (Nordin et al., 2020). As the E-MCC level increases, the H-bonds between the molecules of starch and microcrystalline cellulose also increase. However, at higher concentrations of E-MCC, the flocculation of the particles reduced the degradation temperature. Thus, the DTG peak temperature of the CS film with 5 wt% E-MCC is less as compared to the one with 1 wt% E-MCC. The residual mass of the neat corn starch film at 600 °C is less than

10%, but all the E-MCC-filled starch films had residue over 10% even after 600 °C (J. Chen et al., 2020). The peak degradation temperatures of the E-MCC-filled films are comparable to other reported corn starch films for food packaging (Collazo-Bigliardi et al., 2019; Souza et al., 2021).

#### 2.3.2.4. Measurement of water contact angle

The effect of the incorporation of different concentrations of E-MCC on the hydrophilic property of the corn starch films is shown in **Fig. 2.9**. Pure corn starch film exhibited the lowest contact angle (19.52°) because of the presence of hydrophilic O–H groups in the native starch. Water contact angle value greater than 65° signifies surface hydrophobicity, while the angle lower than 65° reflects hydrophilicity (Ghosh et al., 2020). From the figure, it was observed that the addition of E-MCC significantly enhanced the water contact angle of the films. With the increased E-MCC loading, the contact angle of the films increased to 33.26°, 91.15°, and 98.83° for 1 wt%, 2.5 wt%, and 5 wt% concentrations of E-MCC, respectively. Thus, the result found in this study implies that E-MCC addition improved the hydrophobicity of the starch films to a great extent. The strong interaction of the E-MCC with corn starch through hydrogen bonds led to the formation of a network between the polymer chains of starch and reduced the interaction between water and the surface of the films, thereby preventing water from entering the films' surface (J. Chen et al., 2020; Slavutsky & Bertuzzi, 2014). Chen et al. (Q. Chen et al., 2020) and Hasan et al. (Hasan et al., 2019) also reported that the addition of microcrystalline cellulose could reduce the hydrophilicity of bio-composite films. The results observed in the current study revealed that E-MCC can be a potential

filler to improve the hydrophobic properties of corn starch films for packaging applications.

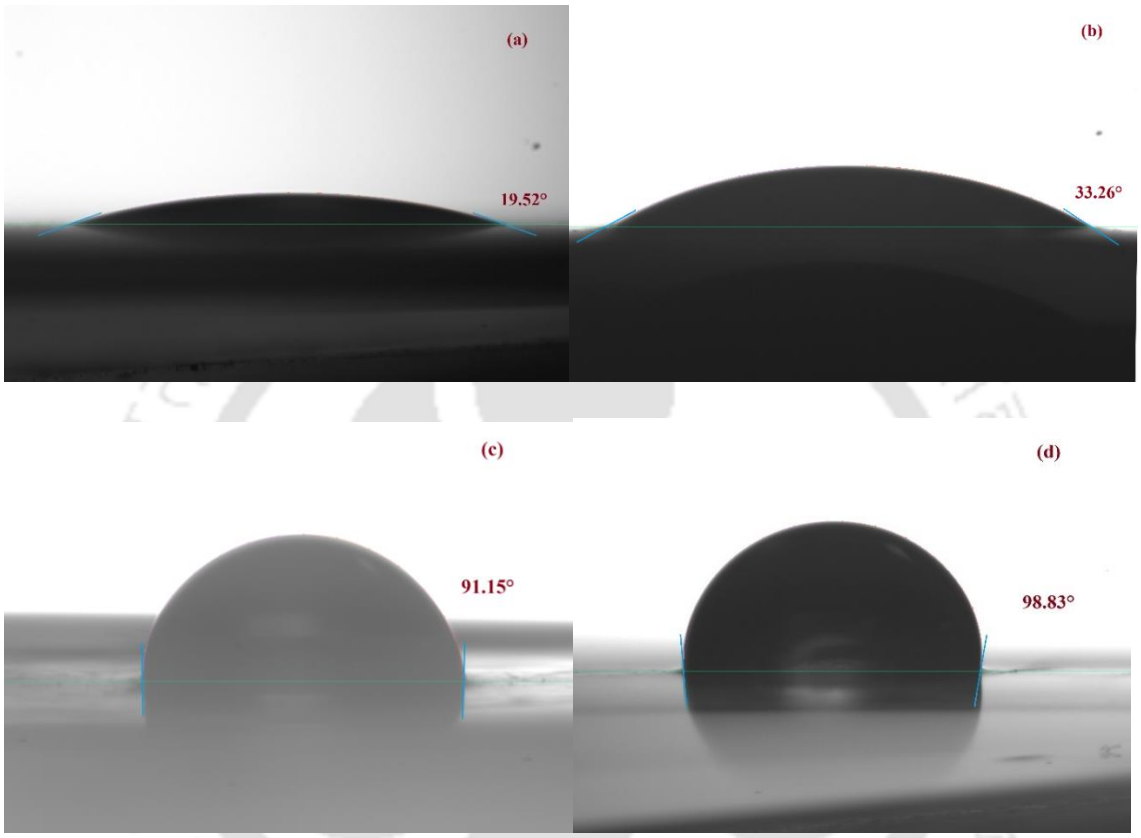


**Figure 2.9** Water contact angle of a) pure corn starch film b) CS/EMCC-1, c) CS/EMCC-2.5, and d) CS/EMCC-5 film

### 2.3.2.5. Determination of thickness, moisture content, and water solubility

The physical properties of the E-MCC/corn starch composite films, such as thickness, moisture content, and solubility in water, are shown in **Table 2.3**. The neat corn starch film was taken as control which had the thickness of 335 μm. The thickness of the films decreased with the addition of E-MCC, which might be attributed to good dispersion of the E-MCC particles in the films leading to less number of cracks and pores in the films (Chen et al., 2019). The moisture content (MC) of the control film was 18.87%, which

decreased with the addition of E-MCC. The film with 1 wt% E-MCC showed an MC of 16.17%. As the concentration of the E-MCC was further increased, the MC of the films kept decreasing and reached to 10.66% at an E-MCC concentration of 5 wt%. A similar trend of the result was observed by Desire et al. (Yao Désiré et al., 2021). Due to the formation of a more intermolecular H-bond between the E-MCC and hydroxyl groups of the corn starch, the number of freely available O–H groups decreased. As a result, the interplay between water and the corn starch–OH groups gets reduced. Hence, the moisture content of the films tends to decline (Hasan et al., 2019; Wang, Sui, et al., 2021).

Water solubility is another important characteristic of packaging materials. **Table 2.3** shows that pure corn starch film has the highest solubility (21.25%) as it is highly hydrophilic and can easily absorb water. Solubility of the films declined with the incorporation of E-MCC and reached the lowest value of 18.05% at an E-MCC concentration of 5 wt%. This reduction in film solubility might be associated with forming a compact network resulting in lower diffusion of water in the corn starch matrix (Chen et al., 2019). The reduction in the water solubility of the films with the increase in E-MCC concentration also indicates that E-MCC increased the crystallinity of the films. The crystalline cellulose promotes the intermolecular interactions between the O–H groups of the corn starch and E-MCC leading to the reduction in solubility. Also, the high crystallinity and compact micro-fibrillary arrangement of cellulose make it less hydrophilic than corn starch, thereby reducing the solubility of corn starch films filled with E-MCC. The results observed in this study are consistent with those found in the case of MCC reinforcement in cassava starch films (Yao Désiré et al., 2021).

**Table 2.3** Physical characteristics of the corn starch films reinforced with different E-MCC concentrations

| Type of film | Thickness (µm) | Moisture content, MC (%) | Water Solubility (%) |
|---|---|---|---|
| Pure corn starch | 335 ± 0.56 | 18.87 ± 1.14 | 21.25 ± 1.06 |
| CS/EMCC-1 | 286 ± 0.97 | 16.17 ± 0.88 | 19.12 ± 0.87 |
| CS/EMCC-2.5 | 296 ± 1.03 | 11.47 ± 0.33 | 18.21 ± 0.44 |
| CS/EMCC-5 | 305 ± 0.48 | 10.66 ± 0.31 | 18.05 ± 0.21 |

### 2.3.2.6. Mechanical properties analysis

The application of bioplastic films as packaging material depends largely on their mechanical behaviour. The strength of a film is measured by its tensile strength, and its flexibility is indicated by elongation at break. The mechanical properties obtained from UTM analysis, i.e., tensile strength, Young's modulus, and elongation at break, of the corn starch composite films with varying levels of E-MCC are shown in **Table 2.4**. The neat corn starch film showed the lowest tensile strength (6.03 ± 0.23 MPa). The addition of 1 wt% E-MCC didn't have much effect on the film tensile strength, but the addition of 2.5 wt% E-MCC increased the strength by 3.3%. The tensile strength of the film containing 5 wt% E-MCC was significantly high (22.33 ± 0.19 MPa). This increase in strength is associated with the proper dispersion and good compatibility between the E-MCC filler and corn starch matrix due to the formation of a strong H-bonded network, already proven in FTIR and FESEM results. As a result, the load transfer between the

interface of the starch matrix and E-MCC network was more uniform and efficient, which minimized stress concentration in a particular area (J. Chen et al., 2020; Khan et al., 2012). The tensile strength of corn starch films reinforced with elephant grass-derived MCC was higher as compared to corn starch films enriched with cellulose nanocrystals synthesized from waste biomass of *Posidonia Oceania* (Benito-González et al., 2021) and Pickering emulsions of cinnamon, cardamom, ho wood essential oils (Souza et al., 2021).

**Table 2.4** Mechanical properties of the corn starch films reinforced with different E-MCC concentrations

| Film | Tensile Strength (MPa) | Young's modulus (MPa) | Elongation at break (%) |
|---|---|---|---|
| Pure corn starch | 6.03 ± 0.23 | 106.47 ± 3.8 | 33.39 ± 2.9 |
| CS/EMCC-1 | 6.04 ± 0.43 | 136.04 ± 4.1 | 29.35 ± 1.3 |
| CS/EMCC-2.5 | 6.23 ± 0.51 | 162.14 ± 6.0 | 24.36 ± 1.7 |
| CS/EMCC-5 | 22.33 ± 0.19 | 493.29 ± 2.9 | 3.49 ± 1.9 |

The substantial increase in Young's modulus of the films with the introduction of E-MCC is attributed to the enhancement of stiffness of the films. As the E-MCC fillers increased the tensile strength and rigidity of the films, it is obvious that the stiffness of the films was also enhanced (Hasan et al., 2019; Othman et al., 2021). As expected, the trend of elongation at the break of the films was found to be reciprocal to that of the tensile strength. This decrease in elongation at break with the addition of E-MCC may

be related to the less flexible or rigid nature of the E-MCC filler. This observation is in accordance with other published literature (J. Chen et al., 2020; Slavutsky & Bertuzzi, 2014).

## 2.4. Comparative study

A comparative assessment of the E-MCC reinforced corn starch films with various other plant material-filled corn starch-based packaging materials is shown in **Table 2.5**. From the table, it is obvious that the incorporation of E-MCC as a reinforcing agent in corn starch matrix results in higher mechanical strength as compared to many filler materials like fireweed extract (Kowalczyk et al., 2021), date palm pits (Alqahtani et al., 2021), guabiroba pulp (Malherbi et al., 2019), *Zanthoxylum bungeanum* essential oil (Wang, Sui, et al., 2021). The hydrophobicity (measured in water contact angle) of the E-MCC loaded corn starch films are better than those filled with virgin coconut oil (Xiao et al., 2022). The moisture content of the corn starch films reinforced with E-MCC are similar to those filled with bamboo leaf volatile oil, date palm pits powder, and virgin coconut oil while significantly lower than those incorporated with fireweed extract, *Zanthoxylum bungeanum* essential oil, and guabiroba pulp. Lower moisture content is desirable for packaging applications of corn starch films. Therefore, it can be stated that E-MCC is an effective filler in corn starch packaging films which is superior to many other reported plant-based filler materials.

**Table 2.5** Comparative analysis of the E-MCC reinforced corn starch films with other plant material filled corn starch-based packaging films

| Films | Filler material | Moisture content (%) | Water contact angle (°) | Tensile strength (MPa) | References |
|---|---|---|---|---|---|
| Corn starch/sodium alginate/gum Arabic | Virgin coconut oil | 12.00-13.70 | 39.9-63.3 | 20.50-27.60 | (Xiao et al., 2022) |
| Corn starch | Fireweed extract | 26.30-26.66 | ----- | 4.32-4.50 | (Kowalczyk et al., 2021) |
| Corn starch | *Zanthoxylum bungeanum* essential oil | 22.96-26.96 | ----- | 1.23-3.98 | (Wang, Sui, et al., 2021) |
| Corn starch | Bamboo leaf volatile oil | 11.41-13.21 | ----- | 10.68-20.64 | (Wang, Yan, et al., 2021) |
| Corn starch | Date palm pits powder | 10.22-17.05 | ----- | 1.30-2.94 | (Alqahtani et al., 2021) |
| Corn starch and gelatin | Guabiroba pulp | 28.84-36.92 | ----- | 4.24-8.67 | (Malherbi et al., 2019) |
| **Corn starch** | **Elephant grass- MCC** | **10.66-16.17** | **33.26-98.83** | **6.04-22.33** | **Present study** |

## 2.5. Summary

This chapter discusses the synthesis of microcrystalline cellulose from elephant grass biomass through successive bleaching with alkaline hydrogen peroxide. The various physicochemical properties of the synthesized product were investigated using XRD, FTIR, FESEM and TGA analysis. The characterization results revealed that the synthesized E-MCC possesses comparable crystallinity, chemical structure, and surface

morphology to those of the commercially available microcrystalline cellulose. The thermal stability of the E-MCC was also comparable to C-MCC. As this synthesis method doesn't involve the usage of any corrosive acid, it can be considered for environment-friendly commercial production of microcrystalline cellulose from the abundant, renewable and cheap waste biomass of elephant grass. The elephant grass derived microcrystalline cellulose was used as a reinforcement agent in corn starch films. The physicochemical properties, thermal stability, water resistance and mechanical properties of fabricated films were determined using various analytical methods. The findings showed that incorporation of E-MCC improved the overall properties of the films considerably, which is due to the good compatibility between the E-MCC molecules and the starch matrix. Strong interaction between the hydroxyl groups of starch and E-MCC enhanced the rigidity, thereby thermal and mechanical properties of the films significantly whereas the hydrophilic properties decreased, which is desirable for packaging applications.

# Chapter 3

# Microwave-assisted synthesis of microcrystalline cellulose from tea industry waste and its characterization

*In this chapter, the detailed experimental method is discussed for the synthesis of microcrystalline cellulose from black tea waste produced in the tea factories using a novel superfast technique involving microwave heating. Tea waste microcrystalline cellulose was also prepared using conventional heating method (without microwave) for comparison with the microwave-assisted extraction technique. FTIR, XRD, FESEM, and TGA analyses were then utilized to characterize the synthesised TWMCC. The properties of the tea waste derived MCC were compared with other conventionally produced biomass based MCCs. The potential of industrial black tea waste to produce valuable microcrystalline cellulose was explored, and the effectiveness of microwave-assisted peroxide bleaching treatment for MCC synthesis was studied in the present chapter. Statistical analysis using RSM (response surface methodology) was also carried out in this study to determine the optimum hydrogen peroxide bleaching condition for synthesizing TWMCC with high crystallinity. The background, state of art literature and the scope of this research have been described in Chapter 1, Section 1.5 and Section 1.7.4., respectively. This work has been published in International Journal of Biological Macromolecules.*

# 3.1. Experimental

## 3.1.1 Materials

Tea waste was collected from Arin Tea Pvt. Ltd. Assam, India. Sodium hydroxide was supplied by HiMedia (India), and hydrogen peroxide (30%) was purchased from Merck (India). Chemicals of analytical grade were used in the present work. Milli-Q water was the solvent used in all the experiments, from solution preparation to sample washing.

## 3.1.2 Preparation of tea waste microcrystalline cellulose

Microcrystalline cellulose was synthesized from black tea waste by microwave-assisted delignification and bleaching. Initially, the raw tea waste collected from the tea factory was boiled in distilled water at a material-to-water ratio of 1:20 (g/mL) at a temperature of 70 °C for 30 min to remove polyphenols and other impurities. Thereafter, the tea waste was allowed to cool to room temperature, then filtered and dried in a hot air oven overnight at a temperature of 50 °C to eliminate any remaining moisture. After drying the sample, a 5 wt% NaOH solution (1:20 g/mL) was added to the sample and was heated in a domestic microwave oven for 2 min. The reaction mixture, which produced a black colour, was allowed to cool to room temperature before being filtered and repeatedly washed with Milli-Q water until the pH was neutral. The filtered solid was then dried in a hot air oven at 50 °C until a constant weight was obtained. Afterwards, the dignified and dried sample was subjected to bleaching for two consecutive times using a mixed solution containing 5 wt% (w/v) sodium hydroxide (NaOH) and 4.5 M

hydrogen peroxide ($H_2O_2$), both at 1:20 (g/mL) tea waste to solvent ratio. The bleaching treatments were carried out under microwave heating for 30seconds. In both the bleaching steps, the white-coloured suspension obtained was cooled to room temperature, filtered, and washed repeatedly with Milli-Q water until the pH reached a neutral value. The solid residue was finally dried in a hot air oven at 50 °C overnight to obtain the tea waste microcrystalline cellulose (TWMCC-MW) in white-coloured powder form (as shown in **Fig. 3.1**).


**Figure 3.1** Schematic illustration of synthesis of tea waste microcrystalline cellulose under microwave (TWMCC-MW)

Tea waste microcrystalline cellulose (denoted as TWMCC-con) was also prepared via conventional heating method (shown in **Fig. 3.2**) for comparison with the microwave-assisted synthesis method. In the conventional heating method, boiled tea waste was delignified using 5 wt% NaOH (at 1:20 material/solvent ratio) in a hot air oven at 80 °C

for 2 h. Then consecutive bleaching treatments were carried out using the same alkaline peroxide solution at 55 °C in a hot air oven for 90 min each time.

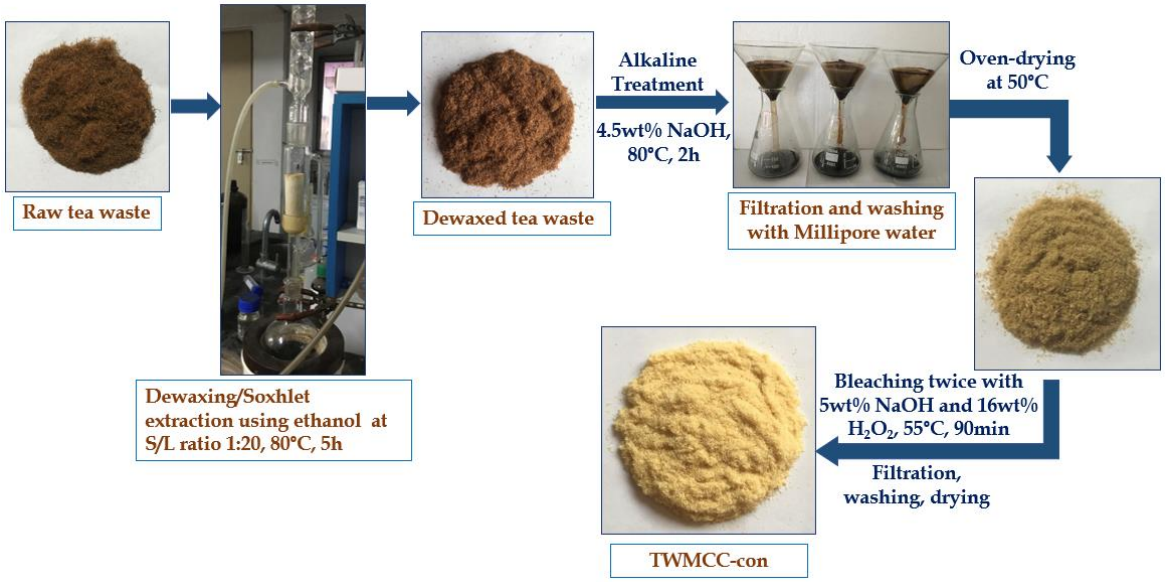


**Figure 3.2** Schematic representation of synthesis of tea waste microcrystalline cellulose under conventional heating (TWMCC-con)

## 3.2. Characterization of the synthesized product

### 3.2.1 Chemical Functionality

A Fourier-transform infrared (FTIR) spectrometer (make: Perkin Elmer, Singapore, model: spectrum two) was used to determine the functional group of the synthesised tea waste MCC. The FTIR spectra were recorded by scanning the samples at the wavelength of 4000–400 $cm^{-1}$.

### 3.2.2 Determination of crystalline structure

Rigaku technology, Japan (model: Smartlab) X-ray diffractometer (XRD) equipped with CuKα radiation was used to examine the crystalline structure of the synthesized product. XRD patterns were obtained in the 2θ (diffraction angle) range of 5–60° with a 0.02° step interval. The crystallinity index (CrI) of the samples was calculated using the Segal equation as follows (Segal et al., 1959):

$$CrI = [(I_{002} - I_{am})/I_{002}] \times 100 \quad (3.1)$$

Where $I_{002}$ is the maximum intensity of the lattice diffraction peak (for plane 002) at 2θ around 22.5°, and $I_{am}$ is the intensity scattered by the amorphous part at 2θ value around 18° (Zhao et al., 2018).

### 3.2.2 Morphology analysis

The surface morphology of the synthesized tea waste microcrystalline cellulose was studied using a Zeiss (model: sigma 300) field emission scanning electron microscope (FESEM). Prior to scanning, the samples were coated with gold to prevent charging. At a 5 kV accelerating voltage, the samples' morphology were then examined.

### 3.2.3 Thermal properties

Thermo-stability of the prepared tea waste MCC was measured employing a Netzsch (model: STA449F3A00) Thermogravimetric instrument. The samples were heated at a 10 °C/min heating rate from room temperature to 600°C under an argon atmosphere

(flowing at a rate of 20 mL/min). Thermogravimetric (TGA) and derivative thermogravimetric (DTG) analysis data were recorded for all the samples.

## 3.3. Statistical analysis using response surface methodology (RSM)

The experiments for RSM study were designed using the Design Expert software (Version 7.0.0) under central composite spherical design to facilitate studies targeting the combined effect of the independent variables on the desired responses or product characteristics. Central composite design (CCD) is the most widely adopted design of experiment for the optimization of process variables. Three control factors of microwave heating time, $H_2O_2$ concentration and tea waste to solvent ratio were selected to investigate the effect of hydrogen peroxide bleaching in the synthesis of tea waste MCC. The response measured was the crystallinity index of the TWMCC-MW to develop the corresponding regression model. The independent process variables and their considered ranges are shown in **Table 3.1.**

**Table 3.1** Independent process variables with ranges

| Factor | Name | Units | Type | Low Actual | High Actual | Low Coded | High Coded | Mean | Std. Dev. |
|---|---|---|---|---|---|---|---|---|---|
| A | Time | Sec | Numeric | 5 | 30 | -1 | 1 | 17.50 | 8.84 |
| B | Hydrogen peroxide | M | Numeric | 3 | 6 | -1 | 1 | 4.50 | 1.06 |

| | | | | | | | | |
|---|---|---|---|---|---|---|---|---|
| | concentration | | | | | | | |
| C | Tea waste to solvent ratio | Numeric | 10 | 30 | -1 | 1 | 20 | 7.07 |

A total of 20 experiments were run as per the three factors-based CCD design of experiments for this optimization. The process control variables and the corresponding responses are summarized in **Table 3.2**. After obtaining all the response values, RSM model-based optimization was conducted to maximize crystallinity. The regression analysis of the responses was carried out using a second order polynomial equation for the evaluation of the best fit model:

$$y_n = \beta_0 + \sum_{i=1}^{k} \beta_i x_i + \sum_{i=1}^{k} \beta_{ii} x_{ii}^2 + \sum_{i=1}^{k} \sum_{j=i+1}^{k-1} \beta_{ij} x_i x_j \quad (3.2)$$

where, $y_n$ denotes the response variables, $\beta_0$ the intercept, $\beta_i$ the linear regression coefficient for the $i^{th}$ factor, $\beta_{ii}$ is the quadratic and $\beta_{ij}$ is the cross-product term, $x_i$ and $x_j$ are the input variables and $k$ is the number of input variables ($k = 3$).

Various alternate models such as linear, two factor interaction, quadratic and cubic models have been considered by the design expert software. The best alternate model has been identified among the alternate models based on the *p*-value (lowest desirable) and *F*-value (highest desirable), which were obtained from the analysis of variance (ANOVA) carried out with constraints set as *p*-value < 0.05 for models to be significant and *p*-value > 0.05 for insignificant lack of value.

**Table 3.2** Design expert software (Version 7.000) design of three variables (microwave heating time, hydrogen peroxide concentration and tea waste to solvent ratio) used for synthesizing MCC from tea waste

| SL. No. | Input variables | | | Response |
|---|---|---|---|---|
| | Time (sec) | $H_2O_2$ concentration (M) | Tea waste to solvent ratio | Crystallinity index (%) |
| 1 | 17.5 | 4.5 | 10 | 88.56 |
| 2 | 5 | 6 | 30 | 70.57 |
| 3 | 5 | 6 | 10 | 88.47 |
| 4 | 30 | 3 | 10 | 87.05 |
| 5 | 17.5 | 4.5 | 30 | 88.23 |
| 6 | 5 | 3 | 10 | 83.13 |
| 7 | 30 | 6 | 10 | 82.11 |
| 8 | 17.50 | 3 | 20 | 88.04 |
| 9 | 30 | 4.5 | 20 | 89.77 |
| 10 | 5 | 4.5 | 20 | 77.03 |
| 11 | 17.50 | 6 | 20 | 87.81 |
| 12 | 30 | 3 | 30 | 85.1 |

| | | | | |
|---|---|---|---|---|
| 13 | 5 | 3 | 30 | 68.25 |
| 14 | 17.5 | 4.5 | 20 | 89.33 |
| 15 | 17.5 | 4.5 | 20 | 89.02 |
| 16 | 17.5 | 4.5 | 20 | 88.89 |
| 17 | 17.5 | 4.5 | 20 | 89.61 |
| 18 | 17.5 | 4.5 | 20 | 89.19 |
| 19 | 17.5 | 4.5 | 20 | 89.53 |
| 20 | 30 | 6 | 30 | 88.25 |

## 3.4 Results and discussion

### 3.4.1 Analysis of chemical structure (FTIR)

The FTIR spectra of raw tea waste, dignified tea waste (DL-TW), single bleached tea waste (TW-BL1), tea waste MCC synthesized by microwave heating (TWMCC-MW) and conventional heating (TWMCC-con) are shown in **Fig. 3.3**. The absorption bands at approximately 3330 $cm^{-1}$, 2900 $cm^{-1}$, 1430 $cm^{-1}$, 890 $cm^{-1}$ appearing in all the spectra correspond to the characteristics of native cellulose. The broad and intense absorption peaks at 3336 $cm^{-1}$ in all the spectra are related to the O-H groups stretching vibrations in cellulose. The peaks located at 2918 $cm^{-1}$ are ascribed to the stretching vibrations of aliphatic saturated C-H bonds present in cellulose (Liu et al., 2018; Ventura-Cruz et al., 2020). The band near 1631 $cm^{-1}$ is associated with the bending of absorbed water in the

cellulose representing cellulose-water interaction in the tea waste fibres (Kian et al., 2020). The absorption peak observed at 1428 $cm^{-1}$, known as the cellulose "crystallinity band", is associated with $-CH_2$ symmetric bending vibration (Rashid et al., 2017; Zhao et al., 2018). The peaks occurring near 1156 $cm^{-1}$ represent the C−O groups stretching vibration in cellulose. The strong bands located at around 1030 $cm^{-1}$ indicate skeletal stretching vibration of the C−O−C pyranose ring of cellulose (Liu et al., 2018; Rashid et al., 2017). The peaks appearing around 895 $cm^{-1}$ indicate the characteristic β-glycosidic linkages present in the cellulose (Zhao et al., 2018). Both the tea waste MCCs prepared via microwave-assisted and conventional heating methods exhibited similar chemical structures containing the same functional groups. Also, comparable absorption spectra were observed in the study by Debnath et al., 2022, demonstrating that the TWMCC synthesized via the microwave-assisted technique in the present study has chemical functionality similar to that of the commercially available MCC (Debnath et al., 2022).

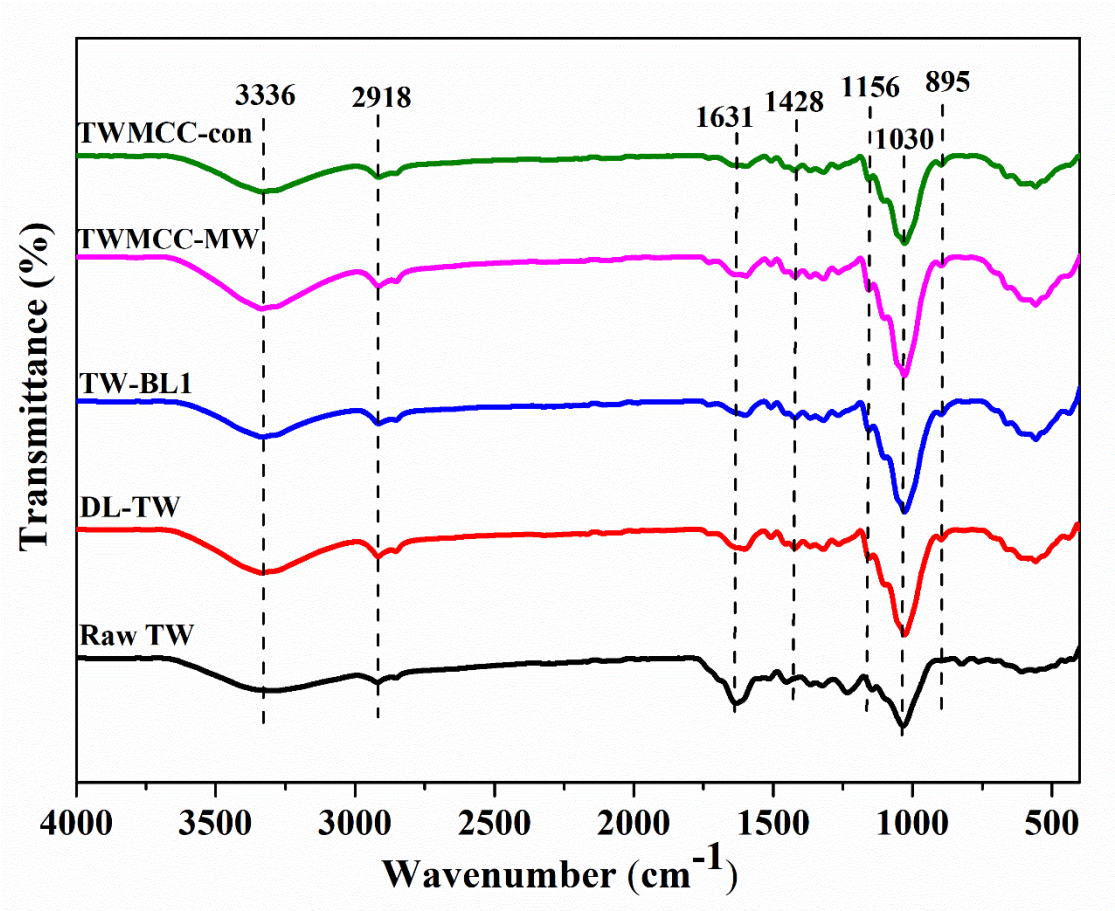


**Figure 3.3.** FTIR spectra of raw tea waste (TW), delignified tea waste (DL-TW), tea waste after first bleaching (TW-BL1), tea waste microcrystalline cellulose prepared under microwave heating (TWMCC-MW) and under conventional heating (TWMCC-con).

### 3.4.2 Determination of crystalline structure (XRD)

The XRD patterns of raw tea waste, DL-TW, TW-BL1, TWMCC-MW and TWMCC-con are presented in **Fig. 3.4**. All the samples exhibited prominent diffraction peaks at 2θ angle values of 15.9°, 22.6° and 34.8°, indicating the presence of cellulose type I. The diffraction angles corresponding to these peaks may be ascribed to the crystalline planes of $1\bar{1}0$, 200, and 004, respectively. The similar diffraction angles appearing in all

the spectra throughout the synthesis process demonstrate that the cellulose structure remains intact during the extraction (Debnath et al., 2022; Ventura-Cruz et al., 2020). The diffraction peak occurring at 22.6° became sharper and narrower from raw TW, with delignification and subsequent bleaching treatments, representing increased cellulose crystallinity resulting from improved intra-and intermolecular H-bonding (Kian et al., 2020). The crystallinity index of the unmodified tea waste was 56.68%. After the delignification and bleaching treatments, the CrI of the biomass increased significantly. The dignified TW exhibited a CrI value of 67.07%, while the sample after the first bleaching and second bleaching or TWMCC-MW showed high crystallinity with CrI of 82.73% and 89.77%, respectively. These findings demonstrate that the quick delignification and bleaching of tea waste under microwave heating progressively increase the crystallinity, indicating the elimination of the amorphous regions of cellulose as well as the non-cellulosic compounds due to the disintegration of β-1,4-glucopyranose linkages releasing the individual crystallites (Ren et al., 2019). Additionally, the similar XRD patterns of the samples reveal that the delignification and consecutive bleaching treatments did not alter the structure of cellulose in the synthesized tea waste microcrystalline cellulose. The crystallinity index of the conventionally synthesized TWMCC-con was found to be 76.83%, which is lower than that of the TWMCC-MW, suggesting that microwave heating is more efficient in comparison to conventional heating for producing MCC with high crystallinity.

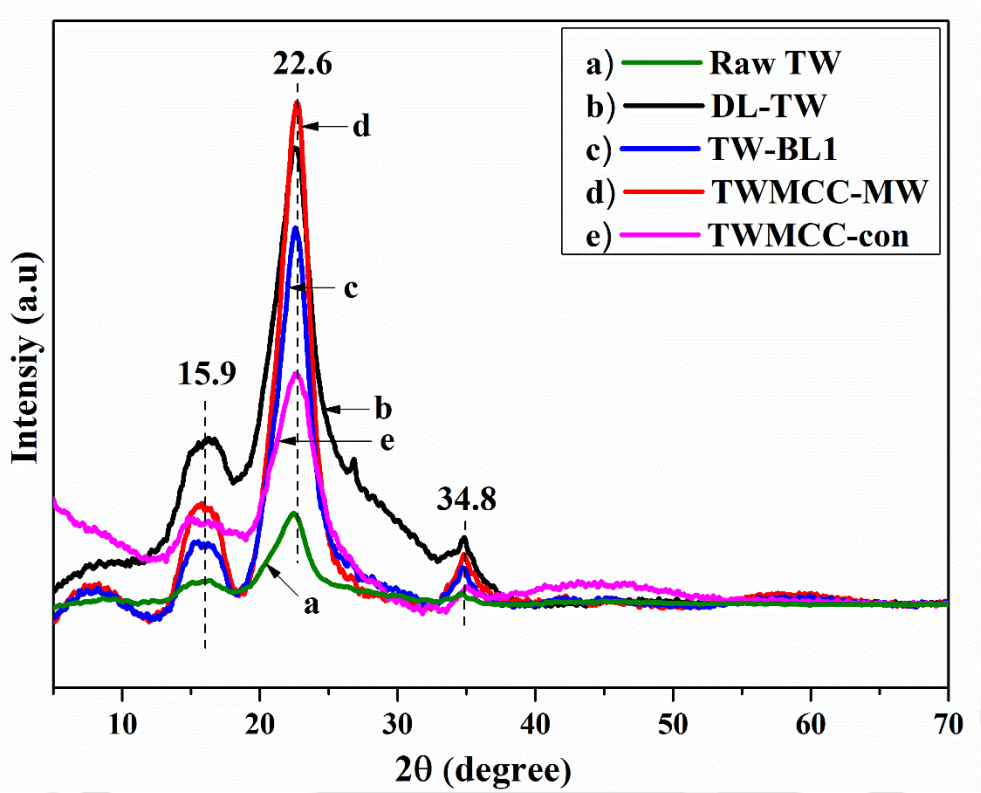


**Figure 3.4** XRD patterns of a) raw TW, b) DL-TW, c) TW-BL1, d) TWMCC-MW, and e) TWMCC-con

A comparison of the crystalline property of tea waste-derived MCC with other biomass-based MCCs are summarized in **Table 3.3**. The crystallinity of the black tea waste MCC synthesized in the present study was higher than a number of biomass-derived MCC such as those synthesized from oolong tea waste via acid hydrolysis (Zhao et al., 2018), olive fibres (Kian et al., 2020), jute (Jahan et al., 2011), rose stems (Ventura-Cruz et al., 2020; Ventura-Cruz & Tecante, 2019), oil palm fronds (Owolabi et al., 2017), rice husk (Sim et al., 2016), soybean hulls (Merci et al., 2015), corncob (Shao et al., 2020) and so on. The crystallinity of the TW-MCC was found to be similar to that of the MCC synthesized from waste cotton fabrics (Hou et al., 2019) and sugarcane bagasse (Thiangtham et al., 2020). Since these MCCs (cotton fabrics waste, sugarcane

bagasse) were isolated via acid hydrolysis, whereas the tea waste MCC was synthesized using alkaline peroxide, it can be concluded that the method of extracting MCC through microwave-assisted alkaline peroxide bleaching is more suitable with respect to industrial aspect.

**Table 3.3** Comparison of the synthesized TWMCC with other reported biomass-based MCCs

| **Biomass** | **Treatment method used** | **Time required for the treatment** | **Crystallinity index (%)** | **References** |
|---|---|---|---|---|
| Jute | Acid hydrolysis: 64 wt% $H_2SO_4$, at 45 °C | 300 min | 74.90 | (Jahan et al., 2011) |
| Waste cotton fabrics | Acid hydrolysis: 3.47 M phosphotungstic acid, at 140 °C | 360 min | 85.20 | (Hou et al., 2019) |
| Rose stems | Acid hydrolysis: 300 g/L $H_2SO_4$, at 80 °C | 120 min | 56.20 | (Ventura-Cruz & Tecante, 2019) |
| Rose stems | Alkaline peroxide bleaching: 5 wt% NaOH and 16% (v/v) $H_2O_2$, at | 90 min | 70.20 | (Ventura-Cruz et al., 2020) |

| | | | | |
|---|---|---|---|---|
| | 55 °C | | | |
| Rice husk | Acid hydrolysis: 4 M $H_2SO_4$, at 60 °C | 60 min | 47.60 | (Sim et al., 2016) |
| Soybean hulls | Reactive extrusion: two step extrusion with NaOH followed by $H_2SO_4$, in a single screw extruder at 110 °C and 100 rpm screw speed | ---- | 70.00 | (Merci et al., 2015) |
| Oil palm empty fruit bunch | Acid hydrolysis: 45% (v/v) $H_2SO_4$, at 45 °C | 45 min | 66.99 | (Pujiasih et al., 2018) |
| Oil palm fronds | Acid hydrolysis: 2.5 N HCl, at 45 °C | 30 min | 62.30 | (Owolabi et al., 2017) |
| Sugarcane bagasse | Acid hydrolysis: 4 M HCl, at 80 °C | 60 min | 84.10 | (Thiangtham et al., 2020) |
| Corncob | Acid hydrolysis: 1 M HCl, at 90 °C | 60 min | 52.82 | (Shao et al., 2020) |
| Oolong tea | Acid hydrolysis: 1.5 M | 90 min | 81.00 | (Zhao et al., |

| | | | | |
|---|---|---|---|---|
| waste | HCl, at 65 °C | | | 2018) |
| Black tea waste | Alkaline peroxide bleaching: 5 wt% NaOH and 4.7 M $H_2O_2$, 55 °C | 90 min | 76.83 | This work |
| Black tea waste | Alkaline peroxide bleaching: 5 wt% NaOH and 4.5 M $H_2O_2$, under microwave heating | **0.5 min** | **89.77** | **This work** |

### 3.4.3 Morphology analysis (FESEM)

The morphology of raw untreated TW, DL-TW, TW-BL1, TWMCC-MW and TWMCC-con, as studied by FESEM, are illustrated in **Fig. 3.5**. It was clearly seen in **Fig. 3.5a** that raw tea waste has thick, well-closed fibres with the smooth surface having a protective layer covering the grooves making the fibres nonporous. After the alkaline treatment, the structure of the fibres got disrupted, resulting in thinner, exposed, and apparently rough surface morphology, as shown in **Fig. 3.5b**. A significant change in the morphology was observed after the bleaching treatments (**Fig. 3.5c and 3.5d**). After the two consecutive bleaching, as shown in **Fig. 3.5d**, the fibres were separated into singular fibres with shorter diameters, more exposed and rougher surfaces, indicating the complete removal of the binding components such as lignin and hemicellulose as a result of which individual fibrillary components are released (Kian et al., 2020; Zhao et al., 2018).

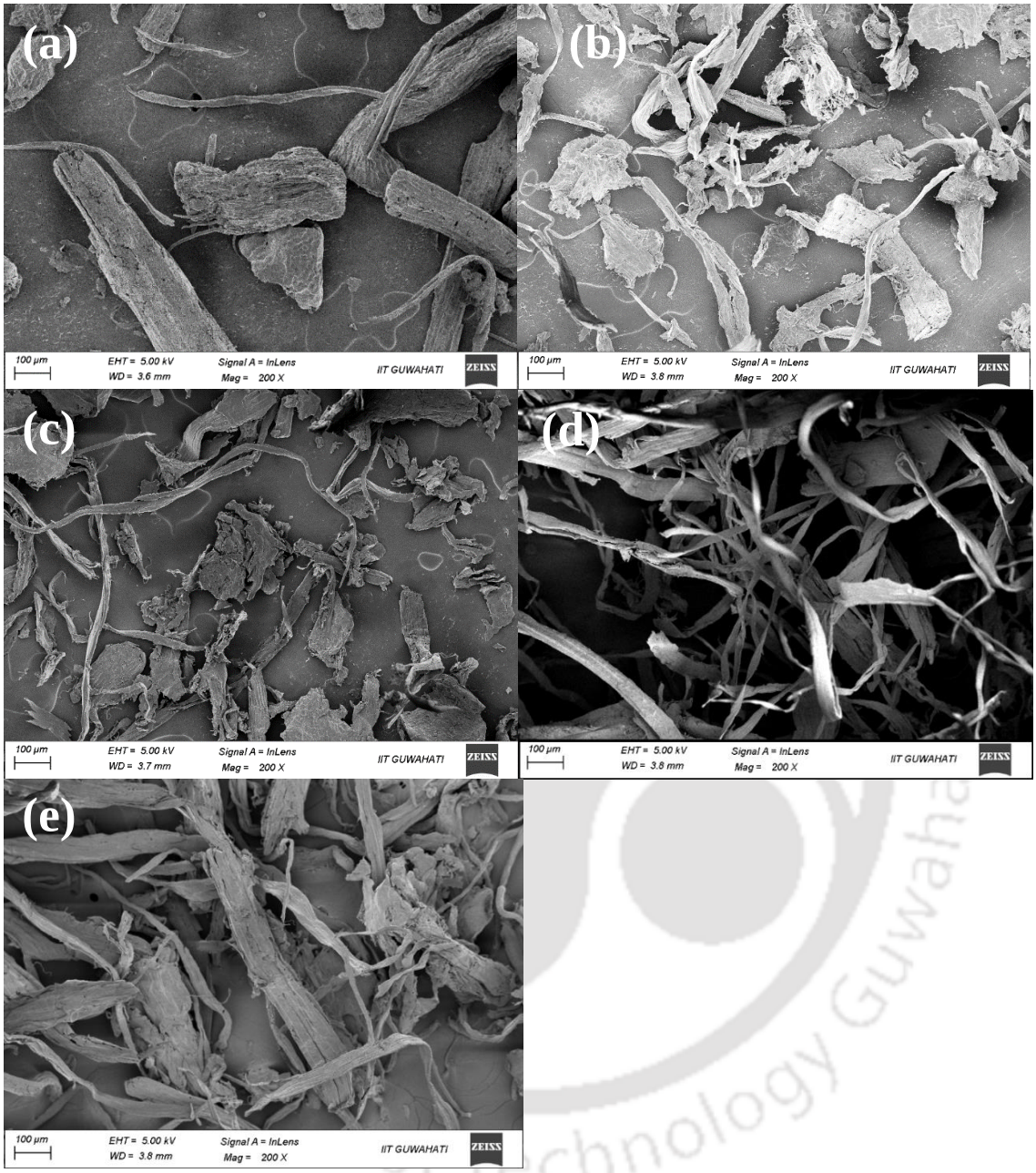


**Figure 3.5** FESEM images of a) raw TW, b) DL-TW, c) TW-BL1, d) TWMCC-MW, and e) TWMCC-con

Consecutive bleaching with alkaline hydrogen peroxide under microwave heating significantly removed the lignin matrix surrounding the tea waste fibres resulting in the formation of looser crystalline cellulosic fibres. Similar results were obtained by

Debnath et al. (Debnath et al., 2022) and Ventura-Cruz et al. (Ventura-Cruz et al., 2020). The diameters of the tea waste MCC fibres were calculated from the FESEM images using ImageJ software. Most of the raw tea waste fibres had diameters in between 86-200 µm. After the microwave-assisted delignification, the diameters of most of the fibres reduced to the range of 22-97 µm, while some fibres still had a diameter of around 150µm. After two consecutive microwave-assisted bleachings, the diameter of the synthesized TWMCC-MW particles was found to be within the range of 11-43 µm, and the average particle diameter was around 23 µm. As shown in **Fig. 3.5e**, the conventionally prepared tea waste MCC (TWMCC-con) had particle sizes ranging from 15-67 µm, having an average diameter of 31 µm. Hence, it can be said that microwave heating produces microcrystalline cellulose with a lower particle size as compared to those prepared by the conventional heating method.

### 3.4.4 Analysis of thermal stability (TGA)

TGA (thermo-gravimetric analysis) and DTG (derivative thermogram) curves of the synthesized tea waste MCCs are depicted in **Fig. 3.6a and 3.6b**, respectively. From **Fig. 3.6a**, it can be observed that the thermal degradation of all the samples resulted in an initial weight loss between the temperatures 45-110 °C, which is due to the elimination of water present in the cellulose samples. The primary decomposition stage occurred between 200-335 °C, which is attributed to the breakdown of cellulose and hemicellulose components. The decomposition of raw tea waste started at around 204 °C, while the delignified tea waste and TWMCC-MW started to degrade at temperatures 220 and 234 °C, respectively. The observations reveal that microwave-assisted quick

delignification and bleaching treatments increased the thermal stability of TWMCC-MW with respect to raw tea waste biomass. This enhancement in thermal stability is related to the removal of amorphous compounds (hemicellulose and lignin) in the synthesized TWMCC-MW because the degradation temperatures of hemicellulose and lignin are lower than cellulose (Liu et al., 2018; Ventura-Cruz et al., 2020). TWMCC-MW exhibited a slightly higher onset degradation temperature than the delignified tea waste, which may be associated with its more crystalline structure with respect to DL-TW (Kian et al., 2020). The black tea waste MCC synthesized by conventional heating method (TWMCC-con) showed a slightly lower onset degradation temperature of around 229 °C. The onset degradation temperature of the MCCs prepared from black tea waste in the present study are almost similar to the MCC isolated from oolong tea waste via conventional acid (hydrochloric acid) hydrolysis that starts to decompose at around 230 °C (Zhao et al., 2018). DTG curves (**Fig. 3.6b**) show that there was no significant change in the peak degradation temperatures of the samples. Raw TW has maximum weight loss at around 317 °C, whereas the maximum decomposition temperature of TWMCC-MW was found to be slightly higher than 323 °C. The conventionally synthesized TWMCC-con showed a similar peak degradation temperature of 319°C, indicating that both the microwave-assisted and conventional methods produced MCC with comparable thermal properties. It was reported that hemicellulose and lignin decompose at around 290 and 450 °C, respectively.

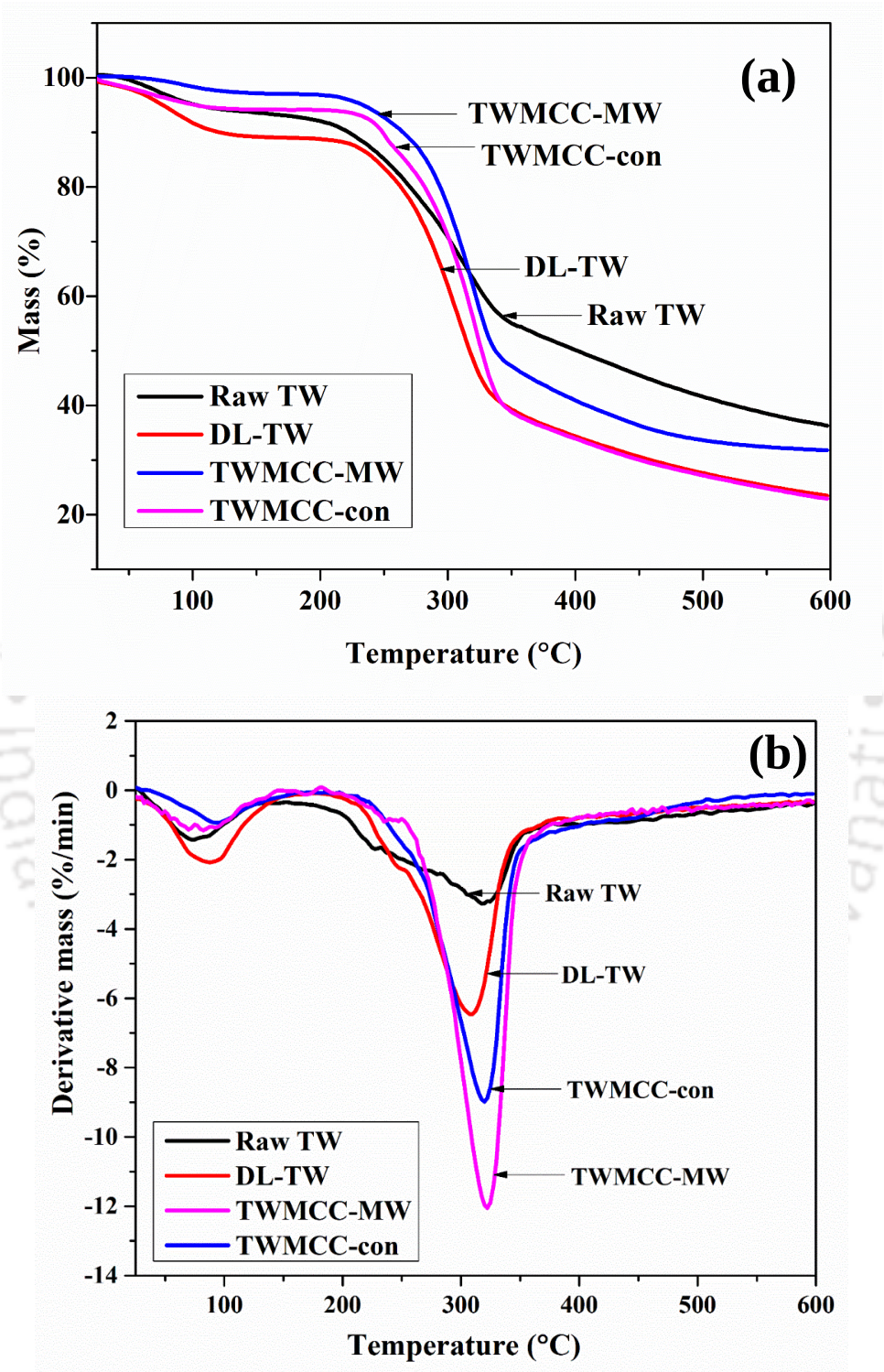


**Figure 3.6** TGA (a) and DTG (b) curves of raw TW, DL-TW, TWMCC-MW, and TWMCC-con

The DTG curve having no weight loss peaks at 290 and 450 °C indicates the absence of hemicellulose and lignin in the synthesized tea waste MCC. This is in agreement with the results obtained in FTIR and XRD analysis (Debnath et al., 2022; Zhao et al., 2018).

## 3.5 Statistical analysis using RSM

The sum of squares, *F* value, and *p* value of the developed model obtained from ANOVA analysis are summarized in **Table 3.4**. The mathematical model for the response variables has been represented using cubic expression that was deduced from the central composite design. The cubic model expression for the response crystallinity index has been presented as follows:

$$\text{Crystallinity index} = +89.20 + 6.37A - 0.12B - 0.16C - 1.18AB + 4.62AC + 0.63BC - 5.71A^2 - 1.18B^2 - 0.71C^2 + 1.39ABC + 0.85A^2B - 3.41A^2C - 2.36AB^2 \quad (3.3)$$

As shown in **Table 3.4**, the *p-values*, *F*-values and R-squared values suggest the significance of the developed cubic model. In any model, *p* values > 0.1 indicates insignificancy of the model. It was observed from the table that the model has *p* values less than 0.0001. The model *F* value 735.85 implies the model is significant and there is only 0.01% error corresponding to high *F* value which can be neglected. The independent variable of heating time (A) has *p* value < 0.0001 indicating its significance, whereas hydrogen peroxide concentration (B) and tea waste to solvent ratio (C) have *p* values greater than 0.1 demonstrating their negligible interaction relative to the product crystallinity. In this case A, AB, AC, BC, ABC, and the various quadratic terms of the independent control variables ($A^2$, $B^2$, $C^2$, $A^2B$, $A^2C$, $AB^2$) are

significant. Microwave heating time exhibited the greatest effect on the crystallinity of the synthesized tea waste MCC by showing the highest *F*-value of 1021.86. The lack of fit was found to be not significant. The predicted $R^2$ value (0.8752) and adjusted $R^2$ value (0.9980) of the developed model show good agreement. Additionally, the lower values of standard deviation (0.28) and the coefficient of variation (0.33%) implies the reproducibility of the developed model. The signal to noise ratio determined in terms of adequate precision must be more than 4 for successful resolution of the model. Here, the designed model shows an adequate precision value of 91.75, representing its acceptability (Das et al., 2022; Karim et al., 2014).

**Table 3.4** ANOVA of the regression parameters of the developed cubic model to identify significant factors

| Source | Sum of Squares | df | Mean Square | *F* Value | *p*-value prob > *F* | Comments |
|---|---|---|---|---|---|---|
| **Model** | 759.71 | 13 | 58.44 | 735.85 | < 0.0001 | significant |
| **A-Time** | 81.15 | 1 | 81.15 | 1021.86 | < 0.0001 | |
| **B-Hydrogen peroxide concentration** | 0.026 | 1 | 0.026 | 0.33 | 0.5849 | |
| **C-Tea waste to solvent ratio** | 0.054 | 1 | 0.054 | 0.69 | 0.4393 | |

| | | | | | |
|---|---|---|---|---|---|
| **AB** | 11.16 | 1 | 11.16 | 140.56 | < 0.0001 |
| **AC** | 170.85 | 1 | 170.85 | 2151.26 | < 0.0001 |
| **BC** | 3.21 | 1 | 3.21 | 40.46 | 0.0007 |
| **$A^2$** | 89.63 | 1 | 89.63 | 1128.63 | < 0.0001 |
| **$B^2$** | 3.86 | 1 | 3.86 | 48.55 | 0.0004 |
| **$C^2$** | 1.40 | 1 | 1.40 | 17.66 | 0.0057 |
| **ABC** | 15.43 | 1 | 15.43 | 194.28 | < 0.0001 |
| **$A^2B$** | 1.15 | 1 | 1.15 | 14.51 | 0.0089 |
| **$A^2C$** | 18.59 | 1 | 18.59 | 234.10 | < 0.0001 |
| **$AB^2$** | 8.90 | 1 | 8.90 | 112.09 | < 0.0001 |
| **$AC^2$** | 0.000 | 0 | | | |
| **$B^2C$** | 0.000 | 0 | | | |
| **$BC^2$** | 0.000 | 0 | | | |
| **$A^3$** | 0.000 | 0 | | | |
| **$B^3$** | 0.000 | 0 | | | |
| **$C^3$** | 0.000 | 0 | | | |

| | | | | | | |
|---|---|---|---|---|---|---|
| **Residual** | 0.48 | 6 | 0.079 | | | |
| **Lack of Fit** | 0.077 | 1 | 0.077 | 0.96 | 0.3719 | not significant |
| **Pure Error** | 0.40 | 5 | 0.080 | | | |
| **Cor Total** | 760.19 | 19 | | | | |

The 3-D RSM plots representing the effect of the different process control variables on the crystallinity index of the synthesized TWMCC-MW are depicted in **Fig. 3.7**. It was observed that as the time of microwave heating was increased, the percentage crystallinity also increased. The reason behind this may be stated that the high heating time would increase the diffusion of the solvents into the amorphous region of cellulose and thereby removing the amorphous components resulting in higher crystallinity (Karim et al., 2014). $H_2O_2$ concentration has moderate effect on the crystallinity. However, a lower level of $H_2O_2$ will be desirable with respect to bulk scale industrial production of MCC to avoid its harsh impacts on the plant equipment. The effect of solvent ratio on the product crystallinity is not much significant. The solvent volume should be kept minimal to eliminate the toxic effects of chemicals on the environment and make the production process cost-effective. The experimental method showed the highest crystallinity of 89.77% for the bleaching conditions of 30sec microwave heating time, 4.5 M $H_2O_2$ concentration and 1:20 tea waste to solvent ratio.

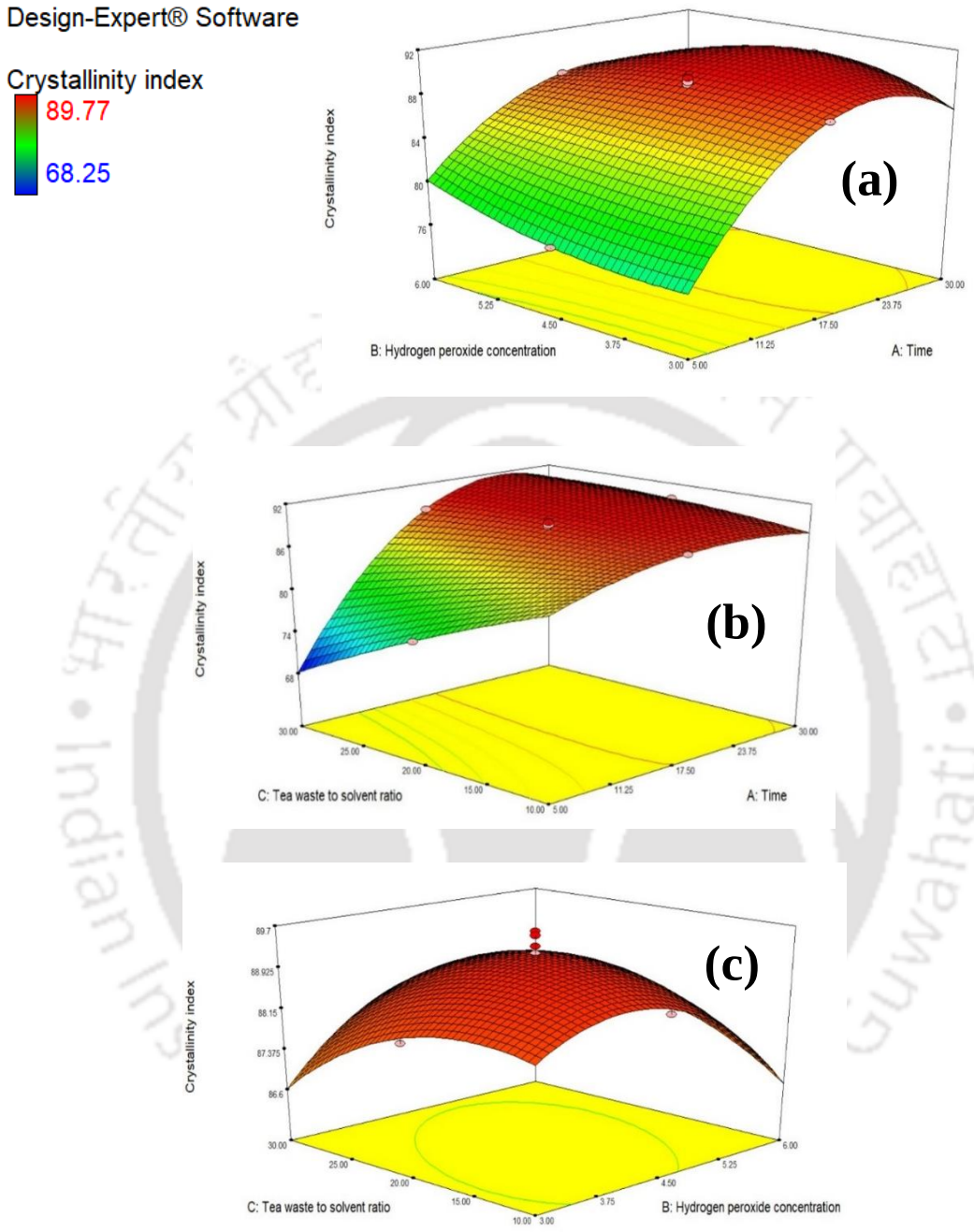


**Figure 3.7** 3-D RSM plots representing the effect of (a) heating time and hydrogen peroxide concentration; (b) heating time and tea waste to solvent ratio, and (c) tea waste to solvent ratio and hydrogen peroxide concentration, on the crystallinity index of the synthesized TWMCC-MW

A numerical optimization was carried out to maximize crystallinity keeping the process control variables within the considered range. The optimal control variable values for the extraction process are 23.70 sec, 4.78 M and 17.37 for microwave heating time, $H_2O_2$ concentration and tea waste to solvent ratio, respectively. The corresponding predicted response variable i.e. crystallinity index is 90.33%. TWMCC-MW was prepared under these optimum conditions and the crystallinity of the sample was found to be 89.12%. The experimental value is in good agreement with the RSM predicted value of crystallinity index and hence the model fitness is highly relevant for the specified range of control variables.

## 3.6 Summary

This chapter emphasizes on the synthesis of microcrystalline cellulose from black tea waste using a quick technique involving microwave heating. The findings of the present work demonstrate that tea waste produced in tea factories during the manufacturing of black tea can be utilized as an abundant, renewable, and cheap source of value-added microcrystalline cellulose. Consecutive bleaching with alkaline hydrogen peroxide is an efficient technique to replace the conventional acid hydrolysis method for the synthesis of microcrystalline cellulose to avoid the corrosive effects of mineral acids. Additionally, the usage of microwave heating in the various treatment steps significantly reduces the time required for the extraction of tea waste microcrystalline cellulose. The optimization of the bleaching conditions (microwave heating time, hydrogen peroxide concentration, tea waste to solvent ratio) was carried out using RSM analysis to obtain microcrystalline cellulose with maximum crystallinity. TWMCC was

also synthesized using conventional heating and its properties were compared with those of the sample synthesized under microwave heating. Microwave heating assisted alkaline peroxide bleaching provides a green, energy-efficient, and fast technique for the production of valuable microcrystalline cellulose from industrial black tea wastes.

# Chapter 4

# Preparation of tea waste microcrystalline cellulose reinforced polyvinyl alcohol packaging films and their application in grapes preservation

*In this chapter, the detailed method for the development of polyvinyl alcohol (PVA) packaging films reinforced with tea industry waste derived microcrystalline cellulose (TWMCC) for preserving fruits has been discussed. The pure PVA film and TWMCC/PVA composite films were prepared via solvent casting approach and their various physicochemical properties then investigated using FTIR, FESEM, TGA, water contact angle measurement, moisture content and solubility analysis, water vapour permeability, tensile strength testing (UTM) and UV-barrier properties analysis. To evaluate the performance of the films for packaging, fresh grapes were wrapped using the prepared films by heat sealing and the change in their visual appearance were studied for a period of 20 days. The background of this work, recent literature and the scope for this work have been discussed in Chapter 1, Section 1.6 and Section 1.7.5, respectively.*

## 4.1. Experimental

### 4.1.1 Materials

Polyvinyl alcohol (PVA) with molecular weight (M.W) 115000 and degree of polymerization (DP) of 1700-1800 was purchased from Loba Chemie, India. Water from the Millipore Milli-Q purification system was used as the solvent throughout the

experiments. Fresh green grapes were collected from a local market. They were thoroughly washed to remove any adhered dust and dirt particles and dried in air.

### 4.1.2 Preparation of tea waste microcrystalline cellulose reinforced PVA films

Microcrystalline cellulose was extracted from tea waste through the microwave-assisted peroxide delignification approach as reported in our prior work (Debnath et al., 2023). To make the pure PVA film, a 5 wt% PVA solution was prepared by dissolving PVA in Milli-Q water at 85 °C for 1h under constant stirring at 500 rpm. Afterwards, 40 mL of the homogenous PVA solution was casted onto a glass petri dish having 18 cm diameter and dried in a hot air oven at 50 °C for 6 h. For preparing the tea waste MCC reinforced PVA films, 1, 3, and 5 wt% of TWMCC (relative to the PVA mass) were initially dispersed in Milli-Q water for 18 h at room temperature under continuous stirring at 700 rpm. After that, PVA was added to the dispersions and the same procedure was followed as the pure PVA film. The dried films were finally peeled off from the petri plates. The volume of the casting solution for each sample was kept constant to attain similar thickness of all the samples. The PVA films with 1, 3 and 5 wt% of TWMCC are denoted as PVA/MCC-1, PVA/MCC-3 and PVA/MCC-5, respectively. All the films were conditioned at 50% relative humidity for 2 days prior to characterization.

## 4.2 Characterization of the prepared films

### 4.2.1 Determination of chemical functionality

Fourier transform infrared (FTIR) spectroscopy was carried out for anyalysing chemical functionality of the prepared PVA composite films. A Perkin Elmer (Spectrum two, Singapore) FTIR spectrometer was used to scan the films in the wavenumber range of 4000–400 $cm^{-1}$.

### 4.2.2 Determination of crystallinity

Crystalline structure of the prepared PVA films were determined using an X-ray diffractometer (smartlab, Rigaku technology, Japan). Each sample was scanned in between the diffraction angles (2θ) of 5–40° with step size 0.02°. The crystallinity index (CrI) of the films were calculated.

### 4.2.3 Surface morphology analysis

The surface morphology of the PVA composite films were analyzed using field emission scanning electron microscopy (FESEM, Zeiss, Sigma 300) at 5 kV accelerating voltage. The films were coated by spraying gold for 2min prior to analysis and scanned at 10000x magnification.

### 4.2.4 Thermogravimetric analysis

Thermogravimetric (TG) and derivative thermogram (DTG) analyses were performed using a Thermogravimetric analyzer (Netzsch, STA449F3A00) to check the thermal stability of the prepared PVA films. About 5mg of the films were heated from room temperature to 600 °C with 10 °C/min heating rate in argon atmosphere (20 mL/min flow rate).

### 4.2.5 Analysis of hydrophilic property

Contact angle meter (Holmarc, HO-IAD-CAM-01B) was used to analyse the surface hydrophilicity of the PVA composite films. At room temperature, 5 μL Milli-Q water was placed on the film surface and contact angle of the water droplet was measured. Water contact angle was measured three times for each of the films and the average values were reported.

### 4.2.6 Determination of water-resistance properties

Moisture content (MC) of the PVA films were determined according to a gravimetric method as described in our previous study (Debnath et al., 2022). 20 mm × 20 mm square samples of the films were initially weighed ($M_0$) and oven-dried at 100 ℃ for 24 h to a constant weight ($M_1$). The following equation was then used to calculate moisture content:

$$MC = \frac{M0-M1}{M0} \times 100\% \quad (4.1)$$

Swelling rate (SR) and water solubility (WS) of the PVA composite films were determined according to the methodology as reported by Lei et al. (Lei et al., 2021). 20 mm × 20 mm square samples of the PVA composite films were oven-dried at 100 ℃ for 24 h and the initial dry weight ($M_1$) were measured. The dried films were next immersed in distilled water at room temperature for 24 h. The films were then taken out of water, the excess water on the film surfaces were wiped off using absorbent paper, and the final weight ($M_2$) of the films were measured. The following equation was then used to calculate swelling rate:

$$SR = \frac{M2-M1}{M1} \times 100\% \quad (4.2)$$

The average values of swelling rate of 3 independent specimen taken from different films are represented in the results.

To determine water solubility, the 2 cm × 2 cm square samples of the films dried at 100 ℃ for 24 h were taken into conical bottles, 100 mL Milli-Q water was added and subjected to continuous agitation in a shaker at 180 rpm speed for 6 h at room temperature. After filtration, the remaining samples were oven-dried at 100 °C for 24 h, and their final weight ($M_3$) were measured. Water solubility of the films was then calculated as per the following equation:

$$WS = \frac{M1-M3}{M1} \times 100\% \quad (4.3)$$

The average values of water solubility of 3 independent specimen taken from different films are represented in the results.

### 4.2.7 Water vapour barrier properties

A digital micrometre (Baker, IP65, India,) with 1µm accuracy was used to measure the thickness of the composite films. Measurements were taken at 10 different locations of each film and the average values are reported. Water vapour transmission rate (WVTR) and water vapour permeability (WVP) of the PVA composite films were determined according to a modified ASTM E96/E96M-16-Standard Test method as described by others (Jiang et al., 2022; Tanwar et al., 2021). Cups were initially filled (more than half) with dry silica gel to maintain a relative humidity of 0%. The mouths of the cups were covered with the fabricated films and sealed using waterproof tapes. The sealed cups were then placed inside desiccators containing ultrapure water to maintain 100%

relative humidity. The desiccators were kept at room temperature (25 °C). The change in weight of the cups were noted every 24 h for 7 days. Tests were conducted three times for each film and the average values were taken. Finally, WVTR and WVP were calculated as per the following equations:

$$\text{WVTR (g h}^{-1}\text{ m}^{-2}) = \frac{\Delta m}{\Delta t \times A} \quad (4.4)$$

$$\text{WVP (g mm h}^{-1}\text{ kPa}^{-1}\text{ m}^{-2}) = \frac{WVTR \times X}{\Delta p} = \frac{WVTR \times X}{P\ (R1-R2)} \quad (4.5)$$

where, Δm = weight change over time (g), X = film thickness (mm), A = exposure area or cup mouth area ($m^2$), Δt = specified time interval (h), ΔP = difference in water vapor pressure of the atmosphere with silica gel and ultrapure water (Pa), P = saturation vapor pressure at 25°C ($3.169 \times 10^3$ Pa), $R_1$ = relative humidity at desiccator (100%), $R_2$ = relative humidity at test cup (0%).

### 4.2.8 Determination of mechanical properties

Tensile strength, elastic modulus, and elongation at break of the composite films were measured with the aid of a universal testing machine (ZwickRoell, Z005TN Proline, load cell 5 KN) at ambient condition. The film specimens were cut into 70 mm × 15 mm rectangular strips. The initial separation of the grip was 40 mm and the crosshead displacement rate was set at 10 mm/min. Three measurements were recorded for each specimen and the average of the results are reported.

### 4.2.9 UV-barrier properties analysis

Light barrier properties of the prepared PVA composite films were studied using a UV–vis spectrophotometer (Shimadzu, UV-2600, Singapore) by measuring the transmission of light within the wavelength region of 200–800 nm.

## 4.3 Packaging performance of the composite films

The real-time packaging performance of the TWMCC reinforced PVA films were studied using grapes. Fresh grapes were purchased from a local fruit shop. Completely sealed bags were prepared with the PVA composite films using a heat-sealing machine and grapes were kept inside them. One grape was kept unwrapped to be used as control. All the samples were preserved at room temperature (~25 °C). The samples were photographed to observe the change in the visual appearance of the grapes and their weight loss was recorded at 2 days interval for a period of 20 days.

## 4.4 Results and discussion

The photographic representations of the PVA films reinforced with different levels of tea waste microcrystalline cellulose are depicted in **Fig. 4.1**. The pure PVA film was transparent and the addition of TWMCC decreased the transparency of the composite films to some extent. All the fabricated films were flexible, had smooth surface, and could be peeled off easily from the casting petri dishes. The various characteristics of the prepared films like functional groups, morphology, thermal behaviour, water and

water vapour barrier properties, mechanical behaviour, and light barrier properties were evaluated and the findings are presented in the following subsections.

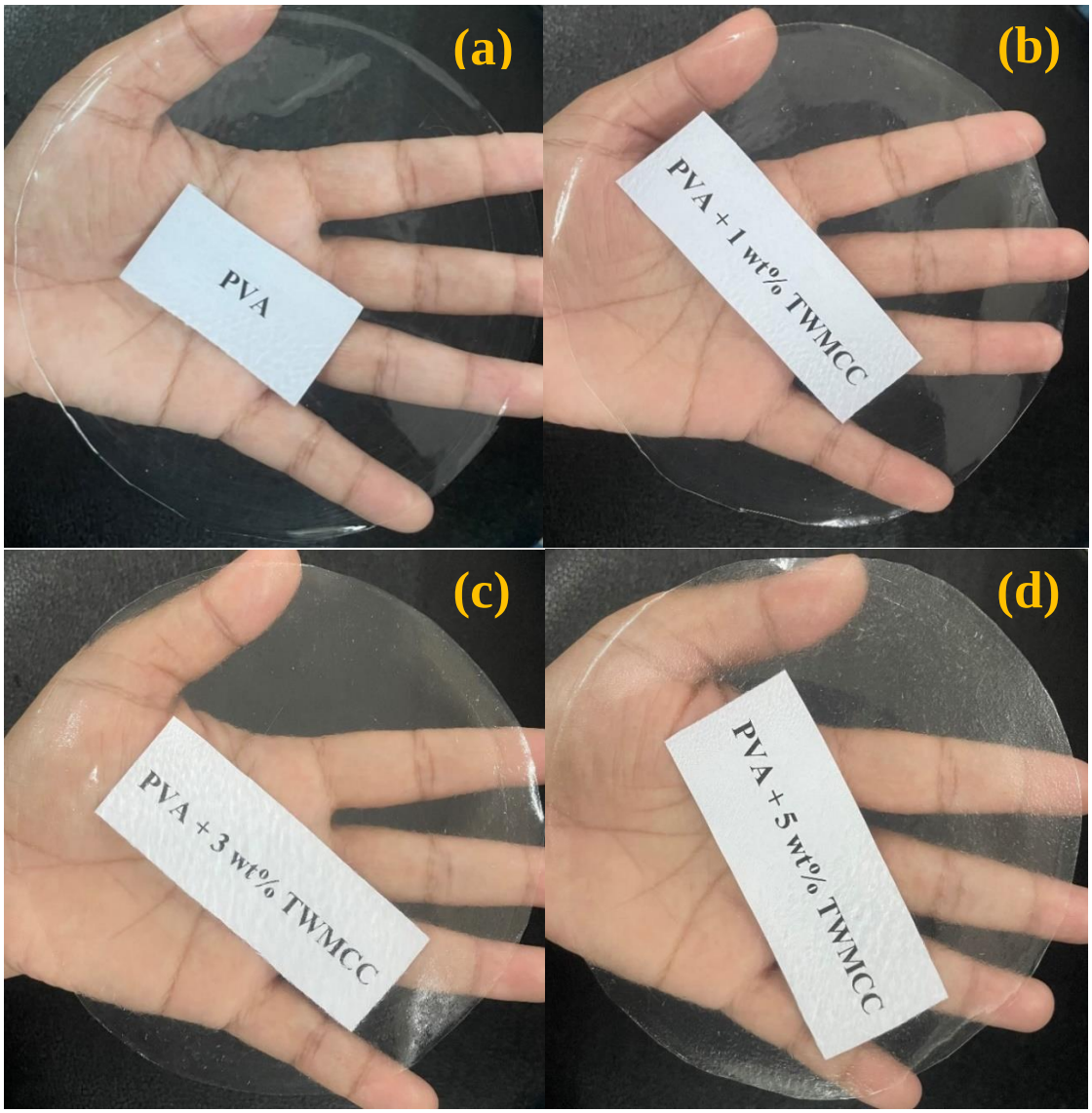


**Figure 4.1** PVA films incorporated with different levels of TWMCC: a) pure PVA, b) PVA/MCC-1, c) PVA/MCC-3, and d) PVA/MCC-5

### 4.4.1 Determination of chemical functionality

The FTIR spectra of PVA, PVA/MCC-1, PVA/MCC-3 and PVA/MCC-5 are illustrated in **Fig. 4.2**. The characteristic peaks at located 3270 $cm^{-1}$ is allotted to the stretching vibration of hydroxyl (O–H) groups of the alcohol and carboxylic acid. This distinctive peak on the FTIR spectrum of pure PVA indicates the presence of free O–H groups due to strong intra and intermolecular bonds. The intensity of this peak decreased after the addition of TWMCC with an increase in peak width. This can be ascribed to the interaction between the hydroxyl groups present in the PVA matrix and on the surface of TWMCC through the formation of solid hydrogen bonds, which reduced freely available O–H groups on the PVA composite films (Baite et al., 2023; Sarwar et al., 2018). The absorption band at 2923 $cm^{-1}$ corresponds to the C–H stretching of the alkyl groups (Zhao et al., 2023). The band located at 1710 $cm^{-1}$ may be related to stretching vibration of C═O group because of the residual acetate group present in PVA as it was made from partial hydrolysis of polyvinyl acetate (Tanwar et al., 2021; Widyaningrum et al., 2022). The peaks appearing at 1419 $cm^{-1}$ are assigned to symmetric bending mode of $CH_2$ groups. The bands at 1086 $cm^{-1}$ correspond to stretching vibrations of C–C and C–O groups. The peaks located at 841 $cm^{-1}$ is associated with stretching vibrations of C–C groups and out of plane bending vibration of O–H groups. The variation in intensities of the spectral bands at 1086 and 841 $cm^{-1}$ of the PVA composite films with respect to pure PVA are indicative of intermolecular interactions between the O–H groups from TWMCC and O–H groups of the PVA polymer matrix, as proposed by other authors (Popescu et al., 2018; Tanwar et al., 2021). The absorption band at 1328

$cm^{-1}$ is ascribed to C-H deformation vibration (Rajesha Shetty & Lakshmeesha Rao, 2022). The peak absorptions of PVA/TWMCC films were similar to that of the neat PVA film, indicating that TWMCC reinforcement did not influence the chemical structure or functionality of the PVA film. This suggests strong inter and intramolecular bonds between PVA matrix and tea waste MCC, thus representing good compatibility between them (Debnath et al., 2022).

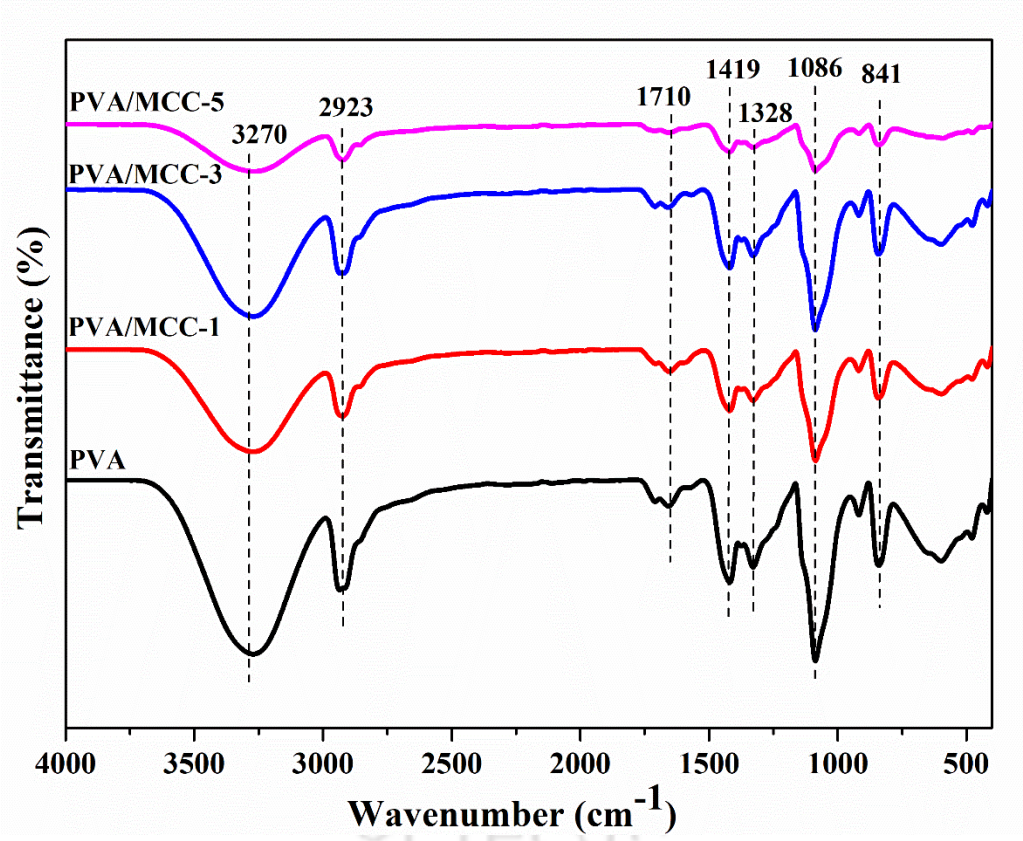


**Figure 4.2** FTIR spectra of PVA films incorporated with different levels of TWMCC

### 4.4.2 Crystallinity of the PVA composite films

The XRD patterns of the pure and TWMCC-incorporated PVA films have been shown in **Fig. 4.3**. All the films exhibited a sharp diffraction peak at 2θ = 19.4° and a shoulder at 22.6°, which are characteristic peaks of PVA corresponding to reflection from the

(101) and (200) crystallographic planes, respectively. The distinctive peak matching with (101) plane represents a semi-crystalline structure of the composite films due to physical interaction through hydrogen bonds in between O–H groups of PVA and TWMCC fillers (Baite et al., 2023; Tanwar et al., 2021). The intensity of the signal increased with the addition of 1 and 3 wt% TWMCC into PVA film, confirming increased crystallinity of the composite films. However, PVA film containing 5 wt% TWMCC showed a very low peak intensity and enhanced peak width indicating that higher concentration of the filler weakens the crystalline behaviour of PVA film (Lei et al., 2021).

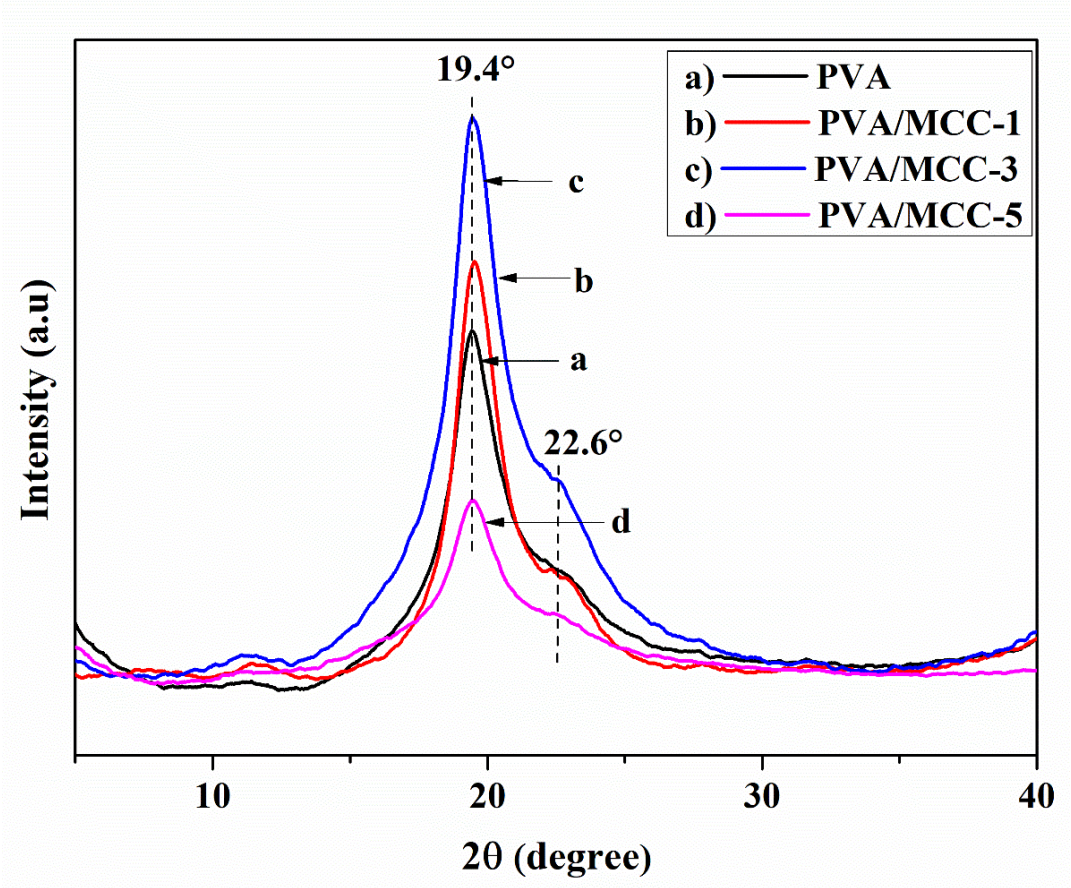


**Figure 4.3** XRD patterns of PVA films reinforced with different levels of TWMCC

The reason behind the decreased crystallinity of PVA/MCC-5 film might be the formation of more H-bonds between the large numbers of TWMCC particles and PVA, due to which the number of hydrogen bonds involved in PVA's crystalline structure get reduced (Popescu et al., 2018). The crystallinity indices of the films were calculated and it was observed that pure PVA film has a CrI of 73.43%. PVA/MCC-1 and PVA/MCC-3 films show increased crystallinity of 84.65 and 87.42%, respectively. The CrI value of the film reinforced with 5 wt% TWMCC decreased to 71.52%.

### 4.4.3 Surface morphology of the films

The surface morphology of neat PVA, PVA/MCC-1, PVA/MCC-3, and PVA/MCC-5 films are shown in **Fig. 4.4.** It can be seen from the **Fig. 4.4a** that the neat PVA film has a uniform and homogeneous smooth surface morphology with no defects or cracks. This specifies the good film-forming property of the polymer during casting. When TWMCC is added at a low concentration (1 wt%) the filler particles dispersed homogeneously in the polymer matrix of the PVA/MCC-1 film, as seen in **Fig. 4.4b**. The existence of only a few agglomerates was observed in the PVA/MCC-3 film as shown in **Fig. 4.4c** as the tea waste MCC concentration was increased to 3 wt%. **Fig. 4.4d** shows that the PVA/MCC-5 film with higher level of TWMCC (5 wt%) exhibits a smooth surface with some blisters or white domain on individual regions resulting from agglomeration of the particles enclosed in the matrix. As reported in the previous chapter, the TWMCC filler particles have diameter in the range of 11-43 μm, with an average diameter of 23.06 μm (Debnath et al., 2023). The diameters of the particles agglomerated in the PVA/MCC-3

and PVA/MCC-5 films were calculated and found to be ranging from 44 to 89 µm. All the tea waste MCC reinforced PVA films showed homogeneous surfaces. The composite films did not show any microscopic phase separation between the components. Such homogeneous surface with no phase separation is an indicative of good compatibility and proper miscibility between PVA and tea waste MCC (Baite et al., 2022; Rajesha Shetty & Lakshmeesha Rao, 2022).

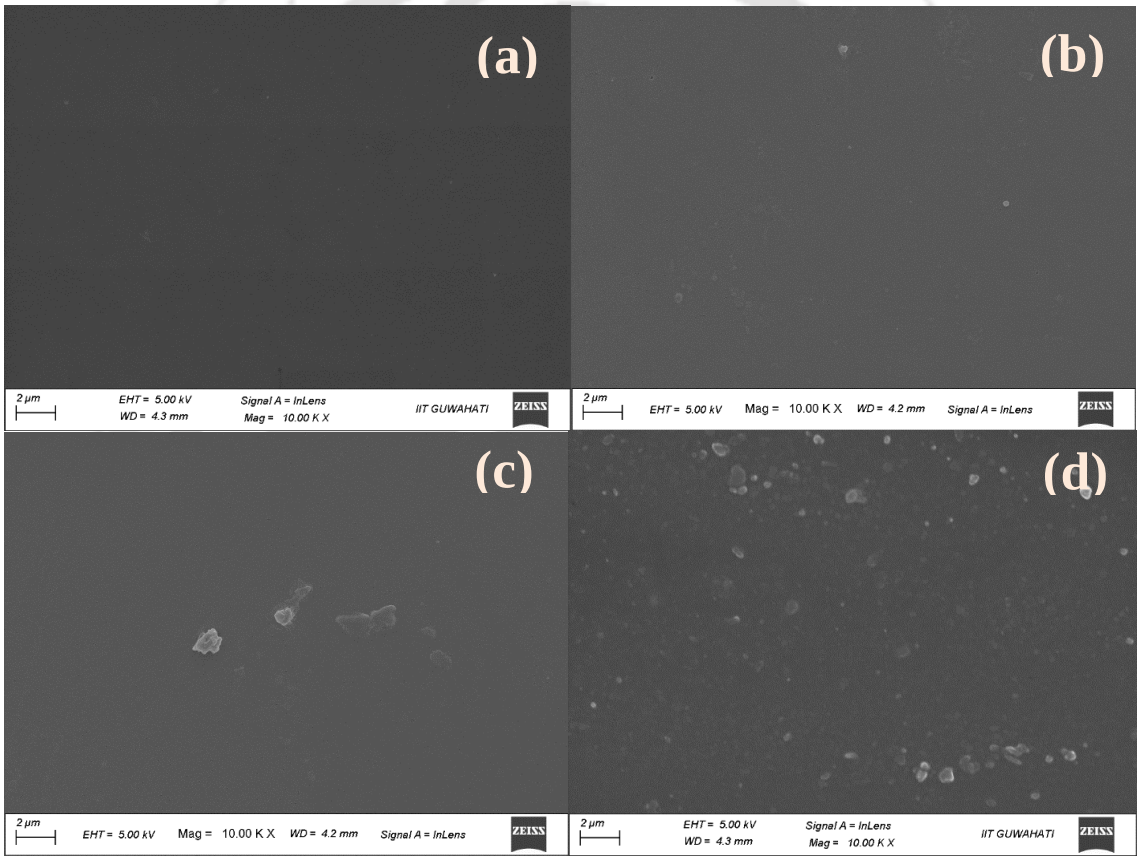


**Figure 4.4** FESEM images of a) neat PVA, b) PVA/MCC-1, c) PVA/MCC-3, and d) PVA/MCC-5 film

### 4.4.4. Thermogravimetric analysis

TGA and DTG curves of PVA films containing varying concentrations of tea waste microcrystalline cellulose are shown in **Fig. 4.5(i)** and **4.5(ii)**, respectively. As seen in **Fig. 4.5(i)**, multi-stage thermal decomposition was shown by all the films. The initial degradation stage observed in between 65–130 °C is associated with the evaporation of weakly bound moisture from the film surface. Following this a sharp degradation was observed in the 240–350 °C range, which is attributed to the starting of the degradation of the main polymer chain, along with the degradation of tea waste MCC. The last stage

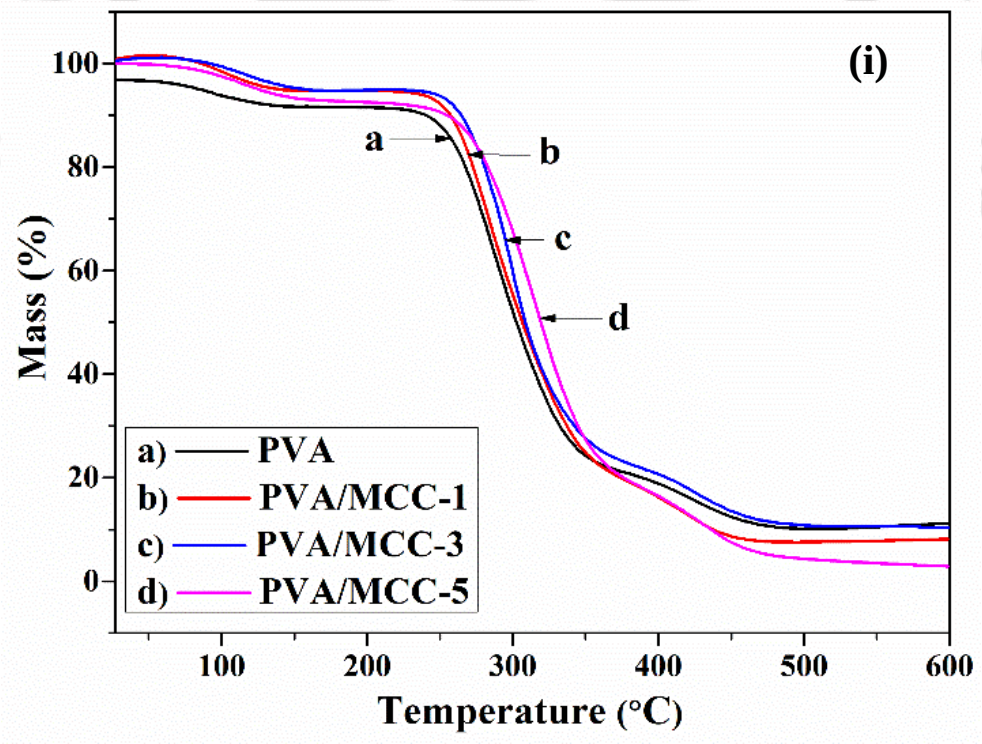

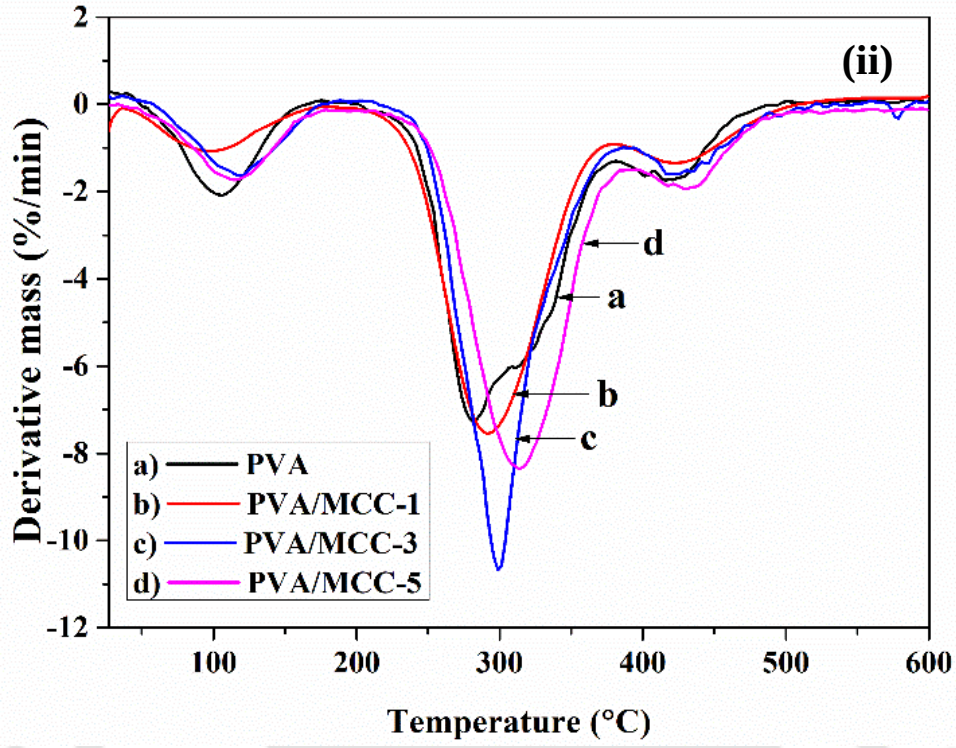


**Figure 4.5** i) TGA and ii) DTG graphs of PVA composite films incorporated with TWMCC at different concentrations

degradation occurring at around 405–452 °C corresponds to the decomposition of the main chain of PVA through the splitting of the C–C backbone (Baite et al., 2022). The pure PVA film started to decompose at about 240 °C, whereas the TWMCC incorporated PVA films exhibited higher degradation temperature. The reinforcement of the PVA films with TWMCC resulted in rightward shift of the TGA curves, suggesting enhancement in their thermal property. **Fig 4.5(ii)** shows that the maximum degradation temperature (Tmax) of the pure PVA film is around 289 °C. PVA/MCC-1 and PVA/MCC-3 showed slightly higher Tmax values of 293 and 298 °C, respectively. The PVA/MCC-5 has the highest Tmax value of around 314 °C, which is significantly higher than the pure PVA film. These findings indicate that the incorporation of 5 wt% of tea waste MCC can enhance the thermal properties of the PVA packaging films to a

great extent (Widyaningrum et al., 2022). XRD analysis results confirmed that PVA films reinforced with TWMCC fillers possess high crystallinity. The incorporation of crystalline cellulose results in increased crystallinity and rigidity of the films due to strong interaction between the TWMCC particles and PVA, and therefore elevated temperatures are required to degrade the composite films. This is the underlying reason behind the improved thermal stability of the TWMCC reinforced PVA films (Debnath et al., 2022).

### 4.4.5. Determination of hydrophilicity

Water contact angle images of the PVA composite films filled with different levels of TWMCC are displayed in **Fig. 4.6**. In general, a high value of water contact angle represents surface hydrophobicity, while a low contact angle indicates hydrophilic nature. Water contact angle of pure PVA film was found to be 29.31°, suggesting high hydrophilicity which is due to the existence of multiple O–H groups (Jiang et al., 2023). The water contact angle of all the composite films increased after the incorporation of tea waste MCC. Addition of 1 wt% TWMCC had little effect on the hydrophilic property of the PVA/MCC-1 film and increased the contact angle up to 37.10°. Further increase in TWMCC level significantly increased the film's surface hydrophobicity as the PVA/MCC-3 film showed a contact angle value around 52.36° and the PVA/MCC-5 film had the highest water contact angle of 81.54°. This reduction in wettability of the PVA films might be because of the dense network structure of the composites, due to which the freedom of O–H groups decreased on the film surface (Feng et al., 2022).

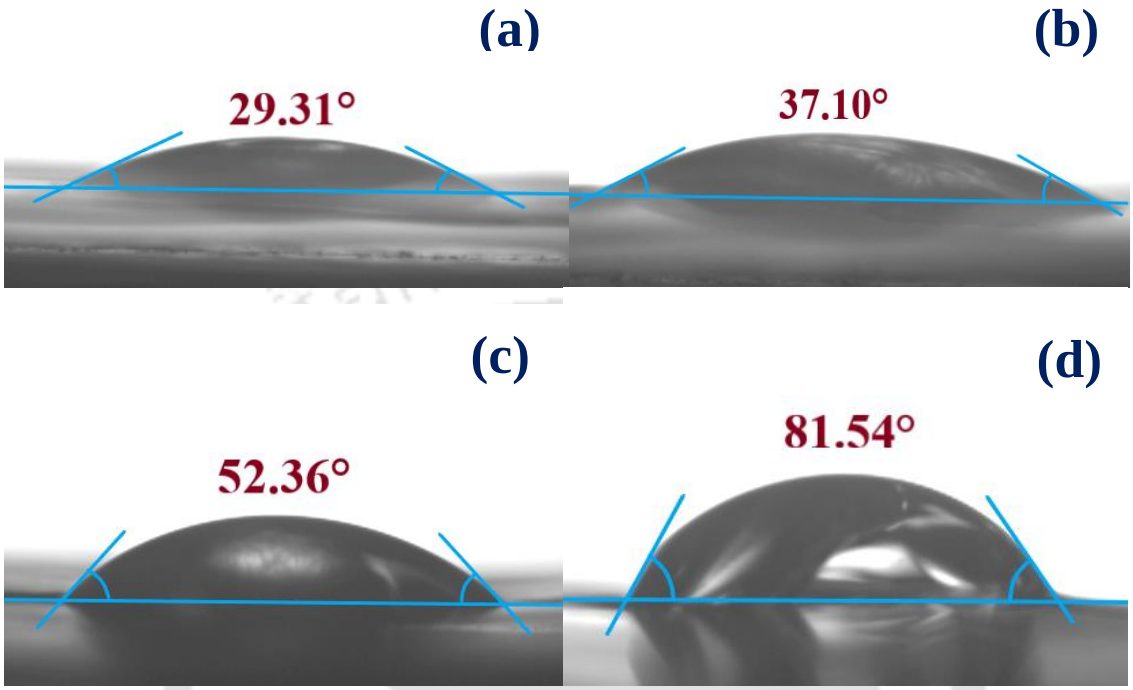


**Figure 4.6** Water contact angle images of a) pure PVA, b) PVA/MCC-1, c) PVA/MCC-3, and d) PVA/MCC-5 film

Microcrystalline cellulose extracted from industrial black tea waste has hydrophilic nature because of the presence of a large number of O–H groups that facilitate interaction with the molecules of water. However, the same O–H groups of TWMCC enables the formation of compact networks within the PVA matrix and thus decreases the interaction between water and film surface (Srivastava et al., 2021).

### 4.4.6 Water-resistance properties

The water resistance properties i.e., moisture content, swelling rate and water solubility of the PVA films reinforced with different concentrations of tea waste MCC are shown in **Table 4.1**. If the adhesion between reinforcing filler and polymer matrix is poor,

moisture easily enters the composite material, leading to increased moisture sensitivity of the composites. In the present study, the observed MC of the pure PVA film was 13.93 ± 1.84% and it showed a declining trend with the incorporation of TWMCC. The PVA/MCC-5 film exhibited the lowest moisture content of 8.17 ± 1.74%. Moisture absorption depends on the crystallinity of polymers. Moisture content decreases with increase in crystallinity of the films. The findings of XRD analysis confirmed that TWMCC filler enhanced the crystallinity of PVA composites, which leads to lower moisture absorption of the reinforced films (Negoro et al., 2016). Solubility of the PVA composite films also decreased when TWMCC content was increased. The WS of pure PVA film was 29.79 ± 0.53% and the PVA/MCC-5 film showed the lowest solubility of 16.67± 0.21%. The reason behind the decrease in moisture content and water solubility of the films is the better interaction between the O–H groups of PVA and TWMCC through hydrogen bonding. The possibility of moisture absorption gets reduced because of the less availability of free O–H groups in the PVA matrix, as they take part in the H-bonding with TWMCC and thus decrease the interplay between PVA-OH and water. Crystalline cellulose promotes the intermolecular interactions between PVA and TWMCC to form a compact network (Debnath et al., 2022). The pure PVA film has the highest swelling rate of 205.01 ± 2.35% owing to the presence of numerous O–H groups on its polymer chains and poor crystalline property, which facilitate the swelling of the polymer network in water. The films reinforced with tea waste MCC exhibited reduced swelling behaviour because of the interaction between PVA and TWMCC that made the films tighter and compact. The lowest SR observed was 128.57 ± 0.23% at the TWMCC level of 5wt%. As the TWMCC concentration was increased in the PVA matrix, more

bonds were developed binding the O–H groups of PVA and hence the swelling of water molecules reduced (Helmiyati et al., 2021; Jiang et al., 2023). Crystalline phase is virtually impermeable to water molecules, and hence the high crystallinity of the TWMCC incorporated PVA films increases the length of the path that water molecules need to cross in the films i.e., tortuosity, resulting in a substantially reduced diffusion of water through the composite films (Trifol et al., 2020). This is the reason behind the improved water-resistance properties of the TWMCC reinforced PVA films with respect to pure PVA. The moisture content, swelling rate and water solubility of pure PVA film differs significantly from the TWMCC reinforced PVA films ($p < 0.05$).

**Table 4.1** Water-resistance properties of the TWMCC reinforced PVA composite films

| Films | Moisture content (%) | Swelling rate (%) | Water solubility (%) |
|---|---|---|---|
| PVA | $13.93 \pm 1.84^{a}$ | $205.01 \pm 2.35^{a}$ | $29.79 \pm 0.53^{a}$ |
| PVA/MCC-1 | $9.08 \pm 2.31^{b}$ | $185.45 \pm 1.76^{b}$ | $21.28 \pm 0.28^{b}$ |
| PVA/MCC-3 | $9.03 \pm 1.77^{b}$ | $157.44 \pm 1.99^{c}$ | $16.82 \pm 0.47^{c}$ |
| PVA/MCC-5 | $8.17 \pm 1.74^{c}$ | $128.57 \pm 0.23^{d}$ | $16.67 \pm 0.21^{c}$ |

All data are the means with standard deviation for three replicates. Different superscript letters within each column indicate significantly different means ($p < 0.05$)

### 4.4.7 Water vapour barrier properties

Water vapour transmission rate (WVTR) and water vapour permeability (WVP) are key parameters in the food packaging context. The tendency of the TWMCC/PVA composite films to resist moisture transmission between the packed food and surrounding atmosphere were determined by water vapour permeability test. Low WVP is ideal for food packaging as it indicates that the films are able to hinder moisture transfer, thus leading to extended food shelf life (Zhao et al., 2023). The thickness, WVTR and WVP of the tea waste MCC reinforced PVA films are shown in **Table 4.2**.

**Table 4.2** Water vapour transmission properties of the PVA composite films filled with TWMCC

| **Films** | **Thickness (μm)** | **WVTR (g $m^{-2}$ $h^{-1}$)** | **WVP ($\times10^{-5}$ g $m^{-1}$ $h^{-1}$ $Pa^{-1}$)** |
|---|---|---|---|
| PVA | $108.32 \pm 1.83^{a}$ | $87.19 \pm 0.53^{a}$ | $3.18 \pm 0.11^{a}$ |
| PVA/MCC-1 | $110.89 \pm 2.42^{a}$ | $86.06 \pm 0.47^{a}$ | $3.05 \pm 0.05^{a}$ |
| PVA/MCC-3 | $118.48 \pm 1.02^{b}$ | $82.66 \pm 1.10^{b}$ | $2.92 \pm 0.02^{b}$ |
| PVA/MCC-5 | $121.20 \pm 1.48^{c}$ | $71.33 \pm 0.85^{c}$ | $2.78 \pm 0.14^{b}$ |

All the values are given as mean ± standard deviation for three replicates. Different superscript letters within each column indicate significant differences ($p < 0.05$)

As tea waste MCC was incorporated into the PVA matrix, WVTR of the films decreased from 87.19 ± 0.53 g $m^{-2}$ $h^{-1}$ for pure PVA film to 71.33 ± 0.85 g $m^{-2}$ $h^{-1}$ for

the PVA composite filled with 5wt% of TWMCC. Pure PVA film exhibited a WVP value of 3.18 ± 0.11×$10^{-5}$ g $m^{-1}$ $h^{-1}$ $Pa^{-1}$ and the WVP of the PVA composite films decreased gradually with the addition of TWMCC. The PVA/MCC-5 film exhibited the lowest WVP of 2.78 ± 0.14×$10^{-5}$ g $m^{-1}$ $h^{-1}$ $Pa^{-1}$. The WVTR and WVP of pure PVA and 1 wt% TWMCC filled PVA films are not significantly different, but the incorporation of 3 and 5 wt% TWMCC significantly reduced the WVTR and WVP of the PVA composites ($p < 0.05$). The reduction in WVP is associated with the crystallinity of the microcrystalline cellulose. Tea waste derived MCC possesses high crystallinity and a compact microfibrillary arrangement. The dense and compact network of H-bonds in between PVA and TWMCC established a tortuous path, thus the water molecules are obstructed to diffuse through the films resulting in lower WVP. As discussed earlier, the interaction between PVA and TWMCC decreases the free O–H groups on the PVA matrix which also leads to reduced interplay with water and thereby lower water vapour transmission (Jiang et al., 2023).

### 4.4.8 Mechanical strength analysis

Mechanical strength of packaging material is important from durability aspect of the packaging to resist the external forces. The mechanical properties of the TWMCC reinforced PVA films including tensile strength, elastic modulus and elongation at break are represented in **Fig. 4.7**. The stress-strain curves of the prepared films are depicted in **Fig. 4.7A**. The tensile strength (TS) of pure PVA film was 9.11 ± 1.15 MPa which is relatively low (**Fig. 4.7B**). The reinforcement with tea waste MCC resulted in a significant increase of TS of the PVA films and the PVA/MCC-1 film showed TS of

14.5 ± 1.37MPa. The PVA film with 3 wt% of TWMCC exhibited the highest TS, around 18.5 ± 1.93MPa which is almost twice that of the unreinforced PVA film. Further increase in TWMCC content (5 wt%) caused a little decrease of tensile strength of the film. However, the TS of the PVA/MCC-5 was still considerably greater than that of the pure PVA film, whereas the tensile strengths of PVA films containing 3 and 5 wt% are not significantly different ($p < 0.05$). The progressive increase in TS of the PVA composite films with increasing TWMCC concentrations may be attributed to the inherent chain stiffness and rigidity of the microcrystalline cellulose, homogeneous distribution of the micro-fillers in the polymer matrix and high compatibility between the TWMCC fillers and PVA matrix. The strong hydrogen bonds between the hydroxyl groups of TWMCC particles and the PVA matrix resulted in the improvement of the mechanical properties of the reinforced PVA films (Mandal & Chakrabarty, 2014; Sarwar et al., 2018). Owing to the good compatibility between TWMCC particles and PVA, the fillers are uniformly dispersed in the polymer matrix. As a result, the load transfer between the interface of the TWMCC and PVA matrix becomes uniform and more efficient reducing the concentration of stress at a particular zone, and therefore the tensile strength of the TWMCC/PVA composite films tend to increase. However, when 5wt% of TWMCC was used some of the filler particles got agglomerated on individual regions of the film matrix as already shown in FESEM result, which leads to increased stress concentration at those areas and the film breaks easily. Thus, the higher flocculation or agglomeration tendency of TWMCC particles when incorporated at higher proportion is associated with the decreased tensile strength of the film (Chen et al., 2020; Khan et al., 2012). As shown in **Fig. 4.7C**, the elastic modulus of the film also

improved with TWMCC reinforcement from 43.9 ± 2.71MPa (pure PVA) to 97.8 ± 6.95MPa (PVA/MCC-5 film). The elastic modulus of PVA film reinforced with 1wt% TWMCC is not significantly different from the pure PVA. However, TWMCC at 3 and 5 wt% proportion significantly increased the elastic modulus of the PVA composite films ($p < 0.05$), which is attributed to the enhanced rigidity and stiffness of the films caused by the incorporation of TWMCC (Debnath et al., 2022). **Fig. 7D** shows that pure PVA film had a lower elongation at break value of around 94.4 ± 3.54%, while all the TWMCC-reinforced PVA films exhibited ductile behaviour with high values of elongation at break (above 150%) and the highest elongation at break was 225 ± 4.18% obtained at 3 wt% of TWMCC. All the TWMCC reinforced films have significantly higher elongation at break as compared to the pure PVA film ( $p < 0.05$), which is ascribed to the increase in crystallinity of the composite films with the incorporation of TWMCC fillers in PVA matrix (Sarwar et al., 2018). General observations show an inverse relation between elongation at break and tensile strength. On the contrary, it was observed in the present study that the percentage elongation of the composite films increased with an increase in TWMCC content. The intramolecular as well as intermolecular H-bonds of pure PVA matrix undergo breakage with the introduction of TWMCC fillers and ductility sets in. The presence of TWMCC particles disturbs the formation of H-bonds amongst PVA chains during the drying of the reinforced PVA films. Microcrystalline cellulose, being a good water carrier, might plasticize the PVA matrix somewhat, resulting in an increase in the film's ductility and thus increasing percentage elongation at break. However, elongation at break falls off beyond the 3 wt% proportion of TWMCC, probably due to the agglomeration of filler particles

(Mandal & Chakrabarty, 2014). These outcomes are consistent with the observations of previous reports (Mandal & Chakrabarty, 2014; Sarwar et al., 2018), where nanocellulose was incorporated as reinforcement in PVA film matrix. The increase in TS of the PVA composite films is attributed to the strong intermolecular hydrogen bonds between the O–H groups of tea waste MCC and PVA, and the uniform distribution of the micro-filler in the PVA matrix (Debnath et al., 2022).

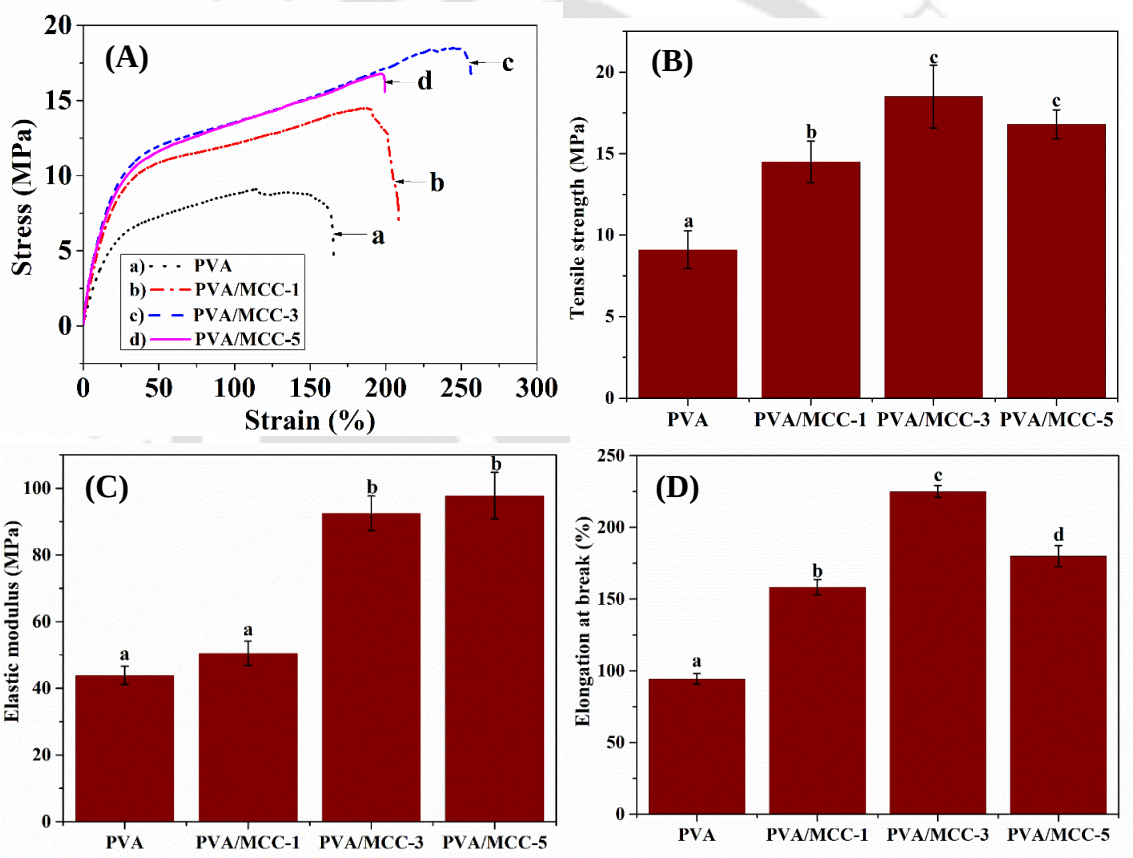


**Figure 4.7** Mechanical properties: A) stress-strain curves, B) tensile strength, C) elastic modulus, and D) elongation at break of the PVA composite films filled with different concentrations of TWMCC (Different superscript letters indicate significant differences at $p < 0.05$)

The high elastic moduli of the PVA composite film with increased TWMCC content might be because of the inherent stiffness and rigidity of microcrystalline cellulose, and high level of compatibility between the TWMCC and polymer matrix. The slight reduction in tensile strength at higher TWMCC concentration (5 wt%) may be ascribed to agglomerating tendency of the TWMCC particles at its higher proportion (Mandal & Chakrabarty, 2014; Sarwar et al., 2018).

### 4.4.9 UV-barrier properties

The UV–Vis transmittance spectra of the fabricated pure PVA film and PVA composite films reinforced with different concentrations of tea waste microcrystalline cellulose are shown in **Fig 4.7**. Pure PVA film exhibited high transmittance of around 100% over the wavelength range of 250-800 nm, which is an indicative of its poor light-blocking properties (Nguyen & Lee, 2022). The high transmittance value in the UV spectral region (200–400 nm) shows that pure PVA film is not able to filter UV irradiation or in other words, it is transparent for UV light (Xiong et al., 2018). In comparison to pure PVA film, the tea waste MCC reinforced PVA films exhibited strong absorption in the UV region. The UV transmittance of composite PVA films gradually decreased as the TWMCC concentration in the composites increased from 1 wt% to 5 wt%. The spectra clearly demonstrate that the transmittance decreased with the increase of TWMCC content due to the scattering of light. The PVA/TWMCC-5 film showed the best performance in UV-blocking, with above 70% reduction of transmittance from 82.99% at 400 nm to 9.44% at 200 nm. The lowest UV-transmittance showed by PVA/TWMCC-5 was 5.26% at 222 nm, while PVA/TWMCC-3 and PVA/TWMCC-1

exhibited lowest transmittance of 8.03% at 201 nm and 9.30% at 202 nm, respectively. The UV light transmittance of the composite films decreased due to the UV-shielding ability of microcrystalline cellulose. Additionally, this transmittance reduction with the incorporation of tea waste MCC indicates that the TWMCC particles are uniformly dispersed in the PVA matrix.

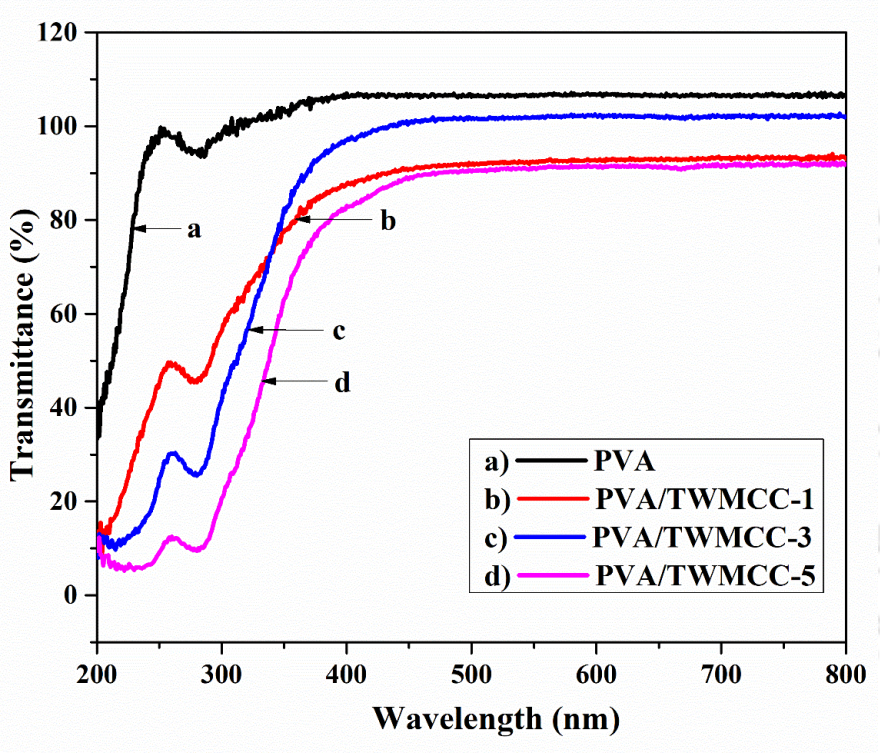


**Figure 4.8** UV-Vis spectra of PVA films reinforced with different concentrations of TWMCC

The cellulose microfibers develop stable interaction through hydrogen bonds between the O–H groups of PVA matrix and cellulose, forming a type of physical barrier to light as the dense network structure restricts the diffusion of light through the films (Srivastava et al., 2021). The decrease in transmittance with the addition of tea waste MCC into PVA matrix may also be correlated with the closeness of the refractive indices of cellulose (1.58) and PVA (1.49–1.52) (Kang et al., 2018). However,

transmittance of all the TWMCC reinforced PVA films remained constant and above 80% in the visible light region (400–800 nm). The findings reveal that incorporation of TWMCC as reinforcing agent in PVA films improves the UV-barrier property of the composite films, with a little impact on their visible light transmittance performance (Feng et al., 2022).

## 4.5 Performance evaluation of the composite films

Grapes are small, tasty, and one of the most popular fruits consumed globally which is rich in carbohydrates, vitamins, organic acids, and many other health-beneficial nutrients. Owing to the thin skin of grapes, they are vulnerable to degradation caused by mechanical impact and microbial infestation during storage and transportation, and hence they possess a very short shelf life. Therefore, it is crucial to extend the shelf life of grapes by preserving them in appropriate packaging. The potential of the TWMCC reinforced PVA films in fruit packaging was assessed by packing grapes as shown in **Table 4.3**. On the 1$^{st}$ day of storage, all the grapes had a smooth green appearance without any wrinkles because of high moisture content. The unpacked grapes started developing dark spots and wrinkles on the 5$^{th}$ day, while the packed samples remained unchanged. After 7days, the spots on the control grapes darkened, the fruits became dull, brown, and lost marketability. By the 13$^{th}$ day they were totally dehydrated, shrunk in size, and brown in colour representing spoilage. The change in the green colour of grapes surface is an indicative of browning which may happen because of high rates of respiration and moisture loss. No significant variations in colour and appearance were observed for the packed grapes till the 7$^{th}$ day. The grapes packed in pure PVA film

started to shrivel after 9days and they turned brown by the 13$^{th}$ day. The grapes packed in PVA/MCC-1 film became slightly brown on the 13$^{th}$ day, whereas the grapes wrapped in PVA/MCC-3 and PVA/MCC-5 films were still green and fresh. The retention of water vapor by the films might have preserved the freshness of these grapes. On the 15$^{th}$ day, the visual appearance of all the grapes degraded and they lost marketability except the grapes packed in PVA/MCC-5 film which remained intact and perfect to use even up to18 days. On the 20$^{th}$ day, wrinkles began to appear on the PVA/MCC-5 film wrapped grapes and they turned yellowish. The PVA composite filled with 5 wt% of TWMCC maintained the moisture required to preserve the quality of the grapes and thus retained their consumer acceptability after 18 days of storage. Such performance of the PVA/MCC-5 film is ascribed to its low water vapour permeability and high water resistance characteristics. In addition to that, the PVA/MCC-5 film is thicker and has the lowest UV transmittance property. Hence, the film protected the grapes from environmental conditions and extended its shelf life (Hadimani et al., 2023; Jiang et al., 2022).

**Table 4.3** Illustration of grapes without packaging and packed using the PVA composite films filled with different levels of tea waste MCC during storage at room temperature

| Day | Control grapes | PVA film | PVA/MCC-1 | PVA/MCC-3 | PVA/MCC-5 |
|---|---|---|---|---|---|
| 1 |  |  |  |  |  |

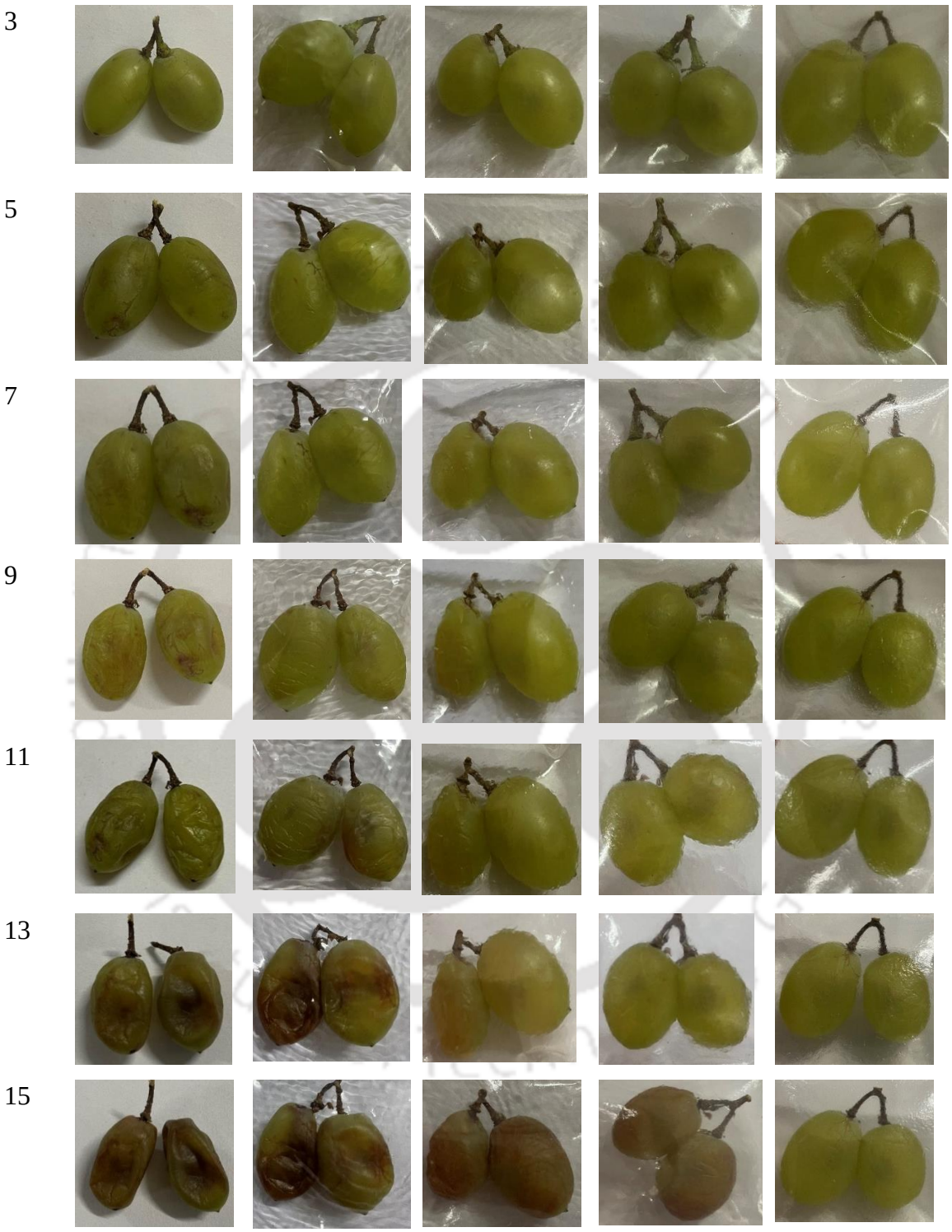


A comparative analysis of the present work with other reported biodegradable packaging materials is represented in **Table 5.4**. From the table, it could be seen that PVA films are reinforced with different organic as well as inorganic additives for improving their packaging properties to extend food shelf life. PVA/nanocellulose composite film prolonged the shelf life of strawberries and kept them fresh up to 6 days, while the unpacked strawberries lost their edible value by that time (Li et al., 2022). PVA composites filled with organic fillers such as citric acid (Jiang et al., 2023), basil leaf extracts (Varghese et al., 2023), and inorganic fillers like silica (Yu et al., 2018), silver nanoparticles (Deng et al., 2019; Yang et al., 2023), zinc oxide nanoparticles (Goudar et al., 2021) could extend the shelf life of fruits and vegetables up to 7-13 days. The tea waste MCC reinforced PVA films prepared in this study exhibited outstanding performance in fruit packaging by preserving grapes for 18 days, which was superior as compared to many other reported biodegradable packaging material for grapes such as chitosan/black cumin extract composite (Karkar et al., 2023) and jackfruit seed starch containing pomegranate peel extract as additive (Bodana et al., 2024) that enhanced grapes shelf life up to 7 and 8 days, respectively.

**Table 4.4** Comparison of the TWMCC reinforced PVA films with other biodegradable composites for food packaging

| Polymer | Fruits/ vegetables stored | Additives/ fillers used | Dosage of the filler (based on polymer weight) | Shelf life (days) | References |
|---|---|---|---|---|---|
| PVA | Strawberries | Nanocellulose | 6wt% | 6 | (Li et al., 2022) |
| PVA/chitosan | Cherries | Citric acid | ----- | 13 | (Jiang et al., 2023) |
| PVA/chitosan | Cherries | Silica | 0.6wt% | 7 | (Yu et al., 2018) |
| PVA/chitosan | Strawberries | Silver nanoparticles | ----- | 9 | (Yang et al., 2023) |
| PVA/starch | Green chilly | Basil leaf extract | 15wt% | 7 | (Varghese et al., 2023) |
| PVA/ *Spathodea campanulata* (African tulip) bud fluid | Black grapes | Zinc Oxide nanoparticles | 0.1wt% | 7 | (Goudar et al., 2021) |
| PVA | Black grapes | Nano silver | ----- | 10 | (Deng et al., 2019) |
| Chitosan | Grapes | Black cumin | ----- | 7 | (Karkar et al., |

| | | | | | |
|---|---|---|---|---|---|
| | | extract | | | 2023) |
| Jackfruit seed starch | Grapes | Pomegranate peel extract | ----- | 8 | (Bodana et al., 2024) |
| **PVA** | **Grapes** | **Tea waste microcrystalline cellulose** | **5wt%** | **18** | **This work** |

## 4.6 Summary

This chapter deals with the preparation of PVA films incorporated with black tea waste microcrystalline cellulose as reinforcement/filler material and inspection of the various physicochemical properties of the composite films. The performance of the prepared films in preserving grapes was also evaluated. The results of FTIR and FESEM analysis revealed good compatibility between the tea waste microcrystalline cellulose and PVA matrix. Reinforcement with TWMCC improved the thermal, mechanical, and UV-blocking properties of PVA films considerably. Water barrier properties such as water solubility, swelling rate, water vapour permeability of the films get reduced with the incorporation of TWMCC. The fabricated TWMCC/PVA composite films showed remarkable performance as packaging material by considerably increasing the shelf life of grapes with respect to unpacked and plain PVA film-packed grapes.

# Chapter 5

# Conclusions and scope for future work

*In this chapter, the main conclusions drawn from each objective and the possible scope for further research are reported. Microcrystalline cellulose was isolated from elephant grass through a non-conventional technique involving successive bleaching using alkaline hydrogen peroxide. The synthesized product was characterized using various analytical methods and its properties were compared with those of the commercially available microcrystalline cellulose. The elephant grass derived microcrystalline cellulose was then incorporated as reinforcement into the polymer matrix of corn starch films and the various physicochemical properties of the fabricated films were investigated that are desirable for food packaging application. Further, the potential of tea industry waste for the synthesis of MCC was explored by using an advance and quick technique involving microwave heating instead of conventional heating. The bleaching treatment conditions were optimized using RSM analysis for maximizing the crystallinity of the tea waste microcrystalline cellulose. The synthesized product was characterized using analytical techniques and its properties were compared with commercial MCC and also with those of the tea waste microcrystalline cellulose synthesized under conventional heating. The TWMCC synthesized under microwave heating was incorporated into PVA films and the composite films were studied for their potential use in grapes packaging to increase the fruit's shelf life. The detailed conclusions are highlighted below, separately for each chapter.*

# Conclusions

## 1. Introduction, Literature Review, Objectives and Organization of the Thesis

- The background of the thesis work, the state of art literature and possible scope of research are reported here.
- Based on the scopes, four research objectives are formulated.
- The organization of the thesis is briefly summarized

## 2. Synthesis of microcrystalline cellulose from elephant grass and its application as reinforcement in corn starch films for food packaging

- Successive bleaching with alkaline hydrogen peroxide efficiently extracted microcrystalline cellulose from elephant grass with a high yield of 89.31%.
- The synthesized elephant grass microcrystalline cellulose possesses polycrystalline structure with a crystallinity index of 74%, which is comparable to commercial MCC that possesses a crystallinity index around 80%.
- The functional groups present in the synthesized E-MCC are hydroxyl, alkyl, aldehyde, and methylene, which are similar to those of the commercial MCC.

- The E-MCC fibers have rough surface and are thinner, more exposed, and disruptive in nature with respect to the raw elephant grass indicating the complete removal of hemicellulose and lignin as a result of successive bleaching treatment.
- The diameter of the particles of E-MCC ranged from 15-48 μm, with an average particle diameter of 29 μm, slightly larger than commercial MCC.
- Thermal degradation of E-MCC starts at around 285 °C, which is close to commercial MCC that starts to degrade at 291°C.
- The onset degradation temperature of the E-MCC (285 °C) is higher than that of the MCC prepared from many other biomass sources like rose stems (232 °C), waste cotton fabrics (240 °C), pomelo peel (280 °C).
- Reinforcement with the synthesized E-MCC improved overall properties of corn starch films considerably.
- Good compatibility between the E-MCC molecules and corn starch matrix occurs through hydrogen bonding.
- An addition of 1 wt% E-MCC increased the maximum degradation temperature of the corn starch film by almost 3%.
- Incorporation of 5 wt% E-MCC increased the water contact angle of the film from 19.52° (pure corn starch film) to 98.83°.
- Mechanical strength of pure corn starch film was 6.03 MPa which increased to 22.33 MPa after the addition of 5 wt% E-MCC.

- Due to the strong interaction between the hydroxyl groups of corn starch and E-MCC, the rigidity, thermal and mechanical properties of the films enhanced significantly, whereas the hydrophilic properties decreased.
- Corn starch films reinforced with the elephant grass derived microcrystalline cellulose possess satisfactory properties for utilization as a food packaging material.

### 3. Microwave-assisted synthesis of microcrystalline cellulose from tea industry waste and its characterization

- Using microwave heating during the various treatment steps can significantly reduce the time required for the extraction of MCC from biomass sources.
- Under microwave heating, delignification of tea waste could be done only in 2 minutes, and bleaching treatments were completed within 30 seconds, while in the case of conventional heating, more than 1 hour time is required to complete these reactions.
- Black tea waste microcrystalline cellulose prepared via microwave-assisted and conventional heating methods exhibit similar chemical structures containing the same functional groups, and their chemical functionality is also as like as the commercial microcrystalline cellulose.
- X-ray diffraction pattern of the TWMCC prepared under microwave shows distinct peaks at diffraction angles of 15.9°, 22.6° and 34.8°, indicating the presence of type I cellulose.

- The crystallinity index of the TWMCC synthesized under conventional and microwave heating was found to be 76.83% and 89.77%, respectively.
- The high crystallinity and good thermal stability make TWMCC a promising filler material for polymer composites.
- Crystallinity of the black tea waste derived microcrystalline cellulose was higher than several biomass-derived MCC such as those isolated from oolong tea waste, olive fibres, jute, rose stems, rice husk and so on.
- TWMCC prepared under microwave heating consist of short cellulosic fibres with a rough surface, polycrystalline structure, and particle diameter in between 11-43 µm.
- RSM analysis revealed that the optimum hydrogen peroxide bleaching time under microwave heating is only 23.70 sec.
- Microwave-assisted peroxide bleaching is a green, energy-efficient, and fast technique for the synthesis of MCC from industrial tea wastes, which will also help in minimizing tea waste management issues by utilizing it in a sustainable way.
- Tea waste can serve as a promising low-cost source of MCC, at the same time promoting the "waste to wealth" strategy.

## 4. Preparation of tea waste microcrystalline cellulose reinforced polyvinyl alcohol packaging films and their application in grapes preservation

- FTIR spectra reveals that the peak absorptions of PVA/TWMCC films are like that of the pure PVA film, indicating that TWMCC reinforcement did not influence the chemical structure of the composite films.
- Strong inter and intramolecular bonds between PVA matrix and tea waste MCC represent good compatibility between them.
- At a lower loading (1 wt%), the TWMCC particles dispersed homogeneously in the polymer matrix, and as the concentration was increased (5 wt%) some of the filler particles got flocculated.
- All the films show homogenous surface representing good compatibility and proper miscibility of the filler in the PVA matrix.
- Reinforcement with TWMCC improves the thermal properties of PVA films considerably because the incorporation of microcrystalline cellulose increases the rigidity of PVA films and hence higher temperatures are required for their degradation.
- Among the PVA composites, the film containing 5 wt% of TWMCC showed the lowest water vapour permeability and the least hydrophilic nature with a water contact angle of 81.54°.
- TWMCC at 3 wt% concentration doubled the tensile strength of the PVA/MCC-3 film as compared to pure PVA film.
- Strong hydrogen bonding between the hydroxyl groups of PVA and TWMCC forms a compact network structure and reduces free O–H groups on the PVA matrix, leading to improvement of the water barrier properties of the films.

- Dense network structures of the PVA/TWMCC composites act as light barrier and thus the reinforced PVA films show excellent UV blocking property.
- PVA film reinforced with 5 wt% TWMCC (PVA/MCC-5) showed excellent performance as packaging material by enhancing the shelf life of grapes up to 18 days.
- Tea waste derived microcrystalline cellulose may be used a promising filler material in biodegradable films for the preparation of sustainable food packaging and this approach can alleviate the global issue of plastic waste.

## Limitations of the study

The present study has some limitations which are listed below

- The purity of the synthesized elephant grass microcrystalline cellulose and tea waste microcrystalline cellulose were not examined in the study.
- The biodegradability of the E-MCC/corn starch composite films and TWMCC/PVA composite films were not investigated.
- Real time packaging performances of the E-MCC reinforced corn starch films were not evaluated.
- The TWMCC reinforced PVA packaging films did not show any radical scavenging or antioxidant activity when tested using DPPH method.

# Recommendation for future works

Considering the observations reported in Chapters 2 to 3, the recommendations for further work are reported below for each chapter

**Chapter 2**

- Extraction of microcrystalline cellulose from other lignocellulosic wastes using the non-conventional alkaline peroxide bleaching method.
- Exploring the potential applications of the elephant grass derived microcrystalline cellulose in the environmental and biomedical fields.
- Studies on the reinforcement effect of elephant grass derived MCC into different other environment friendly and biodegradable food packaging films.

**Chapter 3**

- Studies on microwave-assisted peroxide bleaching synthesis of microcrystalline cellulose from various other lignocellulosic wastes.
- Pilot scale study including cost estimation for the commercialization of MCC production from tea industry wastes.
- Study on one step synthesis of nanocrystalline cellulose from the tea waste derived microcrystalline cellulose.
- Studies on the applications of tea industry waste derived microcrystalline cellulose in the environmental and biomedical field.

## Chapter 4

- Studies on the biodegradability, antioxidant, and antimicrobial properties of TWMCC reinforced PVA packaging films.
- Investigation on the changes in various components (metabolites) of the grapes packaged in TWMCC reinforced PVA films with respect to the unpacked ones.
- Determination of the oxygen transmission rates through the TWMCC/PVA composite films and composition of the gases inside the packages.
- Studies on the reinforcement potential of tea waste derived microcrystalline cellulose into other biopolymer-based food packaging films such as starch, chitosan.

**References**

Abdul Khalil, H. P. S., Lai, T. K., Tye, Y. Y., Paridah, M. T., Fazita, M. R. N., Azniwati, A. A., . . . Rizal, S. (2018). Preparation and Characterization of Microcrystalline Cellulose from Sacred Bali Bamboo as Reinforcing Filler in Seaweed-based Composite Film. *Fibers Polym., 19*(2), 423-434. doi:https://10.1007/s12221-018-7672-7

Abdul Rahman, N. H., Chieng, B. W., Ibrahim, N. A., & Abdul Rahman, N. (2017). Extraction and Characterization of Cellulose Nanocrystals from Tea Leaf Waste Fibers. *Polymers, 9*(11). doi:https://10.3390/polym9110588

Abu-Thabit, N. Y., Judeh, A. A., Hakeem, A. S., Ul-Hamid, A., Umar, Y., & Ahmad, A. (2020). Isolation and characterization of microcrystalline cellulose from date seeds (*Phoenix dactylifera L.). Int. J. Biol. Macromol., 155*, 730-739. doi:https://doi.org/10.1016/j.ijbiomac.2020.03.255

Aloui, H., Khwaldia, K., Hamdi, M., Fortunati, E., Kenny, J. M., Buonocore, G. G., & Lavorgna, M. (2016). Synergistic Effect of Halloysite and Cellulose Nanocrystals on the Functional Properties of PVA Based Nanocomposites. *ACS Sustain. Chem. Eng., 4*(3), 794-800. doi:https://10.1021/acssuschemeng.5b00806

Alqahtani, N., Alnemr, T., & Ali, S. (2021). Development of low-cost biodegradable films from corn starch and date palm pits (*Phoenix dactylifera*). *Food Biosci., 42*, 101199. doi:https://doi.org/10.1016/j.fbio.2021.101199

Arsyad, M., Wardana, I., Pratikto, & Irawan, Y. (2015). The morphology of coconut fiber surface under chemical treatment. *Revista Materia, 20*, 169-177. doi:https://10.1590/S1517-707620150001.0017

Azlan, N. S. M., Yap, C. L., Gan, S., & Rahman, M. B. A. (2022). Effectiveness of various solvents in the microwave-assisted extraction of cellulose from oil palm mesocarp fiber. *Mater. Today: Proc., 59*, 583-590. doi:https://doi.org/10.1016/j.matpr.2021.12.086

Baite, T. N., Mandal, B., & Purkait, M. K. (2022). Antioxidant-Incorporated Poly(vinyl alcohol) Coating: Preparation, Characterization, and Influence on Ripening of Green Bananas. *ACS omega, 7*(46), 42320-42330. doi:https://10.1021/acsomega.2c05271

Baite, T. N., Purkait, M. K., & Mandal, B. (2023). Synthesis of lignin from waste leaves and its potential application for bread packaging: A waste valorization approach. *Int. J. Biol. Macromol., 235*, 123880. doi:https://doi.org/10.1016/j.ijbiomac.2023.123880

Baruah, J., Deka, R. C., & Kalita, E. (2020). Greener production of microcrystalline cellulose (MCC) from *Saccharum spontaneum* (Kans grass): Statistical optimization. *Int. J. Biol. Macromol., 154*, 672-682. doi:https://doi.org/10.1016/j.ijbiomac.2020.03.158

Basumatary, V., Saikia, R., Narzari, R., Bordoloi, N., Gogoi, L., Sut, D., . . . Kataki, R. (2018). Tea factory waste as a feedstock for thermo-chemical conversion to biofuel and biomaterial. *Mater. Today: Proc., 5*(11, Part 2), 23413-23422. doi:https://doi.org/10.1016/j.matpr.2018.11.081

Benito-González, I., Göksen, G., Pérez-Bassart, Z., López-Rubio, A., Sánchez, R., Alonso, J. M., . . . Martínez-Sanz, M. (2021). Pilot plant scale-up of the production of optimized starch-based biocomposites loaded with cellulosic nanocrystals from *Posidonia oceanica* waste biomass. *Food Packag. Shelf Life, 30*, 100730. doi:https://doi.org/10.1016/j.fpsl.2021.100730

Bessa, W., Tarchoun, A. F., Trache, D., & Derradji, M. (2021). Preparation of amino-functionalized microcrystalline cellulose from *Arundo Donax L.* and its effect on the curing behavior of bisphenol A–based benzoxazine. *Thermochim. Acta, 698*, 178882. doi:https://doi.org/10.1016/j.tca.2021.178882

Bodana, V., Swer, T. L., Kumar, N., Singh, A., Samtiya, M., Sari, T. P., & Babar, O. A. (2024). Development and characterization of pomegranate peel extract-functionalized jackfruit seed starch-based edible films and coatings for prolonging the shelf life of white grapes.

*Int. J. Biol. Macromol., 254*, 127234. doi:https://doi.org/10.1016/j.ijbiomac.2023.127234

Castillo, L. A., Farenzena, S., Pintos, E., Rodríguez, M. S., Villar, M. A., García, M. A., & López, O. V. (2017). Active films based on thermoplastic corn starch and chitosan oligomer for food packaging applications. *Food Packag. Shelf Life, 14*, 128-136. doi:https://doi.org/10.1016/j.fpsl.2017.10.004

Chen, J., Chen, F., Meng, Y., Wang, S., & Long, Z. (2019). Oxidized microcrystalline cellulose improve thermoplastic starch-based composite films: Thermal, mechanical and water-solubility properties. *Polymer, 168*, 228-235. doi:https://doi.org/10.1016/j.polymer.2019.02.026

Chen, J., Wang, X., Long, Z., Wang, S., Zhang, J., & Wang, L. (2020). Preparation and performance of thermoplastic starch and microcrystalline cellulose for packaging composites: Extrusion and hot pressing. *Int. J. Biol. Macromol., 165*, 2295-2302. doi:https://doi.org/10.1016/j.ijbiomac.2020.10.117

Chen, Q., Shi, Y., Chen, G., & Cai, M. (2020). Enhanced mechanical and hydrophobic properties of composite cassava starch films with stearic acid modified MCC (microcrystalline cellulose)/NCC (nanocellulose) as strength agent. *Int. J. Biol. Macromol., 142*, 846-854. doi:https://doi.org/10.1016/j.ijbiomac.2019.10.024

Chowdhury, A., Sarkar, S., Chowdhury, A., Bardhan, S., Mandal, P., & Chowdhury, M. (2016). Tea waste management: a case study from West Bengal, India. *Ind. J. Sci. Technol., 9*(42), 1-6. doi:https://10.17485/ijst/2016/v9i42/89790

Collazo-Bigliardi, S., Ortega-Toro, R., & Chiralt, A. (2019a). Improving properties of thermoplastic starch films by incorporating active extracts and cellulose fibres isolated from rice or coffee husk. *Food Packag. Shelf Life, 22*, 100383. doi:https://doi.org/10.1016/j.fpsl.2019.100383

Collazo-Bigliardi, S., Ortega-Toro, R., & Chiralt, A. (2019b). Using lignocellulosic fractions of coffee husk to improve properties of compatibilised starch-PLA blend films. *Food Packag. Shelf Life, 22*, 100423. doi:https://doi.org/10.1016/j.fpsl.2019.100423

Debnath, B., Duarah, P., Haldar, D., & Purkait, M. K. (2022). Improving the properties of corn starch films for application as packaging material via reinforcement with microcrystalline cellulose synthesized from elephant grass. *Food Packag. Shelf Life, 34*, 100937. doi:https://doi.org/10.1016/j.fpsl.2022.100937

Debnath, B., Duarah, P., & Purkait, M. K. (2023). Microwave-assisted quick synthesis of microcrystalline cellulose from black tea waste (*Camellia sinensis*) and characterization. *Int. J. Biol. Macromol., 244*, 125354. doi:https://doi.org/10.1016/j.ijbiomac.2023.125354

Debnath, B., Haldar, D., & Purkait, M. K. (2021a). A critical review on the techniques used for the synthesis and applications of crystalline cellulose derived from agricultural wastes and forest residues. *Carbohydr. Polym., 273*, 118537. doi:https://doi.org/10.1016/j.carbpol.2021.118537

Debnath, B., Haldar, D., & Purkait, M. K. (2021b). Potential and sustainable utilization of tea waste: A review on present status and future trends. *J. Environ. Chem. Eng., 9*(5), 106179. doi:https://doi.org/10.1016/j.jece.2021.106179

Debnath, B., Haldar, D., & Purkait, M. K. (2022). Environmental remediation by tea waste and its derivative products: A review on present status and technological advancements. *Chemosphere, 300*, 134480. doi:https://doi.org/10.1016/j.chemosphere.2022.134480

Deng, J., Chen, Q. J., Peng, Z. Y., Wang, J. H., Li, W., Ding, Q. M., . . . Shi, Y. (2019). Nano-silver-containing polyvinyl alcohol composite film for grape fresh-keeping. *Mater. Express, 9*(9), 985-992. doi:https://doi.org/10.1166/mex.2019.1592

Duarah, P., Haldar, D., Singhania, R. R., Dong, C.-D., Patel, A. K., & Purkait, M. K. (2023). Sustainable management of tea wastes: resource recovery and conversion techniques. *Crit. Rev. Biotechnol.*, 1-20. doi:https://10.1080/07388551.2022.2157701

Fan, G.-Z., Wang, Y.-X., Song, G.-S., Yan, J.-T., & Li, J.-F. (2017). Preparation of microcrystalline cellulose from rice straw under microwave irradiation. *J. Appl. Polym. Sci., 134*(22). doi:https://doi.org/10.1002/app.44901

Feng, Z., Xu, D., Shao, Z., Zhu, P., Qiu, J., & Zhu, L. (2022). Rice straw cellulose microfiber reinforcing PVA composite film of ultraviolet blocking through pre-cross-linking. *Carbohydr. Polym., 296*, 119886. doi:https://doi.org/10.1016/j.carbpol.2022.119886

Ghosh, T., Bhasney, S. M., & Katiyar, V. (2020). Blown films fabrication of poly lactic acid based biocomposites: Thermomechanical and migration studies. *Mater. Today Commun., 22*, 100737. doi:https://doi.org/10.1016/j.mtcomm.2019.100737

Goudar, N., Vanjeri, V. N., Kasai, D., Gouripur, G., Malabadi, R. B., Masti, S. P., & Chougale, R. B. (2021). ZnO NPs Doped PVA/*Spathodea campanulata* Thin Films for Food Packaging. *J. Polym. Environ., 29*(9), 2797-2812. doi:https://10.1007/s10924-021-02070-0

Hadimani, S., Supriya, D., Roopa, K., Soujanya, S. K., Rakshata, V., Netravati, A., . . . Jogaiah, S. (2023). Biodegradable hybrid biopolymer film based on carboxy methyl cellulose and selenium nanoparticles with antifungal properties to enhance grapes shelf life. *Int. J. Biol. Macromol., 237*, 124076. doi:https://doi.org/10.1016/j.ijbiomac.2023.124076

Haldar, D., & Purkait, M. K. (2020a). Lignocellulosic conversion into value-added products: A review. *Process Biochem., 89*, 110-133. doi:https://doi.org/10.1016/j.procbio.2019.10.001

Haldar, D., & Purkait, M. K. (2020b). Micro and nanocrystalline cellulose derivatives of lignocellulosic biomass: A review on synthesis, applications and advancements. *Carbohydr. Polym., 250*, 116937. doi:https://doi.org/10.1016/j.carbpol.2020.116937

Haldar, D., & Purkait, M. K. (2020c). Thermochemical pretreatment enhanced bioconversion of elephant grass (*Pennisetum purpureum*): insight on the production of sugars and lignin. *Biomass Convers. Biorefinery*, 1-14. doi:https://10.1007/s13399-020-00689-y

Haldar, D., & Purkait, M. K. (2021). A review on the environment-friendly emerging techniques for pretreatment of lignocellulosic biomass: Mechanistic insight and advancements. *Chemosphere, 264*, 128523. doi:https://doi.org/10.1016/j.chemosphere.2020.128523

Halder, P., Kundu, S., Patel, S., Setiawan, A., Atkin, R., Parthasarthy, R., . . . Shah, K. (2019). Progress on the pre-treatment of lignocellulosic biomass employing ionic liquids. *Renew. Sustain. Energy Rev., 105*, 268-292. doi:https://doi.org/10.1016/j.rser.2019.01.052

Handoko, F., & Yusuf, Y. (2021). Synthesis and Physicochemical Properties of Poly(vinyl) Alcohol Nanocomposites Reinforced with Nanocrystalline Cellulose from Tea (*Camellia sinensis*) Waste. *Materials, 14*(23). doi:https://10.3390/ma14237154

Hasan, M., Lai, T. K., Gopakumar, D. A., Jawaid, M., Owolabi, F. A. T., Mistar, E. M., . . . Abdul Khalil, H. P. S. (2019). Micro Crystalline Bamboo Cellulose Based Seaweed Biodegradable Composite Films for Sustainable Packaging Material. *J. Polym. Environ., 27*(7), 1602-1612. doi:https://10.1007/s10924-019-01457-4

Helmiyati, H., Hidayat, Z. S. Z., Sitanggang, I. F. R., & Liftyawati, D. (2021). Antimicrobial packaging of ZnO–Nps infused into CMC–PVA nanocomposite films effectively enhances the physicochemical properties. *Polym. Test., 104*, 107412. doi:https://doi.org/10.1016/j.polymertesting.2021.107412

Holilah, H., Prasetyoko, D., Ediati, R., Bahruji, H., Jalil, A. A., Asranudin, A., & Anggraini, S. D. (2021). Hydrothermal assisted isolation of microcrystalline cellulose from pepper (*Piper nigrum L.*) processing waste for making sustainable bio-composite. *J. Clean. Prod., 305*, 127229. doi:https://doi.org/10.1016/j.jclepro.2021.127229

Hou, W., Ling, C., Shi, S., & Yan, Z. (2019). Preparation and characterization of microcrystalline cellulose from waste cotton fabrics by using phosphotungstic acid. *Int. J. Biol. Macromol., 123*, 363-368. doi:https://doi.org/10.1016/j.ijbiomac.2018.11.112

Jahan, M. S., Saeed, A., He, Z., & Ni, Y. (2011). Jute as raw material for the preparation of microcrystalline cellulose. *Cellulose, 18*, 451-459. doi:https://10.1007/s10570-010-9481-z

Jiang, S., Qiao, C., Liu, R., Liu, Q., Xu, J., & Yao, J. (2023). Structure and properties of citric acid cross-linked chitosan/poly(vinyl alcohol) composite films for food packaging applications. *Carbohydr. Polym., 312*, 120842. doi:https://doi.org/10.1016/j.carbpol.2023.120842

Jiang, S., Qiao, C., Wang, X., Li, Z., & Yang, G. (2022). Structure and properties of chitosan/sodium dodecyl sulfate composite films. *RSC Adv., 12*(7), 3969-3978. doi:https://10.1039/D1RA08218C

Kambli, N. D., Mageshwaran, V., Patil, P. G., Saxena, S., & Deshmukh, R. R. (2017). Synthesis and characterization of microcrystalline cellulose powder from corn husk fibres using bio-chemical route. *Cellulose, 24*(12), 5355-5369. doi:https://10.1007/s10570-017-1522-4

Kang, X., Kuga, S., Wang, C., Zhao, Y., Wu, M., & Huang, Y. (2018). Green Preparation of Cellulose Nanocrystal and Its Application. *ACS Sustain. Chem. Eng., 6*(3), 2954-2960. doi:https://10.1021/acssuschemeng.7b02363

Karkar, B., Patır, İ., Eyüboğlu, S., & Şahin, S. (2023). Development of an edible active chitosan film loaded with *Nigella sativa* L. extract to extend the shelf life of grapes. *Biocatal. Agric. Biotechnol., 50*, 102708. doi:https://doi.org/10.1016/j.bcab.2023.102708

Karim, M. Z., Chowdhury, Z. Z., Abd Hamid, S. B., & Ali, M. E. (2014). Statistical optimization for acid hydrolysis of microcrystalline cellulose and its physiochemical characterization by using metal ion catalyst. *Materials, 7*(10), 6982-6999. doi:https://doi.org/10.3390/ma7106982

Khan, A., Khan, R. A., Salmieri, S., Le Tien, C., Riedl, B., Bouchard, J., . . . Lacroix, M. (2012). Mechanical and barrier properties of nanocrystalline cellulose reinforced chitosan based nanocomposite films. *Carbohydr. Polym., 90*(4), 1601-1608. doi:https://doi.org/10.1016/j.carbpol.2012.07.037

Kian, L. K., Jawaid, M., Ariffin, H., & Alothman, O. Y. (2017). Isolation and characterization of microcrystalline cellulose from roselle fibers. *Int. J. Biol. Macromol., 103*, 931-940. doi:https://doi.org/10.1016/j.ijbiomac.2017.05.135

Kian, L. K., Saba, N., Jawaid, M., & Fouad, H. (2020). Characterization of microcrystalline cellulose extracted from olive fiber. *Int. J. Biol. Macromol., 156*, 347-353. doi:https://doi.org/10.1016/j.ijbiomac.2020.04.015

Kongkeitkajorn, M. B., Sae-Kuay, C., & Reungsang, A. (2020). Evaluation of Napier Grass for Bioethanol Production through a Fermentation Process. *Processes, 8*(5). doi:https://10.3390/pr8050567

Kowalczyk, D., Szymanowska, U., Skrzypek, T., Basiura-Cembala, M., Materska, M., & Łupina, K. (2021). Corn starch and methylcellulose edible films incorporated with fireweed (*Chamaenerion angustifolium* L.) extract: Comparison of physicochemical and antioxidant properties. *Int. J. Biol. Macromol., 190*, 969-977. doi:https://doi.org/10.1016/j.ijbiomac.2021.09.079

Krivokapić, J., Ivanović, J., Djuriš, J., Medarević, D., Potpara, Z., Maksimović, Z., & Ibrić, S. (2020). Tableting properties of microcrystalline cellulose obtained from wheat straw measured with a single punch bench top tablet press. *Saudi Pharm. J., 28*(6), 710-718. doi:https://doi.org/10.1016/j.jsps.2020.04.013

Kumar, K. R., Dashora, K., Krishnan, N., Sanyal, S., Chandra, H., Dharmaraja, S., & Kumari, V. (2021). Feasibility assessment of renewable energy resources for tea plantation and industry in India - A review. Renew. *Sustain. Energy Rev., 145*, 111083. doi:https://doi.org/10.1016/j.rser.2021.111083

Kuznetsov, B. N., Sudakova, I. G., Yatsenkova, O. V., Garyntseva, N. V., Rataboul, F., & Djakovitch, L. (2018). Optimizing Single-Stage Processes of Microcrystalline Cellulose Production via the Peroxide Delignification of Wood in the Presence of a Titania Catalyst. *Catal. Ind., 10*(4), 360-367. doi:https://10.1134/S2070050418040116

Lei, Y., Mao, L., Yao, J., & Zhu, H. (2021). Improved mechanical, antibacterial and UV barrier properties of catechol-functionalized chitosan/polyvinyl alcohol biodegradable composites for active food packaging. *Carbohydr. Polym., 264*, 117997. doi:https://doi.org/10.1016/j.carbpol.2021.117997

Li, L., Wang, W., Sun, J., Chen, Z., Ma, Q., Ke, H., & Yang, J. (2022). Improved properties of polyvinyl alcohol films blended with aligned nanocellulose particles induced by a magnetic field. *Food Packag. Shelf Life, 34*, 100985. doi:https://doi.org/10.1016/j.fpsl.2022.100985

Liu, Y., Liu, A., Ibrahim, S. A., Yang, H., & Huang, W. (2018). Isolation and characterization of microcrystalline cellulose from pomelo peel. *Int. J. Biol. Macromol., 111*, 717-721. doi:https://doi.org/10.1016/j.ijbiomac.2018.01.098

Mandal, A., & Chakrabarty, D. (2014). Studies on the mechanical, thermal, morphological and barrier properties of nanocomposites based on poly(vinyl alcohol) and nanocellulose

from sugarcane bagasse. *J. Ind. Eng. Chem., 20*(2), 462-473. doi:https://doi.org/10.1016/j.jiec.2013.05.003

Malherbi, N. M., Schmitz, A. C., Grando, R. C., Bilck, A. P., Yamashita, F., Tormen, L., . . . Bertan, L. C. (2019). Corn starch and gelatin-based films added with guabiroba pulp for application in food packaging. *Food Packag. Shelf Life, 19*, 140-146. doi:https://doi.org/10.1016/j.fpsl.2018.12.008

Mao, Y., Gerrow, A., Ray, E., Perez, N. D., Edler, K., Wolf, B., & Binner, E. (2023). Lignin recovery from cocoa bean shell using microwave-assisted extraction and deep eutectic solvents. *Bioresour. Technol., 372*, 128680. doi:https://doi.org/10.1016/j.biortech.2023.128680

Merci, A., Marim, R. G., Urbano, A., & Mali, S. (2019). Films based on cassava starch reinforced with soybean hulls or microcrystalline cellulose from soybean hulls. *Food Packag. Shelf Life, 20*, 100321. doi:https://doi.org/10.1016/j.fpsl.2019.100321

Merci, A., Urbano, A., Grossmann, M. V. E., Tischer, C. A., & Mali, S. (2015). Properties of microcrystalline cellulose extracted from soybean hulls by reactive extrusion. *Food Res. Int., 73*, 38-43. doi:https://doi.org/10.1016/j.foodres.2015.03.020

Mishra, S., Kharkar, P. S., & Pethe, A. M. (2019). Biomass and waste materials as potential sources of nanocrystalline cellulose: Comparative review of preparation methods (2016 – Till date). *Carbohydr. Polym., 207*, 418-427. doi:https://doi.org/10.1016/j.carbpol.2018.12.004

Moustakas, K., Parmaxidou, P., & Vakalis, S. (2020). Anaerobic digestion for energy production from agricultural biomass waste in Greece: Capacity assessment for the region of Thessaly. *Energy, 191*, 116556. doi:https://doi.org/10.1016/j.energy.2019.116556

Mujtaba, M., Fernandes Fraceto, L., Fazeli, M., Mukherjee, S., Savassa, S. M., Araujo de Medeiros, G., . . . Vilaplana, F. (2023). Lignocellulosic biomass from agricultural waste to the circular economy: a review with focus on biofuels, biocomposites and bioplastics. *J. Clean. Prod., 402*, 136815. doi:https://doi.org/10.1016/j.jclepro.2023.136815

Naduparambath, S., & Purushothaman, E. (2016). Sago seed shell: determination of the composition and isolation of microcrystalline cellulose (MCC). *Cellulose, 23*(3), 1803-1812. doi:https://10.1007/s10570-016-0904-3

Naduparambath, S., Sreejith, M. P., Shaniba, V., Balan, A. K., Jinitha, T. V., & Purushothaman, E. (2018). Poly (vinyl alcohol) green composites reinforced with microcrystalline cellulose through sonication. *Mater. Today: Proc., 5*(8, Part 3), 16411-16417. doi:https://doi.org/10.1016/j.matpr.2018.05.139

Negoro, T., Thodsaratpreeyakul, W., Takada, Y., Thumsorn, S., Inoya, H., & Hamada, H. (2016). Role of crystallinity on moisture absorption and mechanical performance of recycled PET compounds. *Energy Procedia, 89*, 323-327. doi:https://10.1016/j.egypro.2016.05.042

Nguyen, S. V., & Lee, B.-K. (2022). PVA/CNC/TiO2 nanocomposite for food-packaging: Improved mechanical, UV/water vapor barrier, and antimicrobial properties. *Carbohydr. Polym., 298*, 120064. doi:https://doi.org/10.1016/j.carbpol.2022.120064

Nordin, N., Othman, S. H., Rashid, S. A., & Basha, R. K. (2020). Effects of glycerol and thymol on physical, mechanical, and thermal properties of corn starch films. *Food Hydrocoll., 106*, 105884. doi:https://doi.org/10.1016/j.foodhyd.2020.105884

Othman, S. H., Nordin, N., Azman, N. A. A., Tawakkal, I. S. M. A., & Basha, R. K. (2021). Effects of nanocellulose fiber and thymol on mechanical, thermal, and barrier properties of corn starch films. *Int. J. Biol. Macromol., 183*, 1352-1361. doi:https://doi.org/10.1016/j.ijbiomac.2021.05.082

Owolabi, A. F., Haafiz, M. K. M., Hossain, M. S., Hussin, M. H., & Fazita, M. R. N. (2017). Influence of alkaline hydrogen peroxide pre-hydrolysis on the isolation of microcrystalline cellulose from oil palm fronds. *Int. J. Biol. Macromol., 95*, 1228-1234. doi:https://doi.org/10.1016/j.ijbiomac.2016.11.016

Phitsuwan, P., Sakka, K., & Ratanakhanokchai, K. (2016). Structural changes and enzymatic response of Napier grass (*Pennisetum purpureum*) stem induced by alkaline pretreatment. *Bioresour. Technol., 218*, 247-256. doi:https://doi.org/10.1016/j.biortech.2016.06.089

Popescu, M.-C., Dogaru, B.-I., Goanta, M., & Timpu, D. (2018). Structural and morphological evaluation of CNC reinforced PVA/Starch biodegradable films. *Int. J. Biol. Macromol., 116*, 385-393. doi:https://doi.org/10.1016/j.ijbiomac.2018.05.036

Pujiasih, S., Kurnia, Masykur, A., Kusumaningsih, T., & Saputra, O. A. (2018). Silylation and characterization of microcrystalline cellulose isolated from indonesian native oil palm empty fruit bunch. *Carbohydr. Polym., 184*, 74-81. doi:https://doi.org/10.1016/j.carbpol.2017.12.060

Puttaswamy, M., Srinikethan, G., & Shetty K, V. (2017). Biocomposite composed of PVA reinforced with cellulose microfibers isolated from biofuel industrial dissipate: *Jatropha Curcus L.* seed shell. *J. Environ. Chem. Eng., 5*(2), 1990-1997. doi:https://doi.org/10.1016/j.jece.2017.04.004

Rajesha Shetty, G., & Lakshmeesha Rao, B. (2022). Preparation and characterization of silk fibroin-polyvinyl alcohol (PVA) blend films for food packaging materials. *Mater. Today: Proc., 55*, 194-200. doi:https://doi.org/10.1016/j.matpr.2022.02.034

Rashid, M., Gafur, M. A., Sharafat, M. K., Minami, H., Miah, M. A. J., & Ahmad, H. (2017). Biocompatible microcrystalline cellulose particles from cotton wool and magnetization

via a simple in situ co-precipitation method. *Carbohydr. Polym., 170*, 72-79. doi:https://doi.org/10.1016/j.carbpol.2017.04.059

Ratna, A. S., Verma, C., Hossain, S., Gupta, B., & Mukhopadhyay, S. (2023). Development of corn husk cellulose reinforced polyvinyl alcohol bio-composite films incorporated with Zinc Oxide nanoparticles. *Bioresour. Technol. Rep.*, 101570. doi:https://doi.org/10.1016/j.biteb.2023.101570

Ren, H., Shen, J., Pei, J., Wang, Z., Peng, Z., Fu, S., & Zheng, Y. (2019). Characteristic microcrystalline cellulose extracted by combined acid and enzyme hydrolysis of sweet sorghum. *Cellulose, 26*(15), 8367-8381. doi:https://10.1007/s10570-019-02712-6

Rizwan, M., Gilani, S. R., Durrani, A. I., & Naseem, S. (2021). Low temperature green extraction of Acer platanoides cellulose using nitrogen protected microwave assisted extraction (NPMAE) technique. *Carbohydr. Polym., 272*, 118465. doi:https://doi.org/10.1016/j.carbpol.2021.118465

Salama, A. (2020). Cellulose/silk fibroin assisted calcium phosphate growth: Novel biocomposite for dye adsorption. *Int. J. Biol. Macromol., 165*, 1970-1977. doi:https://doi.org/10.1016/j.ijbiomac.2020.10.074

Sarwar, M. S., Niazi, M. B. K., Jahan, Z., Ahmad, T., & Hussain, A. (2018). Preparation and characterization of PVA/nanocellulose/Ag nanocomposite films for antimicrobial food packaging. *Carbohydr. Polym., 184*, 453-464. doi:https://doi.org/10.1016/j.carbpol.2017.12.068

Segal, L., Creely, J. J., Martin Jr, A., & Conrad, C. (1959). An empirical method for estimating the degree of crystallinity of native cellulose using the X-ray diffractometer. *Text. Res. J., 29*(10), 786-794. doi:https://doi.org/10.1177/004051755902901003

Shao, X., Wang, J., Liu, Z., Hu, N., Liu, M., & Xu, Y. (2020). Preparation and Characterization of Porous Microcrystalline Cellulose from Corncob. *Ind. Crops Prod., 151*, 112457. doi:https://doi.org/10.1016/j.indcrop.2020.112457

Shi, S., Zhang, M., Ling, C., Hou, W., & Yan, Z. (2018). Extraction and characterization of microcrystalline cellulose from waste cotton fabrics via hydrothermal method. *Waste Management, 82*, 139-146. doi:https://doi.org/10.1016/j.wasman.2018.10.023

Shih, Y.-T., & Zhao, Y. (2021). Development, characterization and validation of starch based biocomposite films reinforced by cellulose nanofiber as edible muffin liner. *Food Packag. Shelf Life, 28*, 100655. doi:https://doi.org/10.1016/j.fpsl.2021.100655

Sim, B., Bae, D., Choi, K., Islam, M. S., & Kao, N. (2016). Fabrication and stimuli response of rice husk-based microcrystalline cellulose particle suspension under electric fields. *Cellulose, 23*. doi:https://10.1007/s10570-015-0836-3

Singh, S., Gaikwad, K. K., Park, S.-I., & Lee, Y. S. (2017). Microwave-assisted step reduced extraction of seaweed (*Gelidiella aceroso*) cellulose nanocrystals. *Int. J. Biol. Macromol., 99*, 506-510. doi:https://doi.org/10.1016/j.ijbiomac.2017.03.004

Slavutsky, A. M., & Bertuzzi, M. A. (2014). Water barrier properties of starch films reinforced with cellulose nanocrystals obtained from sugarcane bagasse. *Carbohydr. Polym., 110*, 53-61. doi:https://doi.org/10.1016/j.carbpol.2014.03.049

Souza, A. G., Ferreira, R. R., Paula, L. C., Mitra, S. K., & Rosa, D. S. (2021). Starch-based films enriched with nanocellulose-stabilized Pickering emulsions containing different essential oils for possible applications in food packaging. *Food Packag. Shelf Life, 27*, 100615. doi:https://doi.org/10.1016/j.fpsl.2020.100615

Srivastava, K. R., Dixit, S., Pal, D. B., Mishra, P. K., Srivastava, P., Srivastava, N., . . . Abd_Allah, E. F. (2021). Effect of nanocellulose on mechanical and barrier properties

of PVA–banana pseudostem fiber composite films. *Environ. Technol. Innov., 21*, 101312. doi:https://doi.org/10.1016/j.eti.2020.101312

Tanwar, R., Gupta, V., Kumar, P., Kumar, A., Singh, S., & Gaikwad, K. K. (2021). Development and characterization of PVA-starch incorporated with coconut shell extract and sepiolite clay as an antioxidant film for active food packaging applications. *Int. J. Biol. Macromol., 185*, 451-461. doi:https://doi.org/10.1016/j.ijbiomac.2021.06.179

Tarchoun, A. F., Trache, D., & Klapötke, T. M. (2019). Microcrystalline cellulose from *Posidonia oceanica* brown algae: Extraction and characterization. *Int. J. Biol. Macromol., 138*, 837-845. doi:https://doi.org/10.1016/j.ijbiomac.2019.07.176

Tea Board of India, Global Tea website. (2022). Retrieved from https://www.teaboard.gov.in/pdf/Global_Tea_Website_pdf8152.pdf

Thiangtham, S., Runt, J., Saito, N., & Manuspiya, H. (2020). Fabrication of biocomposite membrane with microcrystalline cellulose (MCC) extracted from sugarcane bagasse by phase inversion method. *Cellulose, 27*(3), 1367-1384. doi:https://10.1007/s10570-019-02866-3

Trache, D., Hussin, M. H., Hui Chuin, C. T., Sabar, S., Fazita, M. R. N., Taiwo, O. F. A., . . . Haafiz, M. K. M. (2016). Microcrystalline cellulose: Isolation, characterization and bio-composites application—A review. *Int. J. Biol. Macromol., 93*, 789-804. doi:https://doi.org/10.1016/j.ijbiomac.2016.09.056

Trifol, J., Plackett, D., Szabo, P., Daugaard, A. E., & Giacinti Baschetti, M. (2020). Effect of crystallinity on water vapor sorption, diffusion, and permeation of PLA-based nanocomposites. *ACS omega, 5*(25), 15362-15369. doi:https://10.1021/acsomega.0c01468

Tummala, G. K., Rojas, R., & Mihranyan, A. (2016). Poly(vinyl alcohol) Hydrogels Reinforced with Nanocellulose for Ophthalmic Applications: General Characteristics and Optical Properties. *J. Phys. Chem. B, 120*(51), 13094-13101. doi:https://10.1021/acs.jpcb.6b10650

Ueda, T., Ishigami, A., Thumsorn, S., Kurose, T., Kobayashi, Y., & Ito, H. (2022). Structural, rheological, and mechanical properties of polyvinyl alcohol composites reinforced with cellulose nanofiber treated by ultrahigh-pressure homogenizer. *Mater. Today Commun., 33*, 104316. doi:https://doi.org/10.1016/j.mtcomm.2022.104316

Ulaganathan, R. K., Mohamad Senusi, N. A., Mohd Amin, M. A., Abdul Razab, M. K. A., Ismardi, A., & Abdullah, N. H. (2022). Effect of cellulose nanocrystals (CNC) on PVA/CNC bio-nanocomposite film as potential food packaging application. *Mater. Today: Proc., 66*, 3150-3153. doi:https://doi.org/10.1016/j.matpr.2022.07.466

Ummartyotin, S., & Pechyen, C. (2016). Microcrystalline-cellulose and polypropylene based composite: A simple, selective and effective material for microwavable packaging. *Carbohydr. Polym., 142*, 133-140. doi:https://doi.org/10.1016/j.carbpol.2016.01.020

Varghese, S. A., Pulikkalparambil, H., Rangappa, S. M., Parameswaranpillai, J., & Siengchin, S. (2023). Antimicrobial active packaging based on PVA/Starch films incorporating basil leaf extracts. *Mater. Today: Proc., 72*, 3056-3062. doi:https://doi.org/10.1016/j.matpr.2022.09.062

Ventura-Cruz, S., Flores-Alamo, N., & Tecante, A. (2020). Preparation of microcrystalline cellulose from residual Rose stems (*Rosa spp.*) by successive delignification with alkaline hydrogen peroxide. *Int. J. Biol. Macromol., 155*, 324-329. doi:https://doi.org/10.1016/j.ijbiomac.2020.03.222

Ventura-Cruz, S., & Tecante, A. (2019). Extraction and characterization of cellulose nanofibers from Rose stems (*Rosa spp.*). *Carbohydr. Polym., 220*, 53-59. doi:https://doi.org/10.1016/j.carbpol.2019.05.053

Wang, B., Dong, F., Chen, M., Zhu, J., Tan, J., Fu, X., . . . Chen, S. (2016). Advances in Recycling and Utilization of Agricultural Wastes in China: Based on Environmental Risk, Crucial Pathways, Influencing Factors, Policy Mechanism. *Procedia Environ. Sci., 31*, 12-17. doi:https://doi.org/10.1016/j.proenv.2016.02.002

Wang, B., Sui, J., Yu, B., Yuan, C., Guo, L., Abd El-Aty, A. M., & Cui, B. (2021). Physicochemical properties and antibacterial activity of corn starch-based films incorporated with *Zanthoxylum bungeanum* essential oil. *Carbohydr. Polym., 254*, 117314. doi:https://doi.org/10.1016/j.carbpol.2020.117314

Wang, B., Yan, S., Gao, W., Kang, X., Yu, B., Liu, P., . . . Abd El-Aty, A. M. (2021). Antibacterial activity, optical, and functional properties of corn starch-based films impregnated with bamboo leaf volatile oil. *Food Chem., 357*, 129743. doi:https://doi.org/10.1016/j.foodchem.2021.129743

Wang, C., Mei, J., & Zhang, L. (2021). High-added-value biomass-derived composites by chemically coupling post-consumer plastics with agricultural and forestry wastes. *J. Clean. Prod., 284*, 124768. doi:https://doi.org/10.1016/j.jclepro.2020.124768

Wang, Z.-C., Qin, C.-Q., Zhang, X., Wang, Q., Li, R.-X., & Ren, D.-F. (2021). Effect of whey protein isolate/chitosan/microcrystalline cellulose/PET multilayer bottles on the shelf life of rosebud beverages. *Food Chem., 347*, 129006. doi:https://doi.org/10.1016/j.foodchem.2021.129006

Wang, Z., Qiao, X., & Sun, K. (2018). Rice straw cellulose nanofibrils reinforced poly(vinyl alcohol) composite films. *Carbohydr. Polym., 197*, 442-450. doi:https://doi.org/10.1016/j.carbpol.2018.06.025

Widyaningrum, B. A., Amanda, P., Pramasari, D. A., Ningrum, R. S., Kusumaningrum, W. B., Kurniawan, Y. D., . . . Kusuma, H. S. (2022). Preparation of a Conductive Cellulose Nanofiber-reinforced PVA Composite Film with Silver Nanowires Loading. *Nano-Struct. Nano-Objects., 31*, 100904. doi:https://doi.org/10.1016/j.nanoso.2022.100904

Xiao, M., Tang, B., Qin, J., Wu, K., & Jiang, F. (2022). Properties of film-forming emulsions and films based on corn starch/sodium alginate/gum Arabic as affected by virgin coconut oil content. *Food Packag. Shelf Life, 32*, 100819. doi:https://doi.org/10.1016/j.fpsl.2022.100819

Xiong, F., Wu, Y., Li, G., Han, Y., & Chu, F. (2018). Transparent Nanocomposite Films of Lignin Nanospheres and Poly(vinyl alcohol) for UV-Absorbing. *Ind. Eng. Chem. Res., 57*(4), 1207-1212. doi:https://10.1021/acs.iecr.7b04108

Xie, H., Du, H., Yang, X., & Si, C. (2018). Recent Strategies in Preparation of Cellulose Nanocrystals and Cellulose Nanofibrils Derived from Raw Cellulose Materials. *Int. J. Polym. Sci., 2018*, 7923068. doi:https://10.1155/2018/7923068

Xu, H., Hao, Z., Gao, J., Zhou, Q., Li, W., Liao, X., . . . Xiao, Y. (2023). Complexation between rice starch and cellulose nanocrystal from black tea residues: Gelatinization properties and digestibility in vitro. *Int. J. Biol. Macromol., 234*, 123695. doi:https://doi.org/10.1016/j.ijbiomac.2023.123695

Yang, D., Liu, Q., Gao, Y., Wan, S., Meng, F., Weng, W., & Zhang, Y. (2023). Characterization of silver nanoparticles loaded chitosan/polyvinyl alcohol antibacterial films for food packaging. *Food Hydrocoll., 136*, 108305. doi:https://doi.org/10.1016/j.foodhyd.2022.108305

Yang, M., Zhang, X., Guan, S., Dou, Y., & Gao, X. (2020). Preparation of lignin containing cellulose nanofibers and its application in PVA nanocomposite films. *Int. J. Biol. Macromol., 158*, 1259-1267. doi:https://doi.org/10.1016/j.ijbiomac.2020.05.044

Yao Désiré, A., Charlemagne, N., Degbeu Claver, K., Fabrice Achille, T., & Marianne, S. (2021). Starch-based edible films of improved cassava varieties Yavo and TMS reinforced with microcrystalline cellulose. *Heliyon, 7*(4), e06804. doi:https://doi.org/10.1016/j.heliyon.2021.e06804

Yuan, Y., & Chen, H. (2021). Preparation and characterization of a biodegradable starch-based antibacterial film containing nanocellulose and polyhexamethylene biguanide. *Food Packag. Shelf Life, 30*, 100718. doi:https://doi.org/10.1016/j.fpsl.2021.100718

Yu, Z., Li, B., Chu, J., & Zhang, P. (2018). Silica in situ enhanced PVA/chitosan biodegradable films for food packages. *Carbohydr. Polym., 184*, 214-220. doi:https://doi.org/10.1016/j.carbpol.2017.12.043

Zhao, T., Chen, Z., Lin, X., Ren, Z., Li, B., & Zhang, Y. (2018). Preparation and characterization of microcrystalline cellulose (MCC) from tea waste. *Carbohydr. Polym., 184*, 164-170. doi:https://doi.org/10.1016/j.carbpol.2017.12.024

Zhao, X., Han, Z., Zhang, S., Abuduaini, G., Wen, X., Liu, T., & Cheng, Z. (2023). Preparation of PVA/*Tremella* polysaccharide and soy protein isolate complex/ε-polylysine active membrane and its application in blueberry preservation. *Food Packag. Shelf Life, 40*, 101163. doi:https://doi.org/10.1016/j.fpsl.2023.101163

Zheng, R., Zhao, T., Lin, X., Chen, Z., Li, B., & Zhang, Y. (2022). Fabrication, characterization, and application of Pickering emulsion stabilized by tea (*Camellia sinensis* L.) O. Kuntze) waste microcrystalline cellulose. *J. Dispers. Sci. Technol*., 1-11. doi:https://10.1080/01932691.2022.2063883